Improving Species Distribution Models with Bias Correction and Geographically Weighted Regression: Tests of Virtual Species and Past and Present Distributions in North American Deserts

by

Richard Inman

A Dissertation Presented in Partial Fulfillment
of the Requirements for the Degree
Doctor of Philosophy

Approved April 2018 by the
Graduate Supervisory Committee:

Janet Franklin, Chair
A. Stewart Fotheringham
Ronald Dorn

ARIZONA STATE UNIVERSITY

May 2018

ABSTRACT

This work investigates the effects of non-random sampling on our understanding of species distributions and their niches. In its most general form, bias is systematic error that can obscure interpretation of analytical results by skewing samples away from the average condition of the system they represent. Here I use species distribution modelling (SDM), virtual species, and multiscale geographically weighted regression (MGWR) to explore how sampling bias can alter our perception of broad patterns of biodiversity by distorting spatial predictions of habitat, a key characteristic in biogeographic studies. I use three separate case studies to explore: 1) How methods to account for sampling bias in species distribution modeling may alter estimates of species distributions and species-environment relationships, 2) How accounting for sampling bias in fossil data may change our understanding of paleo-distributions and interpretation of niche stability through time (i.e. niche conservation), and 3) How a novel use of MGWR can account for environmental sampling bias to reveal landscape patterns of local niche differences among proximal, but non-overlapping sister taxa. Broadly, my work shows that sampling bias present in commonly used federated global biodiversity observations is more than enough to degrade model performance of spatial predictions and niche characteristics. Measures commonly used to account for this bias can negate much loss, but only in certain conditions, and did not improve the ability to correctly identify explanatory variables or recreate species-environment relationships. Paleo-distributions calibrated on biased fossil records were improved with the use of a novel method to directly estimate the biased sampling distribution, which can be generalized to finer time slices for further paleontological studies. Finally, I show how a novel coupling of SDM and MGWR can

illuminate local differences in niche separation that more closely match landscape genotypic variability in the two North American desert tortoise species than does their current taxonomic delineation.

DEDICATION

This dissertation is dedicated to my wife, Kerstin, who has been a constant source of support and encouragement. I am truly thankful for having you in my life. This work is also dedicated to my parents, Rod and Katherine, who inspired my fascination with the natural world.

ACKNOWLEDGMENTS

I am very fortunate to have had Janet Franklin as an advisor, mentor and friend. Her attention to detail, positive and constructive critique, and her endless energy has shaped my view of academia and scientific productivity. She is an inspiration to us all. I am very thankful for the support Ron Dorn provided throughout my time at ASU; our discussions of geomorphology and tortoise habitat during mountain biking adventures were invaluable. And for Stewart Fotheringham, whose professionalism and intellectual rigor kept me limber during statistical gymnastics. And finally, I could not have finished this work without the support of Todd Esque and Ken Nussear, who have shaped and supported my early career work.

TABLE OF CONTENTS

Page

CHAPTER Page

CHAPTER Page

CHAPTER Page

APPENDIX Page

APPENDIX Page

LIST OF TABLES

LIST OF FIGURES

CHAPTER 1

INTRODUCTION

Sampling bias is an issue that obscures statistical inference across a wide range of disciplines, including the natural and social sciences. Both of these broad realms of scientific inquiry have benefitted from the quantitative revolution in the late 1960's and early 70's, and more recently, have seen a proliferation in the availability of large crowd-sourced and federated datasets. This is especially true in the discipline of quantitative geography, where new analytical methods are continually being developed to analyze newly available data (Fotheringham et al. 2000). Most of these methods rely on statistical models, many of which are sensitive to biases and have implicit assumptions such as being free of spatial dependence (Besag and Newell 1991). Research on topics such as spatial dependence and spatial heterogeneity have helped address some of these assumptions (Anselin 2003), and have spilled over to benefit countless other fields of research in the social and natural sciences (Fotheringham et al. 2000). In particular, the fusion of quantitative geography and spatial ecology has led to improved methods for dealing with environmental sampling bias in species distribution modelling (SDM), a set of methods that has become common in the fields of ecology and biogeography.

SDM is a quantitative modeling approach that relates locations of species occurrences to environmental covariates hypothesized to influence or define the suitability of habitat of the species and is often used to predict the geographic distribution of species or to generate maps of habitat potential (Franklin 2010a). SDM is especially well suited for tasks such as designing conservation and monitoring programs, evaluating the efficacy of proposed land management actions, and developing recovery planning for

threatened or endangered species (Franklin 2013). Additionally, SDMs are being used to assess large-scale patterns of species richness (Graham and Hijmans 2006, Franklin 2010a) and to evaluate potential changes in species distributions resulting from climate change (e.g. Pearson and Dawson 2003, Sinclair et al. 2010), as well as to hindcast distributions under past climates based on current species-environment relationships (Svenning et al. 2011, Varela et al. 2011, Franklin et al. 2015).

SDM quantifies relationships between environmental conditions at locations where a species occurs (presence) and where it does not (absence) to make spatial predictions about where the species may occur. While presence locations are often readily available, locations where an organism is absent are not always known or available, and are far more difficult to ascertain (MacKenzie et al. 2002, Elith and Leathwick 2009). This lack of absence observations is becoming more common due to the increased availability of occurrence records found in online museum databases now available for thousands of species (Graham et al. 2004a, Frey 2009, Newbold 2010), and has contributed to the development of presence-background (PB) modeling methods that compare environmental conditions at locations where a species has been observed to environmental conditions across the entire study area (background). These methods do not rely on knowledge of locations where a species is absent, and as such, software for PB data (e.g. MaxEnt; Phillips et al. 2006) have become primary tools for SDM research in recent years (Guillera-Arroita et al. 2015).

However, while PB methods offer many advantages (e.g., availability of data, prevalence of software), they make several assumptions that are not always acknowledged in practice (Elith and Leathwick 2009). One key assumption with PB

methods is that the sampling of occurrence localities is unbiased and that any sampling bias is proportional to the background distribution of environmental covariates (Araújo and Guisan 2006, Phillips et al. 2009). This assumption is routinely ignored or only cursorily addressed (Guillera-Arroita et al. 2015) due to the high cost of conducting random or stratified sampling and because many studies using SDM draw on historical museum records that generally represent haphazard and opportunistic sampling (Elith and Leathwick 2007, Newbold 2010). Because of this, SDM often relies on observations that are highly clustered and/or non-randomly distributed in geographic and environmental-space (Loiselle et al. 2007, Hortal et al. 2008). In lieu of starting with bias-free calibration data, several methods to reduce the effects of environmental sampling bias have been proposed and used with varying degrees of success over the past decade. I address three of the most commonly used bias-correction methods in Chapter 2 with a simulation approach to explore the effects of sampling bias on SDM in PB frameworks. Specifically, I aim to identify which of these three methods is best able to account for sampling bias across a wide range of species. Where these methods have been compared previously, emphasis has been on spatial predictions of habitat potential. Here I dig deeper into the use of these correction methods by exploring how sampling bias not only affects predictions of habitat potential, but also our understanding of niche characteristics such as which explanatory variables and species-environment relationships best represent the niche.

In Chapter 3, I investigate sampling bias in another growing segment of SDM applications: paleo-distribution modeling. Paleo-distribution modeling (paleo-SDM) has become an important tool for paleontological studies, allowing researchers to estimate

species' past distributions for questioning how organisms used resources and their environment historically (Guillera-Arroita et al. 2015). Paleo-SDM draws on the recent development of paleoecological archives providing geo-located fossil observations and reconstructions of historical environmental conditions. Paleoecological archives are used directly for calibrating models under past environmental conditions, and any sampling bias in the calibration dataset has the potential to affect these reconstructed distributions and therefore skew results of archeological and paleobiogeographic questions.

In general, areas with more recent geologic formations have a greater prevalence of fossils due to the larger volume of sedimentary rock and because more recent formations will have had fewer destructive erosional forces (Raup 1972). While these patterns are generally attributed to time scales describing changes in the fossil record from the Cambrian through the Permian and into the Tertiary periods, they can influence the distribution of fossils during the Late Quaternary - such as the distribution of *Neotoma* (North American packrat) middens. These nests can contain an immense wealth of plant and animal remains preserved by crystallized urine in arid environments (Wells 1976), which have been ^{14}C dated and are geo-referenced. However, while the analysis of packrat middens has spanned the past 50 years, this wealth of geo-referenced macrofossil information has rarely been used in paleo-SDM studies. In Chapter 3, I explore potential effects of sampling bias in the North American *Neotoma* packrat plant macrofossil record (Strickland et al. 2013, Williams et al. 2018), and test whether (1) the spatial sampling bias inherent in this record can influence estimates of paleo-distributions, (2) this bias can alter our ability to measure shifts in distributions from the early/mid Holocene (11.5 ka –

5 ka) to present day (1950 – present), and (3) bias correction methods can improve paleo-distributions and analyses of range shifts and niche breadth.

Another issue gaining recognition in biogeographical research is that of spatial non-stationarity, which has drawn recent attention from the infusion of geographic thought to the spatial ecology domain (Foody 2008, Miller and Hanham 2011, Miller 2012). Most applications of SDM rely on the assumption that species-environment relationships are constant across a species' geographic distribution. In a regression framework, species-environment relationships are treated as stationary by estimating a single parameter (or possibly several for non-linear relationships) for the entire study area (i.e. 'global') for each covariate of interest. Spatial non-stationarity suggests that instead of remaining constant across a species' distribution, a species-environment relationship may change across a landscape such that in one part of a species' range, a relationship may be positive, but in another part, negative. This idea has been explored in context of macroecology patterns such as species richness (Rahbek and Graves 2001, Willis and Whittaker 2002, Foody 2004, Bickford and Laffan 2006), but has only recently been extended to species distribution modeling (Miller 2012) – likely due to the complexity of the many factors that influence a species' distribution.

In biophysical ecology, many relationships of an organism's physiology and its environment are assumed to be stationary due to their foundation in first principles (e.g. an organism's thermodynamic exchange with its proximal environment; Porter and Gates 1969). These relationships (such as an organism's rate of water loss) are governed by physical properties such as an organism's size, shape, solar reflectance, insulation, metabolic rate and so forth, which do not vary as an organism moves across a landscape.

However, population level manifestations of these relationships can be affected by heterogeneity in local conditions (e.g. interactions between temperature and soil moisture), resulting in apparent macro-scale variation in species-environment relationships across a species' distribution. Similarly, spatial non-stationarity may be apparent when key variables are omitted or the model functional form is mis-specified (Fotheringham 1997). Variable omission is likely when proxies are used instead of mechanistic causal factors (Kearney and Porter 2009), especially when the proxies are non-linearly related to the unmeasured factors they are supposed to represent. In this case, an environmental covariate, such as 'mean annual temperature' may serve as a proxy for the more mechanistically relevant factor of hourly surface substrate temperature (Kearney et al. 2014), and as such may show a changing relationship across a species' range as a function of another unmeasured variable such as substrate type. Due to these issues, and likely a misunderstanding of how spatial non-stationarity can arise in broad ecological patterns, very few published works have incorporated spatial non-stationarity with species distribution modeling (Kupfer and Farris 2006, Miller 2012).

Geographically weighted regression (GWR; Fotheringham et al. 2003) has become a dominant method to incorporate spatial non-stationarity in a regression framework and uses local statistics to explore evidence of spatially varying relationships. GWR uses spatially explicit kernel weighting schemes to create local parameter estimates (coefficients, t-values, standard errors and R^2) for each observation. These weighting schemes rely on a bandwidth parameter used to define the shape of the spatial weighting scheme and can be fixed or allowed to shrink and expand in geographic space (i.e. 'adaptive kernel') to include an optimal number of observations to accommodate

variations in observation density. A single GWR model is an amalgamation of many separate regression models, and results in locally varying estimates of the relationships between covariates and response variable. Obvious benefits to SDM are the ability to model spatial non-stationarity and to account for spatial autocorrelation in calibration data through a spatial weights matrix. While the latter has been addressed through the development of hierarchical Bayesian models (e.g. Chakraborty et al. 2010) and spatial dependence terms (e.g. Miller et al. 2007), the former presents a new paradigm with which to view SDM.

Another obvious benefit of the GWR framework is the estimation of locally varying intercepts, which have the potential to account for sampling bias by offsetting the intercept parameter in a given area to account for locally intense sampling efforts. This is because at fine local scales, the geographic variation in survey effort can be assumed to be constant. Therefore, as long as the bandwidth can approximate the local scale of the survey effort bias, locally varying intercepts may reduce environmental sampling bias caused by biased survey efforts. However, at very fine local scales, calibration of logistic regression models may fail to converge due to complete separation of response classes if some areas contain only presence or only absence observations. This problem is magnified under extreme sampling bias, and generally forces SDM cast in a GWR framework to use large bandwidths approximating global models (Miller 2012). In Chapter 4, I use a novel application of SDM and GWR to investigate differences in habitat use between two species of North American tortoise, *Gopherus agassizii* (Agassiz's desert tortoise) and *Gopherus morafkai* (Morafka's desert tortoise). Specifically, I 1) identify landscape boundaries in habitat use between the two species,

and 2) determine which of three hypothesized delineations better describes landscape patterns of genotype variation. These hypothesized delineations include A) the current geographic boundary defining each species, B) the Mojave and Sonoran Basin and Range ecotone, and C) geographic similarities in local habitat use. The results of this study have implications for land management in and around the secondary contact zone due to the difference in protection status between these two species. Further, this work will inform conservation planning in other regions where local habitat use is of concern.

CHAPTER 2

COMPARING SAMPLE BIAS CORRECTION METHODS FOR SPECIES DISTRIBUTION MODELING USING VIRTUAL SPECIES

ABSTRACT

1. A key assumption in species distribution modeling (SDM) with presence-background (PB) methods is that sampling of occurrence localities is unbiased and that any sampling bias is proportional to the background distribution of environmental covariates. This assumption is routinely violated when federated museum records from natural history collections are used due to their incomplete and biased survey methods.

2. I use a simulation approach to explore the effectiveness of three methods developed to account for sampling bias in SDM with PB frameworks. Two of the methods rely on careful filtering of observation data: geographical thinning (G-Filter) and environmental thinning (E-Filter); while a third method, FactorBiasOut, creates selection weights for background data to bias their locations towards areas where the observation dataset was sampled. Where these methods have been assessed previously, emphasis has been on spatial predictions of habitat potential. Here I dig deeper into the effectiveness of these methods by exploring how sampling bias not only affects predictions of habitat potential, but also our understanding of fundamental niche characteristics such as which explanatory variables and response curves best represent species-environment relationships. I simulate 100 virtual species ranging from generalists to specialists in terms of habitat preferences and introduce geographical and environmental bias at three intensity levels to measure the effectiveness of each correction method to: 1) identify true

explanatory variables, 2) recreate true species-environment relationships, and 3) predict the true probability of occurrence across the study area.

3. I find that the FactorBiasOut method most often showed the greatest improvement in recreating known distributions but did no better at correctly identifying environmental covariates or recreating species-environment relationships than the G-Filter or E-Filter methods. Narrow niche species are most problematic for biased calibration datasets, such that correction methods can, in some cases, make predictions worse.

4. I highlight the need for SDM practitioners to be cognizant of sampling bias when inferring species-environment relationships using historical museum records or other biased occurrence data.

INTRODUCTION

A methodology that has taken the forefront in conservation biology, spatial ecology and biogeography is species distribution modeling (SDM), a statistical modeling approach that relates locations of species observations to environmental covariates hypothesized to influence or define an organism's niche (Franklin 2010b). SDM using discriminative statistical methods characterizes the relationships between environmental conditions at locations where a species has been observed to those locations where it has not in order to predict how likely it is to occur at other unobserved locations (Mateo et al. 2010). Unfortunately, locations where an organism is absent are not always known or readily available, and can be difficult to ascertain (MacKenzie et al. 2002, Elith and Leathwick 2009). This has contributed to the development of so-called presence-background (PB) modeling methods that compare environmental conditions at locations where a species has been observed to environmental conditions across the entire study

area (background). Methods not relying on locations where species are absent have propelled software for PB data (e.g. Maxent; Phillips et al. 2006) to become primary tools for SDM research in recent years (Guillera-Arroita et al. 2015).

However, while PB methods have many advantages over presence-absence methods, (e.g. availability of data and software), they make several assumptions that are not always acknowledged in practice (Elith and Leathwick 2009). One key assumption of PB methods is that any sampling bias is proportional to the background distribution of environmental covariates (Araújo and Guisan 2006), and that a species' niche is sampled over the full range of environmental conditions in which they occur (Phillips et al. 2009). To meet these assumptions, an obvious solution is to use random or stratified-random sampling designs to collect observations in a manner free of sampling bias (Hirzel and Guisan 2002, Edwards et al. 2006). Unfortunately, the high cost of conducting these surveys often precludes their use and has resulted in widespread use of a growing number of federated museum records to describe species occurrences for SDM. These natural history collections generally represent haphazard and opportunistic sampling (Elith and Leathwick 2007, Loiselle et al. 2007, Hortal et al. 2008, Newbold 2010), and introduce sampling bias to the locality information for thousands of species.

There are two types of bias problematic for SDM: 1) incomplete sampling, and 2) over-sampling; both result in spatial heterogeneity in the sampling intensity across a landscape. The former occurs when not all parts of environmental space where a species can occur (realized niche space) is sampled, leaving certain combinations of environmental conditions absent from the observation dataset. This may occur when some regions of a species' range are unavailable for sampling, resulting in few

observations in certain areas that are otherwise occupied. Over-sampling occurs when some occupied regions of environmental space are sampled at higher intensities than others, thereby shifting model coefficients towards conditions represented by those heavily sample regions and away from regions that may be equally suitable for the species. This may result when some geographic areas are sampled at higher intensities than others, such as when areas proximal to roadways and access routes are more heavily sampled than remote and inaccessible areas (Kadmon et al. 2004). Other species may suffer from heterogeneity in sampling intensity caused by administrative boundaries, such as when national parks, wildlife refuges or other locations of interest are sampled more heavily, thereby biasing model coefficients towards environmental conditions found in those areas. These two types of bias can occur in museum records because these sources rarely stem from systematic sampling regimes (Ponder et al. 2001, Frey 2009, Newbold 2010).

Another factor affecting sampling bias is the size of a species' geographic range or prevalence of occupied areas across a landscape. SDMs for species with large geographic ranges and high prevalence have shown poorer model fit than rarer species with smaller ranges and lower prevalence (Brotons et al. 2004, Elith et al. 2006, Marmion et al. 2008, Franklin et al. 2009) because smaller ranges require fewer observations to obtain an unbiased sampling distribution than larger ranges. Similarly, species with high landscape prevalence and large ranges are often generalists, that is, occurring across a wide range of habitats or environmental conditions (Brown 1984, Pulliam 2000, Slatyer et al. 2013). The difficulty in distinguishing their niches from the available background may result in poor model performance (Segurado and Araujo 2004, Luoto et al. 2005).

Two of the more straightforward methods to reduce sampling bias rely on careful filtering of observation data. The first method, geographical filtering (G-Filter), has been used in numerous applications in SDM and, in its simplest form, involves removing occurrence records from areas with high sample densities (Boria et al. 2014). In contrast, the second filtering method, environmental filtering (E-Filter), involves filtering observation data based on environmental clustering rather than geographic clustering (Varela et al. 2014). Here, clusters in n-dimensional environmental space are identified and random samples are selected from each cluster; thereby ensuring that all combinations of covariate space are equally represented in the observation dataset. While subtly different in their implementation, these two methods both rely on filtering observations to create a smaller observation dataset with minimal bias. A third approach uses the complete (but biased) observation dataset, and instead manipulates the selection of background records to mimic the spatial sampling bias found in the observations using a background weight correction. This method is implemented using the FactorBiasOut algorithm (Dudik et al. 2005) in MaxEnt (Phillips et al. 2006) and has gained popularity due to the ease with which it can be applied.

I use a simulation approach to explore the effects of sampling bias on SDM in PB frameworks. Specifically, I aim to identify which of these three commonly used methods is best able to account for sampling bias across a wide range of diverse species. Where these methods have been addressed previously emphasis has been on spatial predictions of habitat potential. Here I dig deeper into the use of these methods by exploring how sampling bias not only affects predictions of habitat potential, but also our understanding of fundamental niche characteristics such as which explanatory variables and species-

environment relationships best represent the niche. Simulated and virtual species (Hirzel et al. 2001, Meynard and Kaplan 2012, Miller 2014, Moudrý 2015) offer a controlled environment with which to assess the performance of these three bias correction methods, and to disentangle the effects of biased observations from niche characteristics such as landscape prevalence and niche breadth. I simulate 100 virtual species ranging from habitat specialists to generalists and introduce geographical and environmental bias at three intensity levels to measure the effectiveness of each correction method to: 1) identify true explanatory variables, 2) recreate true species-environment relationships, and 3) predict the true habitat potential across my study area. The work flow used here is shown in Figure 2.1.

MATERIALS AND METHODS

Study Area

I use environmental maps of an arid, interior southwestern region of the USA to define the environment and environmental correlates of realistic, but virtual, species distributions. My study area covered 918,557 km^2 and incorporated a broad range of ecosystems ranging from Southern and Central California Chaparral and Oak Woodlands to the southwestern Mojave, Sonoran and Chihuahuan Deserts. I chose this area for the availability of a rich set of environmental data (e.g. Vandergast et al. 2013, Inman et al. 2014) describing a broad range of physiographic (e.g. landform type, surface texture and geologic character) and climatic (e.g. temperature, precipitation norms and extremes) environmental conditions available to develop distributions of virtual species that could plausibly inhabit this region.

Simulated Species

I created distributions for 100 virtual species using the package *virtualspecies* (Leroy et al. 2015) in R 3.3.2 (R Core Team 2016). Each species' niche was defined using two to five randomly selected environmental covariates from a suite of ten possible explanatory variables spanning physiographic and climatic constraints. These raster layers represented environmental conditions hypothesized to influence the distribution of many actual species in the region (Inman et al. 2014), and were generalized to a spatial resolution of 1 km (Appendix 2.1). For simplicity, I set the realized niches of these species equal to their fundamental niches, precluding the need to simulate predation or competition, and assumed that these virtual species were in equilibrium with their environment and therefore exhibited stable population sizes. The 'true' habitat potential for each species in each grid cell was deterministically defined using response curves that included linear, quadratic, logistic or Gaussian functions in an additive approach. In order to create realistic species distributions and habitat preferences, I ensured that response curves could not contradict one another on the landscape (e.g. result in species living simultaneously in the hottest and coldest portions of my study area) using an iterative approach, wherein mechanistic response curves were created sequentially. In the first step, a single response curve was randomly generated and applied to its corresponding environmental covariate to create a grid surface representing habitat potential for the virtual species based only a single environmental descriptor. An 'occupied' raster layer was created from this habitat potential for each species using a probabilistic approach wherein occupied cells were selected with the probability:

$$P_i = \frac{1}{1+e^{\frac{x_i-0.65}{-0.05}}} \quad (2.1)$$

Where x_i is the habitat potential value for cell i for x explanatory variable. For the next explanatory variable, a response curve was randomly developed for areas considered occupied from the first covariate, and a new grid surface representing habitat potential for the virtual species was created by combining the two response curves in an additive approach and applying them to the entire study area. If additional environmental explanatory variables were assigned, these steps were repeated resulting in a 'true' habitat potential value for each grid cell wherein each explanatory variable was given an equal weight. I created an occupied raster layer from the true habitat potential, which was then used to calculate the prevalence of occupied areas for each species, ranging from 0.05% to over 97% of the study area. I attempted to create a range of specialist and generalist species by modifying the shape parameters for each of the linear, quadratic, logistic and Gaussian functions. The resulting virtual species had mean landscape values of their 'true' habitat potential ranging from 0.13 to 0.94.

I hypothesized that the breadth of each species' niche and their landscape prevalence would affect how much biased sampling distributions degraded SDM performance. Specifically, I hypothesized that specialists would show erratic responses to differing types and levels of sampling bias, because while rare species may require fewer samples to adequately estimate their distributions (Franklin et al. 2009), they may also be missed entirely or only sparsely sampled at extreme levels of sampling bias. In cases of the latter I assumed that SDM performance would be severely degraded. I measured landscape prevalence as the occupied proportion of the study area, and niche breadth with a novel approach quantifying the uniqueness of the environmental conditions defining each species' geographic distribution. Metrics of niche breadth can range from

volumetric measurements of n-dimensional hypervolumes (e.g. Blonder et al. 2014), reduced principle component axes of presumed occupied regions of environmental space (e.g. Saupe et al. 2015) to counts of unique habitat types presumed to be occupied (e.g. Harnik et al. 2012, Nürnberg and Aberhan 2013). I developed a novel approach quantifying the environmental uniqueness of occupied habitat drawing on Mahalanobis distances in environmental space because I was most interested in how unique the occupied habitat was from the rest of the study area across all environmental explanatory variables. The niche breadth value for each species was defined as the median of the squared Mahalanobis distance of all occupied cells:

$$\widetilde{D^2} = (\mathrm{X}_o - \mu_a)'\Sigma^{-1}(\mathrm{X}_a - \mu_a) \quad (2.2)$$

Where X_o is the matrix of explanatory variables used to define the species' niche over all occupied cells, X_a is the matrix of the same explanatory variables over all cells in the study area, μ_a is a vector of variable means of the study area and Σ is the covariance matrix of X_a. Occupied cells with high D^2 values have greater environmental distance from all other cells and are therefore more unique, indicative of specialist species. $\widetilde{D^2}$ values can range from near 0 to well over 400, a completely unrealistic value representing the most specialist species possible in my study area; namely a species occurring on a single grid cell with the most unique environmental conditions. I therefore rescaled $\widetilde{D^2}$ into niche breadth values as the inverse of the realistic minimum and maximum possible values in my study area (zero and ten) with the equation:

$$Niche\ Breadth = 1 - \frac{\widetilde{D^2}}{10} \quad (2.3)$$

This index ranges from 0 - 1, wherein a niche breadth value of 0 indicates extreme

uniqueness of environmental variables at occupied cells, and results from a median squared Mahalanobis distance value of 10, the maximum realistic value in my study area. In contrast, a niche breadth value of 1 indicates the most generalist species possible, namely, one that occupies every cell with Mahalanobis distances near 0. Species with small niche breadths also had low landscape prevalence, although the opposite was not always true (Figure 2.2).

Sampling Bias

I introduced two types of sampling bias, geographic and environmental, into observation datasets derived from the virtual species' distributions to explore the potential effects of each type of bias on the performance of SDM. For each type of bias, I created biased observation samples for each species to represent three levels of bias intensity (Low, Medium and High). These three levels ranged from almost no bias (nearly indistinguishable from a randomly sampled set of observations) to an extreme level greater than that expected to be found in most presence-only observation datasets. Bias was introduced with spatial inclusion weights, which were used to preferentially sample N occupied cells for inclusion to each biased observation dataset. Each biased dataset assumes perfect detection such that if an organism occurs in a given area, it would be detected with a probability of 1. While this may not always be the case (MacKenzie et al. 2002), I assume perfect detection in order to focus on the differences between methods to correct sampling bias. An additional observation dataset with no bias was created for each species by randomly selecting N observations from the occupied cells.

Inclusion weights for the geographically biased observation datasets were calculated using a spatially clustered sampling schema by randomly seeding 5, 8, or 10

cluster centers for the Low, Medium and High intensities of bias, respectively (Figure 2.3). For each level of intensity, I created a Gaussian density kernel raster using the equal split method of Okabe et al. (2009) with a bandwidth of 500 , 250, or 100 km for the 5, 8, or 10 cluster centers, respectively, in GRASS GIS (Neteler et al. 2012). The inclusion weight for each occupied cell was defined by rescaling each Gaussian density kernel raster to 0-1. This spatially clustered sampling schema ensures that occupied cells closest to the randomly seeded cluster were selected with higher probabilities than those further away. I create biased observation datasets by randomly selecting occupied cells according to their inclusion weights. The number of cells selected (N) for each species was determined by the prevalence of occupied cells across the study area, and was calculated as:

$$N = p * 500 \quad (2.4)$$

Where p is the prevalence of occupied cells across the study area. I limited the maximum number of observations to 500 to ensure a realistic sample size for each biased observation dataset. I assessed the degree of sampling bias in each dataset using a generalization of the Ripley's K function for inhomogeneous point processes (Baddeley et al. 2000), which describes the density of observations in the point process over multiple distances, *r*. I measure the mean difference between the theoretical K(r) and border-corrected K(r) density functions of the spatial point pattern for each biased dataset out to a maximum distance of 350 km with the package *spatstat* (Baddeley et al. 2015) in R 3.3.2 (R Core Team 2016). Spatial point patterns with theoretical K(r) and border-corrected K(r) differences near 0 are close to spatially random, while higher values indicate increased levels of spatial bias. Spatial bias among the unbiased and biased

observation datasets for the 100 virtual species ranged from 1 to 197 (Figure 2.4A), and each class (No, Low, Medium and High Bias) was significantly different when accounting for repeated measures of the 100 virtual species ($F_{3,272}$=121.5716; p<0.0001). Inclusion weights for the environmentally biased datasets were defined by identifying 15 unique clusters in the multivariate space of the 10 possible explanatory variables used to create the 100 virtual species. The clusters were identified using a partitioning-around-medoids clustering algorithm in the package *cluster* (Maechler et al. 2016) in R 3.3.2 (R Core Team 2016) and were mapped to geographic space. Inclusion weights were assigned to occupied cells in each mapped cluster based on the total area of each cluster with the equation:

$$P_i = \left(\frac{1}{ClusterArea_{(i)}}\right)^a \quad (2.5)$$

Where *a* equals 1, 3, or 5 for the Low, Medium, or High bias scenarios, and *ClusterArea* is the proportion of the study area that is covered by the mapped cluster containing cell *i*. This method ensures that mapped clusters with larger areas are less likely to be selected, whereas areas with smaller areas were more likely to be sampled. Inclusion weights were rescaled to 0 - 1 prior to use. As with the geographically biased observation datasets, I randomly selected N occupied cells according to their inclusion weights (equation 2.1). The degree of sampling bias for each level was assessed with the random Skewers method of covariance similarity (Cheverud 1996) in the package *phytools* (Revell 2012) in R 3.3.2 (R Core Team 2016), measuring the collinearity between two random selection vectors, each operating on a single covariance matrix (Cheverud and Marroig 2007). This method is used increasingly in evolutionary biology and genetics to estimate similarity among genetic covariance matrices due to its simple

implementation and use of random permutations that can be cast as null hypotheses of the complete un-relatedness between two matrices (Roff et al. 2012). Here I use this method to estimate the relatedness between the covariance matrix of the environmental explanatory variables at locations in the biased observation datasets and the covariance matrix of the environmental explanatory variables at all of the occupied cells. The random Skewers covariance similarity coefficient among the 100 virtual species ranged from 0.997 to 0.904 for each of the four levels of environmentally biased datasets (Figure 2.4B), and each class (No, Low, Medium and High Bias) was significantly different when accounting for repeated measures of the 100 virtual species ($F_{3,273}$=31.19; $p<0.0001$).

Bias Correction Methods

I implemented the geographic filtering (G-Filter) method of bias correction using a sampling mesh with equally sized rectangular cells, each 225 km^2 in area, resulting in 4119 unique sampling areas throughout the study area (Figure 2.5). I limited observations in each sampling area to 2 observations per 225 km^2, a rate that has been effective in minimizing sampling bias for other desert species (Inman et al. 2014). I implemented the environmental filtering (E-Filter) correction by sampling observations at a uniform rate across multiple clusters identified in the n-dimensional environmental space defined by the explanatory variables for a given model specification. I used the same partitioning around medoids clustering algorithm used to introduce environmental sampling bias into the observation datasets, but since the true number of clusters or degree of bias in a biased sampling distribution is rarely known, I estimate an optimal number by maximizing the average silhouette width with package *fpc* (Hennig 2015) in R (R Core Team 2016). In each cluster a random sample with a size equal to the minimum number

of observations in any cluster was selected, and these were pooled to create an observation dataset. This method ensures an equal sampling intensity across each cluster in environmental space, though it does not necessarily result in an even sampling intensity across geographic space.

I implement background weight correction with the FactorBiasOut algorithm (Dudik et al. 2005) in Maxent (Phillips et al. 2006). FactorBiasOut estimates the combined distribution of the biased sample selection distribution (biased survey effort; σ) and the true species distribution (π) and factors out σ, which is assumed to be known and represented as an auxiliary variable (Phillips et al. 2009), often in the form of a bias grid (Elith et al. 2011). This method relies on the knowledge of the biased sample selection distribution (σ), which in practice, is rarely known. However, because the biased observation dataset is a sample of σ, (the observations are sampled with the biased sampling distribution), σ can be estimated when the observation dataset is large (Phillips et al. 2009). I use a bias grid as an estimate of σ by creating a kernel density raster of each biased observation dataset and use it to alter background selection weights. The bandwidth for each kernel was estimated using cross-validation to minimize mean-square error (Baddeley et al. 2015). The resulting kernel density raster was rescaled to 1 - 20, to give greater selection probability to areas with higher densities of observations (Elith et al. 2011).

Models and Performance Criteria

I used MaxEnt v. 3.4.0 (Phillips et al. 2018) to create distribution models for each virtual species and to assess the three bias correction methods in their ability to: 1) identify correct explanatory variables, 2) recreate the shape of the species-environment

relationships, and 3) correctly predict habitat potential across the study area. To address the first objective, I considered all unique combinations of two to five of the 10 possible explanatory variables. Interaction terms were not included and pairs of explanatory variables with correlation coefficients greater than 0.7 were excluded. To reduce processing time, I randomly selected 10 virtual species to evaluate the first objective. For the second and third objectives I created a single model for each of the 100 virtual species specified with the true explanatory variables because for these analyses I assumed that the true explanatory variables were known. The latest versions of Maxent software (e.g. version 3.4.0) implement a new function to produce an estimate of occurrence probability: the complementary log-log function (Phillips et al. 2017). I use this transformation as an indication of habitat potential, and allow inclusion of all feature classes (linear, quadratic, product, threshold and hinge).

The two filtering methods were applied in a replicated fashion because each involves random thinning to remove observations. I replicated the G-Filter and E-Filter methods 20 times each to generate a set of filtered calibration datasets for each biased observation dataset. I estimated a Maxent model for each of the replicated filtered datasets. The background weight correction was implemented using FactorBiasOut in Maxent with the bootstrap option, also with 20 replications. For each of the 800 biased observation datasets (2 bias types, 4 bias intensities, 100 virtual species) and 4 bias correction methods (no correction, G-Filter, E-Filter, FactorBiasOut), I selected the single best performing model with the average Area Under the receiver operating characteristic Curve value (AUC; Fielding and Bell 1997) across the 20 replicates, one of the most commonly used test measures in SDM literature. AUC provides a robust measure of a

model's ability to discriminate between presence and absence localities, independent of an arbitrary cutoff threshold (Cumming 2000), although it has been criticized for its sensitivity to areal extent, among other factors (Lobo et al. 2008). However, because my models were evaluated using the same geographic extent, and because my goal was to select a single model with which to evaluate the bias correction methods, I used AUC to evaluate each model.

Variable selection is a key step in SDM development (Elith and Leathwick 2009, Williams et al. 2012, Bell and Schlaepfer 2016), and yet few studies investigate or comment on the choice of potential environmental covariates, often including widely available climatic variables with little justification (Bell and Schlaepfer 2016). I evaluated each of the bias correction method's ability to identify the correct explanatory variables with the Jaccard similarity coefficient using the equation:

$$J(A, B) = (A \cap B)/(A \cup B) \tag{2.6}$$

Where A is the set of true explanatory variables, B is the set of explanatory variables selected by the model, and $A \cap B$ is the count of the correctly identified explanatory variables and $A \cup B$ is the count of unique explanatory variables in the "true" virtual species model and the best model identified by a given bias correction method. Higher values indicate a greater ability to discriminate the correct set of variables used to define the distribution of the virtual species. The ability to recreate the form of the true species-environment relationships for each explanatory variable was assessed with the Pearson's correlation coefficient between the true relationship and that estimated by the model (Appendix 2.2). I measured collinearity between the marginal response curves produced by Maxent, and those used to create each corresponding virtual species.

Marginal response curves represent the average response curves for each explanatory variable by holding all other variables at their mean for the study area (Phillips et al. 2006). Finally, I assessed the performance of each bias correction method to correctly estimate the true habitat potential for each virtual species in the study area using the Expected fraction of Shared Presences (ESP; Godsoe 2013) by comparing the estimated habitat potential to the true habitat potential across all cells with the equation:

$$ESP = \frac{2\sum_j P_{1j}P_{2j}}{\sum_j (P_{1j}P_{2j})} \quad (2.7)$$

Where P_{1j} denotes the true habitat potential at location j and P_{2j} denotes the prediction generated from the model at location j. This index is a modified Sorenson similarity index (Sørensen, 1948) used to compare predicted probabilities that each species is present at a given cell rather than relying on presence/absence information (Godsoe 2013). Scores of 1 indicate perfect agreement between the two maps, while an ESP value of 0 indicates complete geographic separation (Godsoe 2013). For all three objectives and their respective performance metrics (Jaccard's similarity, Pearson's correlation coefficient, and ESP), I test for loss in performance due to each type and level of bias intensity, as well as a gain in performance due to the 3 correction methods. I use mixed models to account for random effects among species and denote differences where significant.

RESULTS

Variable Selection

In the absence of sampling bias, the mean Jaccard Index score of the randomly selected 10 virtual species was 0.62 (sd=0.22), with the true set of explanatory variables being selected only 15% of the time. When bias was introduced, reductions in Jaccard

Index scores ranged from -0.06 (environmental) and -0.10 (geographic) for low intensity bias to -0.14 (environmental) and -0.10 (geographic) for the high intensity bias (Table 2.1). This translated to reductions in Jaccard Index scores of up to 22% for the high intensity environmental bias level and resulted in the correct set of explanatory variables being selected only 3% of the time. In general, Maxent models of specialist species did better at identifying the correct variables than generalist species, though effect was only marginally significant ($F_{1,18}$=3.927; p=0.063). Bias correction methods rarely improved the ability to select the correct explanatory variables (Table 2.1), and I found no difference among the three correction methods in their ability to improve Jaccard Index scores ($F_{2,168}$= 0.377, p=0.686). Similarly, I found no relationship between niche breadth and the three methods' ability to improve Jaccard Index scores ($F_{2,166}$= 1.065; p=0.347).

Species-Environment Relationships

On average, the correlation between true and estimated response curves was 0.797 (sd=0.341) when no sampling bias was present, though Pearson's correlation coefficients ranged from -0.974 to 0.999 (Table 2.2). This suggested that when the true explanatory variables are known, Maxent was able to recreate response curves reasonably well (fewer than 10% of response curve correlation coefficients were below 0.5). It was rare for the estimated response curve to be completely wrong (e.g. negative correlation), with correlation coefficients below 0 only occurring 2% of the time. There was no apparent relationship between niche breadth ($F_{1,182}$=1.734; p=0.190) or landscape prevalence ($F_{1,182}$=3.115; p=0.080) with estimated response curves, though the variability of correlation coefficients was greater among species with wide niches.

When bias was introduced, the mean of the correlations between actual and estimated response curves dropped significantly ($F_{3,2630}$=24.478; p<0.001) to 0.760 (sd=0.386), 0.687 (sd=0.452) and 0.633 (sd=0.486) for the Low, Medium and High levels of environmental bias, respectively (Table 2.2). This translated to mean proportional reductions of 10%, 17% and 16% for the Low, Medium and High environmental bias levels, respectively. Geographic bias caused greater overall reductions in correlation coefficients, with 26%, 18% and 36% for the Low, Medium and High levels of bias, respectively (Table 2.2). There was no apparent relationship between losses in correlation coefficients and niche breadth ($F_{1,90}$=1.119; p=0.293); specialist species showed the same reduction in correlation coefficients as generalist species. This pattern held for landscape prevalence as well, with no discernable difference between rare and widespread species ($F_{1,90}$=0.079; p=0.780). In general, bias correction methods did not provide any improvement in estimating response curves ($F_{3,10440}$=0.118; p=0.950), though there was extreme variability in improvement among species with respect to both niche breadth (Figure 2.6A) and prevalence (Figure 2.6B).

Habitat potential Predictions

When using unbiased observation data, ESP scores measuring the similarity between virtual species' true and estimated distributions ranged from 0.177 to 0.756, with a mean of 0.487 (sd=0.128) across all virtual species. Generalist species showed greater agreement between the true and estimated distributions (Figure 2.7A), as did species with high landscape prevalence (Figure 2.7B). When bias was introduced, ESP scores were reduced (less accurate estimation of true habitat potential), with mean scores for the 100 virtual species of 0.461 (sd=0.128), 0.442 (sd=0.125), and 0.397 (sd=0.140), for the Low,

Medium and High bias levels of both types of bias, respectively. Reductions were greatest for the high environmental bias level, equating to an average reduction of 26% in ESP scores across all species (Table 2.3). However, not all species showed reduced ESP scores when bias was introduced; ~20% resulted in higher ESP scores when bias was introduced, and nearly half of these were at the low bias level (shown as a negative loss in Figure 2.8A). Species with an increase in ESP after bias was introduced tended to be very rare, with low landscape prevalence. Only 20% of the instances where biased observation data resulted in improved ESP scores were at the high bias level, suggesting that highly biased observation datasets rarely resulted in improved prediction ability. I found a slight effect of niche breadth ($F_{1,90}$=5.369; p=0.003) on loss of ESP scores, suggesting that specialist species were more susceptible to sampling bias than were the most generalist species in my study area (Figure 2.8B); though this effect was most pronounced in the high bias level. Interesting, I found no effect of landscape prevalence on the loss of ESP scores ($F_{1,90}$=0.086; p=0.770), though rare species showed the greatest variability in loss of ESP scores (Figure 2.8A).

Bias correction methods were usually able to increase prediction ability, though the E-Filter method resulted in lower ESP scores 43% of the time. This loss was nearly equally distributed among the three bias levels, suggesting that the E-Filter correction method was poor at compensating for any level of bias. The environmentally biased datasets saw greater improvement than the geographically biased ones, especially with the FactorBiasOut correction method (Figure 2.9). Overall, FactorBiasOut provided the greatest improvements of the three methods across both types of bias ($F_{2,1560}$=331.856; p<0.001), with an average 11% greater increase in ESP than the other two methods

(Figure 2.9). In addition, FactorBiasOut was able to improve ESP scores in 96% of the cases, whereas the G-Filter and E-Filter only improved ESP scores 82% and 55% of the time, respectively. On average, all three correction methods provided 2% greater improvements with the environmentally biased datasets than with the geographically biased datasets ($F_{1,1377}$=29.269; $p<0.001$); suggesting that while environmental bias caused the greatest reduction in ESP scores, it was also improved the most by correction methods. I found an interaction effect between niche breadth and the bias correction methods ($F_{2,1558}$=83.259; $p<0.001$); specialist species and rare species showed greater improvements with the FactorBiasOut method.

DISCUSSION

I use a simulation study with virtual species to compare three easily implemented sampling bias correction methods that are often used in presence-only SDM but have not been systematically compared. I found that even in the presence of low levels of bias, model performance was degraded, and that correction methods did not improve the ability to correctly identify explanatory variables or recreate species-environment relationships. It seems that identifying true drivers of distributions is difficult, at best. Bias correction methods did, however, improve the accuracy of mapped predictions of habitat potential, which is often the focus of SDM studies. For studies focusing on spatial patterns of habitat potential rather than an understanding of the mechanisms driving those patterns, the FactorBiasOut correction method is well suited. I found that for spatial predictions of habitat potential, FactorBiasOut outperformed the G-Filter and E-Filter bias correction methods across all levels and types of bias. However, when for identifying and understanding drivers of species distributions, SDM with unbiased

presence *and* absence data (Guisan and Zimmermann 2000, Hirzel and Guisan 2002), or mechanistic models incorporating biophysical ecology and functional traits (e.g. Kearney et al. 2010, Higgins et al. 2012), may be better suited.

Estimating Distributions

SDM is most often used for estimating spatial predictions of distributions, and in these cases, the use of bias correction methods is clearly recommended. Previous work has shown contrasting results, however, with some studies suggesting that G-Filter methods may outperform the FactorBiasOut method in some instances (Kramer-Schadt et al. 2013, Fourcade et al. 2014, Stolar and Nielsen 2015), and others showing E-Filter methods as superior to G-Filter methods (Varela et al. 2014). Yet other work suggests that the FactorBiasOut is superior, especially when target group background data are incorporated (Syfert et al. 2013, Fourcade 2016). The target group background approach estimates the biased sampling distribution (σ) from pooled observations of multiple species within a 'target group' of similar taxa whose locality data were collected in the same way as the modelled species, and has shown promise for reducing sampling bias (Phillips and Dudik 2008, Elith et al. 2011, Ranc et al. 2016). The benefit of pooling observations from multiple taxa is increasing the sample size to estimate σ, thereby improving its precision (Phillips and Dudik 2008). However, this method assumes that σ is the same across all species of the target group, which may not be true for many species represented in biodiversity repositories composed of aggregate survey efforts (Ponder et al. 2001, Hortal et al. 2008, Newbold 2010).

My results suggest that the FactorBiasOut method consistently outperformed both of the two filtering methods in their ability to accurately estimate geographic

distributions. While my results may contradict some previous findings, they are not too dissimilar. For example, Kramer-Schadt et al. (2013) found that a G-Filter method resulted in lower omission errors than the FactorBiasOut method, but those differences were within 7%, a margin that was found only in a single, wide ranging species. Similarly, other work has shown considerable variability in the performance of correction methods among differing levels of bias, with the FactorBiasOut method outperforming other methods in a single virtual species, but not two (actual) species (Fourcade et al. 2014). To address this ambiguity, I simulated 100 virtual species with niche characteristics ranging from rare specialists to common generalists and found that the difference among correction methods was independent of niche breadth.

Niche Breadth, landscape prevalence and rarity

In the absence of sampling bias, my results confirm the previously well-established relationship between sample size, and therefore landscape prevalence, with the ability to estimate true distributions (e.g. Hernandez et al. 2006, Wisz et al. 2008, van Proosdij et al. 2015). However, the relationship between niche breadth and sampling bias is not well understood. Previous work has suggested that occupied niches may be more difficult to distinguish from background environmental space in generalists with broad tolerances than for specialists (Brotons et al. 2004, Elith et al. 2006, Franklin et al. 2009); on the other hand, recent work has shown that specialist species are more susceptible to sampling noise and may require larger sample sizes to quantify their distributions (Soultan and Safi 2017). If distributions of specialists are in fact more easily estimated than generalists, this would suggest that specialists may be *less* susceptible to biased sampling than generalists because their smaller niches are likely to be sampled more

completely than larger ones. However, in previous studies, niche breadth is often conflated with landscape prevalence (or rarity), assuming that generalists with wide niches are less rare than specialists.

Species with wide niches may in fact also be rare if the areas they occupy are similar to the conditions throughout the study area with respect to all but a single environmental variable. This can result in wide niche breadths, but low landscape prevalence. I found evidence that specialists with narrow niches are more susceptible to high intensities of biased sampling than generalists, but this effect was weak, at best. There was no effect of landscape prevalence on susceptibility to sampling bias, and no interaction between landscape prevalence and niche breadth, suggesting that any susceptibility to sampling bias was due to niche breadth alone, not rarity. My results suggest that niche breadth is therefore more important than landscape prevalence, except in cases of extreme rarity: biased sampling actually improved predictions of habitat potential in a few, very rare, species. By design, my study sampled each species proportional to landscape prevalence, resulting in small sample sizes for rare species. However, this may not represent reality for rare species that are well-studied and heavily sampled; in these cases, rare species may be more easily modelled than generalists, as previously suggested.

Contrast of methods

Of the three bias correction methods compared here, the FactorBiasOut and G-Filter methods are used most often. These methods are rather straight forward to implement, though each require tuning with parameters and little guidance is provided in the literature. The FactorBiasOut method implemented in Maxent requires a bias grid

representing hypothesized sampling intensity across the study area. Where documented, these grids are often created as Gaussian kernel densities of observations as recommended by Elith et al. (2010), though the choice of standard deviation (SD) for the kernel is not often reported. This choice influences the distance at which adjacent cells affect estimated densities, wherein a small SD equates to a local influence among neighboring cells. The consequences of different choices of SD are not well understood. Elith et al. (2010) suggest SD might reflect some property of a species' dispersal ability to capture the possibility of animal movement between surveys. However, the haphazard nature of opportunistic sampling inherent in museum databases likely confounds the interpretation of SD, and therefore I chose a cross-validation approach based on the spatial pattern of observations to estimate an optimal value for SD. This method minimizes the mean squared error in the Gaussian kernel density field at multiple SD values and identifies an optimum value for a given observation data set (Diggle et al. 1998). The tradeoffs and implications of using statistical measures over biological knowledge are not well understood; additional work is needed to provide guidelines for selecting SD and developing bias grids.

The G-Filter method also relies on selecting a spatial parameter, namely the bandwidth used, to identify areas with high observation densities. Previous studies have filtered observations based on nearest neighbor distances, such as removing observations that are within a certain distance of one another (e.g. Dormann 2007, Veloz 2009, Anderson and Raza 2010, Kramer-Schadt et al. 2013, Boria et al. 2014, Aiello-Lammens et al. 2015), while others use spatial grids to filter observations from cells with high densities (Vandergast et al. 2013, Inman et al. 2014, Varela et al. 2014). The decision for

the bandwidth size is rarely discussed, though Veloz et al. (2009) use a novel method of exploring spatial autocorrelation in model residuals to determine an optimal value. My selection of bandwidth and choice of filtering methods were based on previous work to reduce sampling bias in aggregated observations for the southwestern USA (Vandergast et al. 2013, Inman et al. 2014). As with the FactorBiasOut method, additional research is needed to explore differences among alternative implementations of the G-Filter method.

In contrast to the G-Filter method, the E-Filter method is less well represented in the literature. This is likely because it is more tedious to implement and is dependent on the set of explanatory variables included in any given model. Whereas thinning using G-Filter occurs entirely in geographic space and results in a single dataset that can be used to calibrate multiple model specifications, the E-Filter method results in a separate calibration dataset for each model specification. This precludes any multi-model inference or complexity metrics, such as Akaike Information Criterion (AIC) or Bayesian Information Criterion (BIC). Model complexity is not often discussed, but has been shown to be an important factor affecting predictions across geographic regions and time periods (Warren and Seifert 2011, Syfert et al. 2013, Merow et al. 2014, Bell and Schlaepfer 2016). Virtual species with wide niches were often characterized with few explanatory variables, but I found no differences between the three bias correction methods in their ability to accurately identify those variables; possibly because I was unable to use multi-model inference or complexity metrics with the E-Filter method.

I chose to implement the E-Filter method with a partitioning around medoids clustering algorithm because it can be optimized for large datasets (Kaufman and Rousseeuw 2008) and because multiple environmental explanatory variables can be

incorporated; previous implementations have used only two (Varela et al. 2014). The use of a clustering algorithm instead of visually assessing 2-dimensional clusters enables the identification of an optimum number of clusters or regions in environmental space that can be thinned to achieve uniform sampling intensity. As implemented here, the E-Filter method resulted in the greatest reduction of sample sizes with an average loss of 32% of the total observations records per dataset. Because sample size is such a critical aspect to model calibration and fit, it is no wonder that the E-Filter method often performed poorly. In contrast, the G-Filter resulted in an average loss of only 9% of observations, thereby resulting in higher sample sizes more of the time. However, not all biased datasets resulted in larger G-Filter than E-Filter calibration datasets; the medium and high biased datasets resulted in E-Filter calibration datasets that were larger than G-Filter calibration datasets 12% of the time. The E-Filter method is therefore highly dependent on the explanatory variables considered and can outperform the G-Filter method in certain instances – but more often I found little improvement with the E-Filter method.

Bias correction in practice

Overall, this research suggests that bias correction improves spatial predictions of habitat potential across a wide range of bias intensity, but thus far, these levels of bias are not tied to observational data. Here I frame my results by comparing the geographic Low, Medium, High, and No Bias levels to bias found for nine species occurring in the southwestern continental USA. These species represent a diverse group of flora and fauna, including squamata, aves, rodentia, asterales, and zygophyllales. Locality records were downloaded from the Global Biodiversity Information Facility (GBIF; www.gbif.org) with the package *rgbif* (Chamberlain 2016) in R 3.3.2 (R Core Team

2016) and are provided in Appendix 2.3. I assessed each observation dataset for geographic sampling bias using the same Ripley's K function for inhomogeneous point processes (Baddeley et al. 2000) used with my virtual species. I did not assess these datasets for environmental bias, as this type of bias is dependent on the hypothesized environmental explanatory variables considered during SDM and can only be assessed after explanatory variables have been identified. Most of the GBIF observational datasets produced Ripley's K function scores indicative of Low or Medium geographic bias levels defined in this study, but two species, *Chionactis occipitalis*, and *Perognathus longimembris*, yielded geographic bias equivalent to my most extreme biased observation datasets (Figure 2.10). Both of these species are well studied and are represented with sample sizes over 1500; I suspect each suffer from extreme study bias wherein observations are locally dense at trap sites or along roads. At these extreme levels of bias, I suggest practitioners be wary of using model fit to identify explanatory variables or infer ecological meaning from species-environment relationships when using SDM in PB frameworks. Moreover, I suggest that further work is needed to quantify bias and assess trends across multiple taxa.

TABLES

Table 2.1. Agreement scores for best models. Mean and standard deviation (SD) Jaccard Index agreement scores for the best models selected by area under the curve (AUC) for 10 virtual species with and without sampling bias. Jaccard Index agreement scores measure the proportion of the true explanatory variables identified by the model with the highest AUC score. Agreement scores without bias (Original) and change (Change), after bias was introduced, or correction methods were applied.

		High Bias				Medium Bias				Low Bias				No Bias	
Bias Type	**Correction Method**	**Original**		**Change**		**Original**		**Change**		**Original**		**Change**		**Original**	
Environmental	None	0.48	(0.19)	-0.14	(0.19)	0.48	(0.17)	-0.14	(0.16)	0.56	(0.23)	-0.06	(0.13)		
	FactorBiasOut			-0.00	(0.09)			-0.04	(0.08)			-0.00	(0.09)		
	G-Filter			-0.00	(0.00)			-0.00	(0.00)			-0.00	(0.00)		
	E-Filter			-0.00	(0.09)			0.02	(0.06)			0.03	(0.07)		
Geographic	None	0.52	(0.22)	-0.10	(0.22)	0.54	(0.21)	-0.08	(0.22)	0.52	(0.19)	-0.10	(0.25)		
	FactorBiasOut			0.04	(0.08)			-0.06	(0.19)			0.04	(0.08)		
	G-Filter			-0.00	(0.09)			-0.04	(0.08)			-0.00	(0.00)		
	E-Filter			-0.05	(0.11)			0.04	(0.08)			-0.00	(0.00)		
No Bias	None													0.62	(0.22)

Table 2.2. Pearson's correlation coefficients for best models. Mean and standard deviation (SD) Pearson's correlation coefficients for models with the true explanatory variables for 100 virtual species with and without sampling bias. Collinearity between the true and estimated response curves assesses the ability to represent mechanistic determinants of species distributions when the true explanatory variables are known. Collinearity scores without bias (Original) and change (Change), after bias was introduced, or correction methods were applied.

		High Bias				Medium Bias				Low Bias				No Bias	
Bias Type	**Correction Method**	**Original**		**% Change**		**Original**		**% Change**		**Original**		**% Change**		**Original**	
Environmental	None	0.633	(0.476)	-16.110	(153.104)	0.687	(0.452)	-16.610	(150.876)	0.760	(0.386)	-10.379	(168.960)		
	FactorBiasOut			-13.969	(87.339)			117.317	(914.175)			-24.472	(221.228)		
	G-Filter			-9.509	(115.195)			-8.735	(59.212)			3.540	(23.933)		
	E-Filter			-6.124	(67.598)			-127.698	(1193.770)			-3.918	(142.925)		
Geographic	None	0.591	0.486	-36.218	(54.881)	0.687	0.447	-18.016	(82.597)	0.674	0.454	-25.799	(67.176)		
	FactorBiasOut			23.985	(333.284)			-11.048	(82.558)			-5.512	(73.364)		
	G-Filter			-5.293	(45.029)			-6.298	(26.030)			4.816	(44.772)		
	E-Filter			4.967	(125.325)			-6.060	(27.372)			14.054	(157.511)		
No Bias	None													0.979	(0.341)

Table 2.3. Expected fraction of Shared Presences for best models. Mean and standard deviation (SD) Expected fraction of Shared Presences (ESP) for models with the true explanatory variables for 100 virtual species with and without environmental (ENV) and geographic (GEO) sampling bias. ESP without bias (Original) and change (Change), after bias was introduced, or correction methods were applied.

		High Bias				Medium Bias				Low Bias				No Bias	
Bias Type	**Correction Method**	**Original**		**% Change**		**Original**		**% Change**		**Original**		**% Change**		**Original**	
ENV	None	0.361	0.149	25.648	(24.514)	0.432	(0.123)	10.047	(18.648)	0.466	0.128	4.073	(14.855)		
	FactorBiasOut			21.668	(14.619)			15.126	(13.721)			9.722	(9.763)		
	G-Filter			5.210	(7.025)			2.631	(3.970)			1.087	(2.097)		
	E-Filter			4.732	(13.727)			1.998	(8.207)			0.443	(7.528)		
GEO	None	0.432	0.122	11.787	(15.869)	0.451	(0.126)	7.797	(13.981)	0.457	0.127	6.827	(16.439)		
	FactorBiasOut			11.310	(7.569)			11.843	(8.938)			10.798	(9.795)		
	G-Filter			2.693	(2.602)			1.393	(1.818)			0.885	(1.560)		
	E-Filter			0.510	(8.653)			2.024	(7.702)			3.143	(8.921)		
No Bias	None													0.487	(0.128)

FIGURES

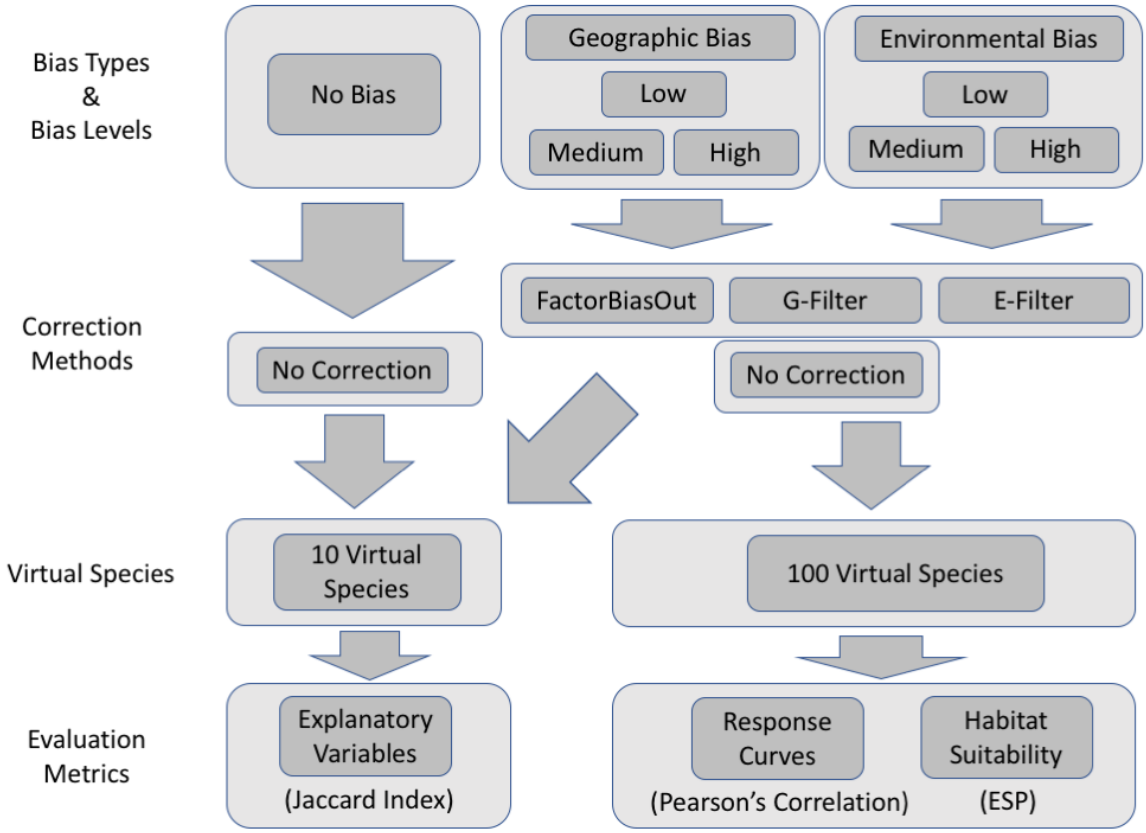

Figure 2.1. Methodology Flow Diagram. For the three types of bias (None, Geographic and Environmental), we assessed three bias correction methods (FactorBiasOut, G-Filter and E-Filter) along with no bias correction in 100 virtual species to assess response curves and habitat potential. We also used 10 virtual species to assess the identification of explanatory variables.

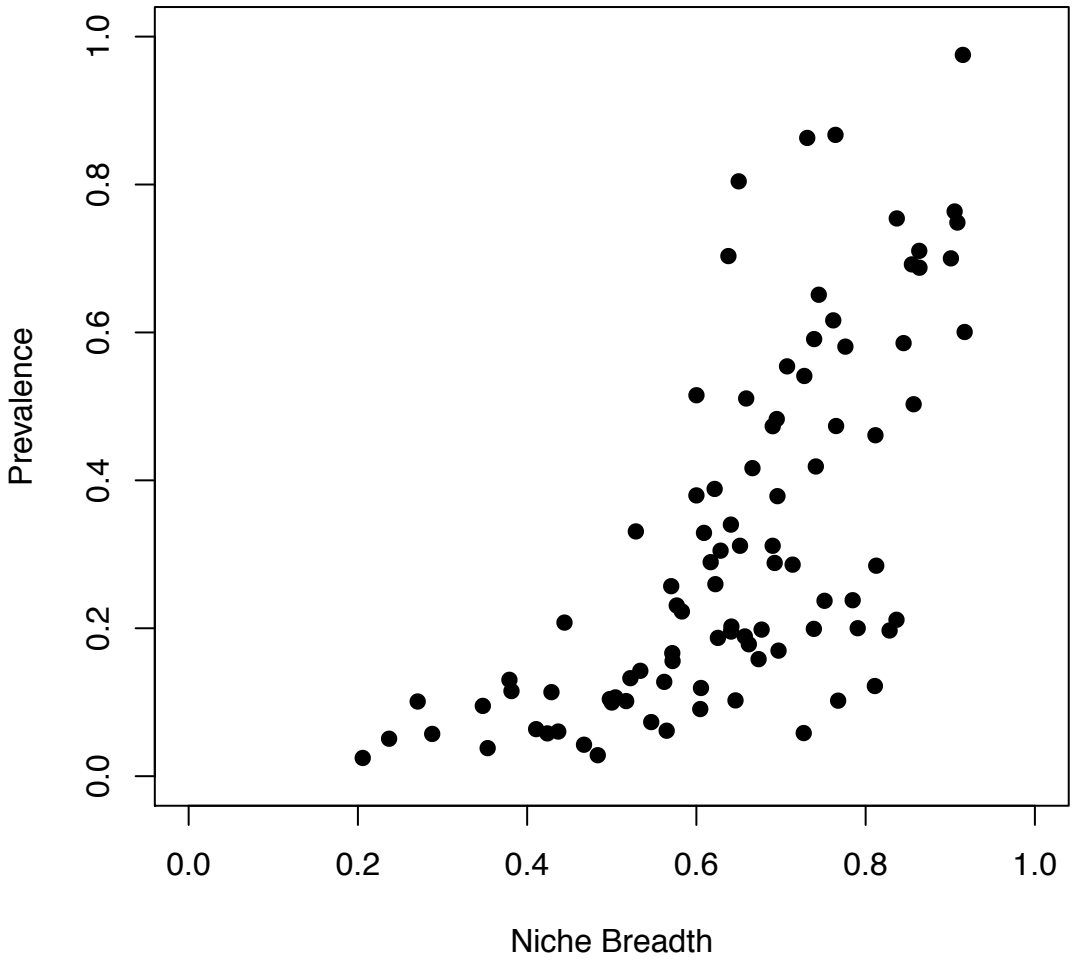

Figure 2.2. Prevalence and Niche Breadth in Virtual Species. Species with low landscape prevalence (y-axis; proportion of study area occupied by species) had narrow niche breadths (x-axis; uniqueness of occupied habitat). However, species with wide niches (low uniqueness of occupied habitat) were not necessarily widely present across the landscape.

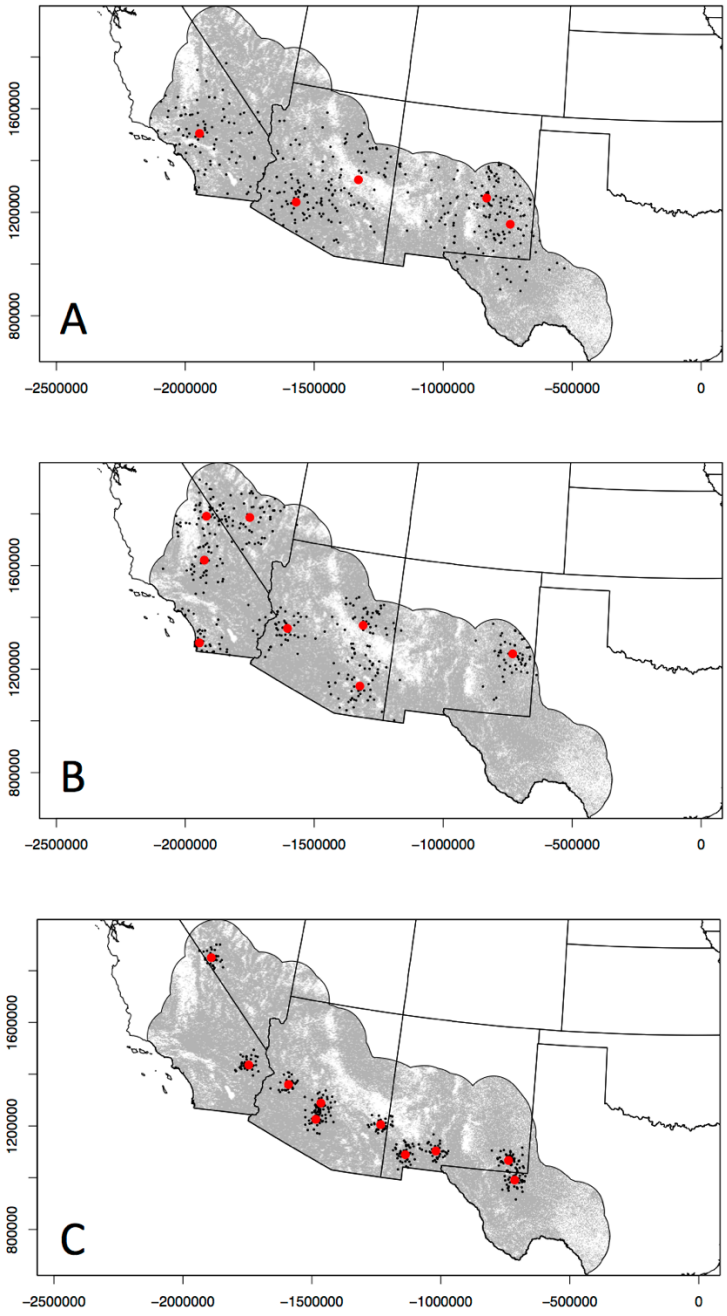

Figure 2.3. Generating Geographic Sampling Bias. Biased observation datasets were created by randomly selecting occupied cells according to their inclusion weights. Inclusion weights for the geographically biased observation datasets were calculated using a spatially clustered sampling schema by randomly seeding 5, 8, or 10 cluster centers (red) for the Low, Medium and High intensities of bias, respectively.

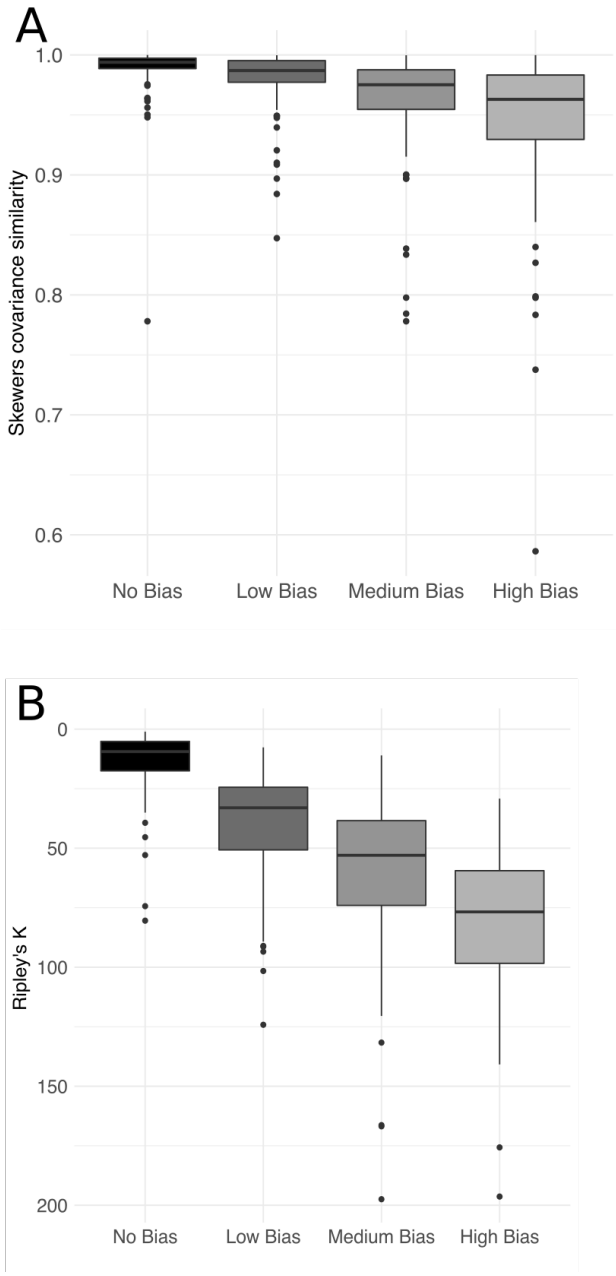

Figure 2.4. Measured Sampling Bias in Observation Datasets. Environmental sampling bias was measured with Skewer's covariance similarity index (A). Observation datasets with No Bias had the highest similarity scores, and each class was significantly different from one another. Geographic sampling bias was measured as the mean difference between t theoretical K(r) and border-corrected K(r) Ripley's K density function for inhomogeneous point processes of the spatial point pattern for each biased dataset out to a maximum distance of 350 km.

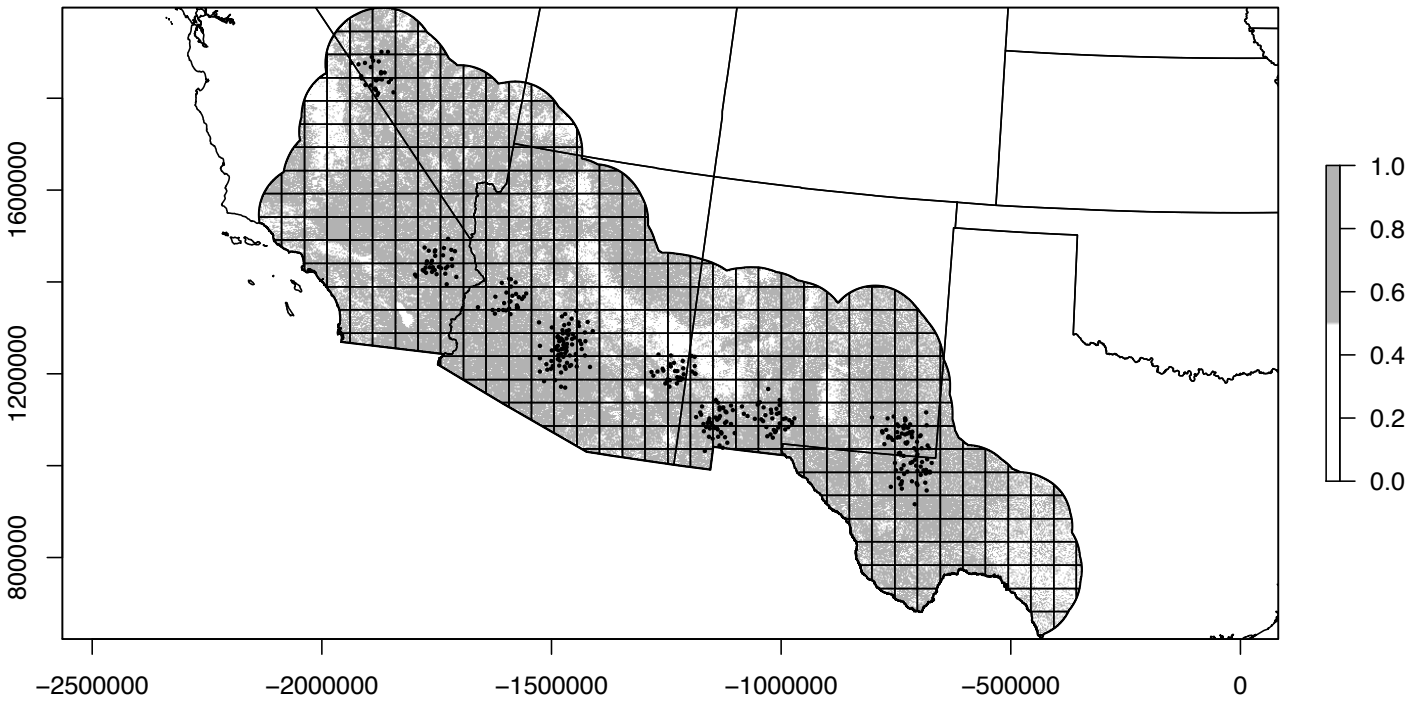

Figure 2.5 Geographic Sampling Mesh. The geographic filtering (G-Filter) method of bias correction used a sampling mesh with equally sized rectangular cells, each 225 km^2 in area, resulting in 4119 unique sampling areas throughout the study area. Occupied habitat (grey) and unoccupied non-habitat (white) are shown for an example simulated species. Bias observations (black) are concentrated around 8 sampling clusters, but are thinned to 2 observations per 225 km^2 cell with the G-Filter method.

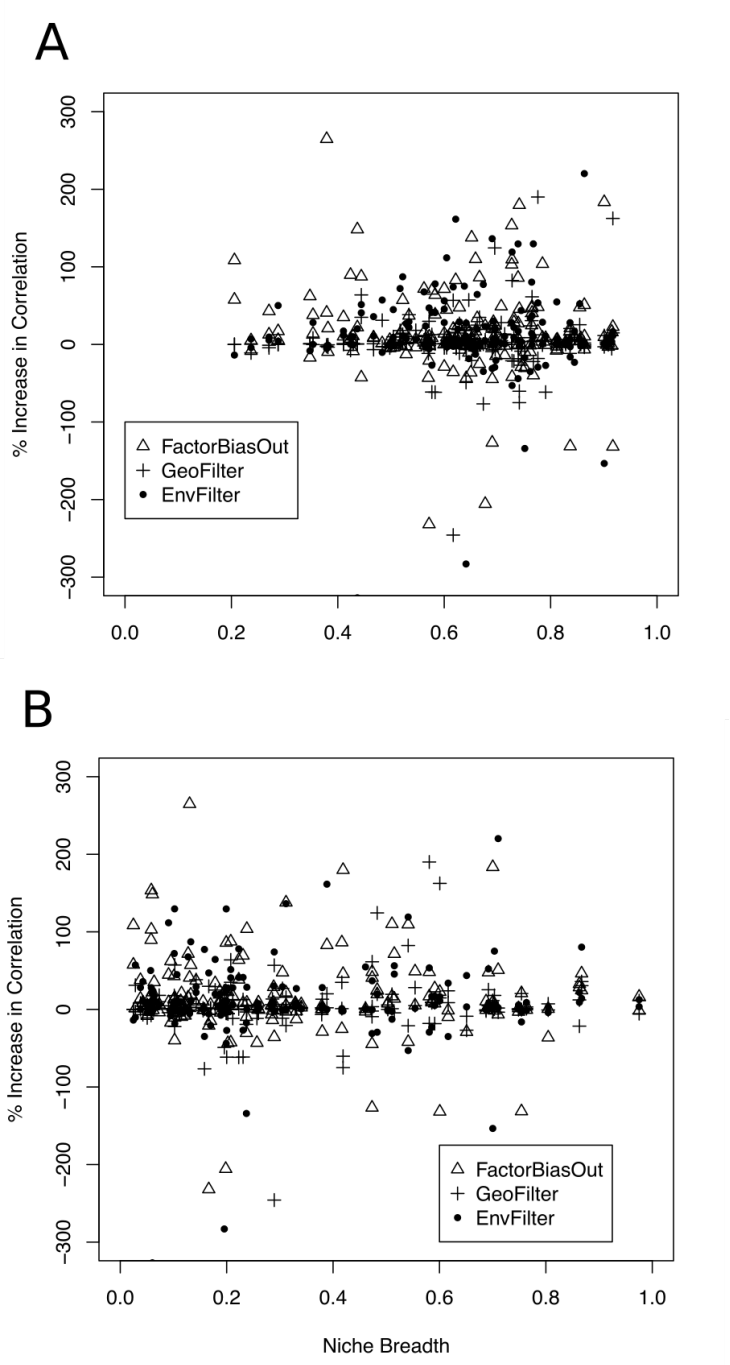

Figure 2.6. Improvement in Predicting Response Curves. In general, bias correction methods did not provide any improvement in estimating response curves though there was extreme variability among species in improvement with respect to both niche breadth (A) and prevalence (B).

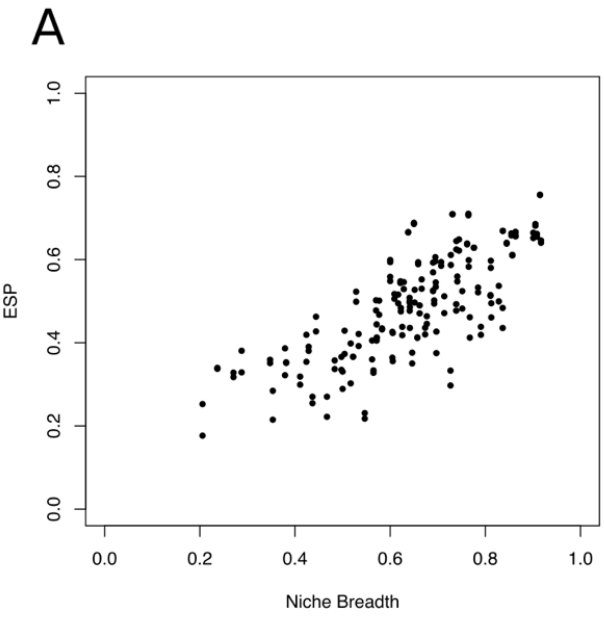

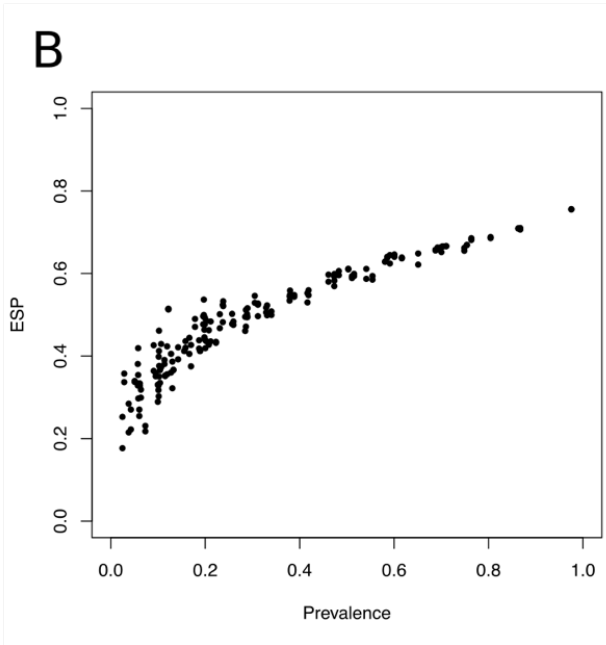

Figure 2.7. Species Traits and Predicting Habitat Potential. Generalist species showed greater agreement between the true and estimated distributions (A), as did species with high landscape prevalence (B). Spatial agreement between predictions of habitat potential were made with Expected fraction of Shared Presences (ESP). Scores of 1 indicate perfect agreement between the two habitat potential maps, while an ESP value of 0 indicates complete geographic separation. In absence of bias, generalists and those that were widely distributed showed higher predictive power.

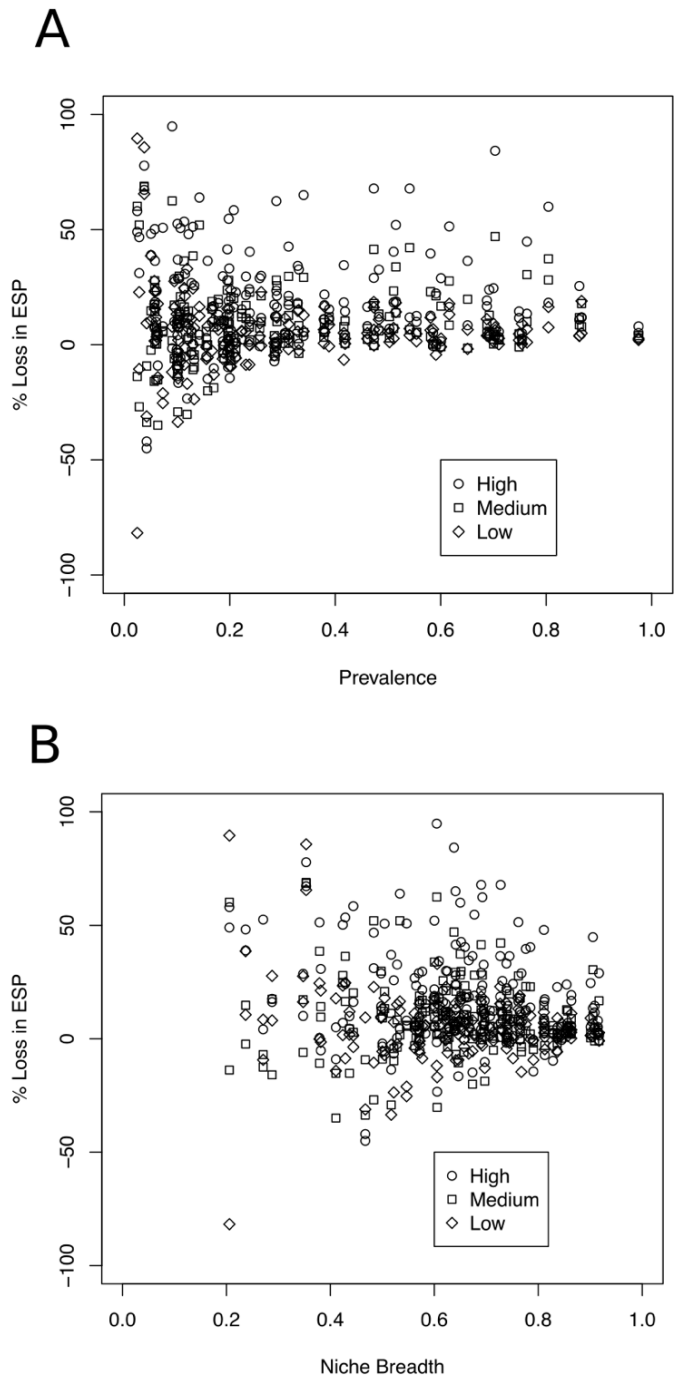

Figure 2.8. Reduction in Predicting Habitat Potential. The majority of habitat potential predictions were worsened when bias was introduced, though some with low landscape prevalence were improved (shown as a negative loss A). There was a slight effect of niche breadth on loss of ESP scores, suggesting that specialist species were more susceptible to sampling bias than were the most generalist species in our study area (B), though this effect was most pronounced in the high bias level.

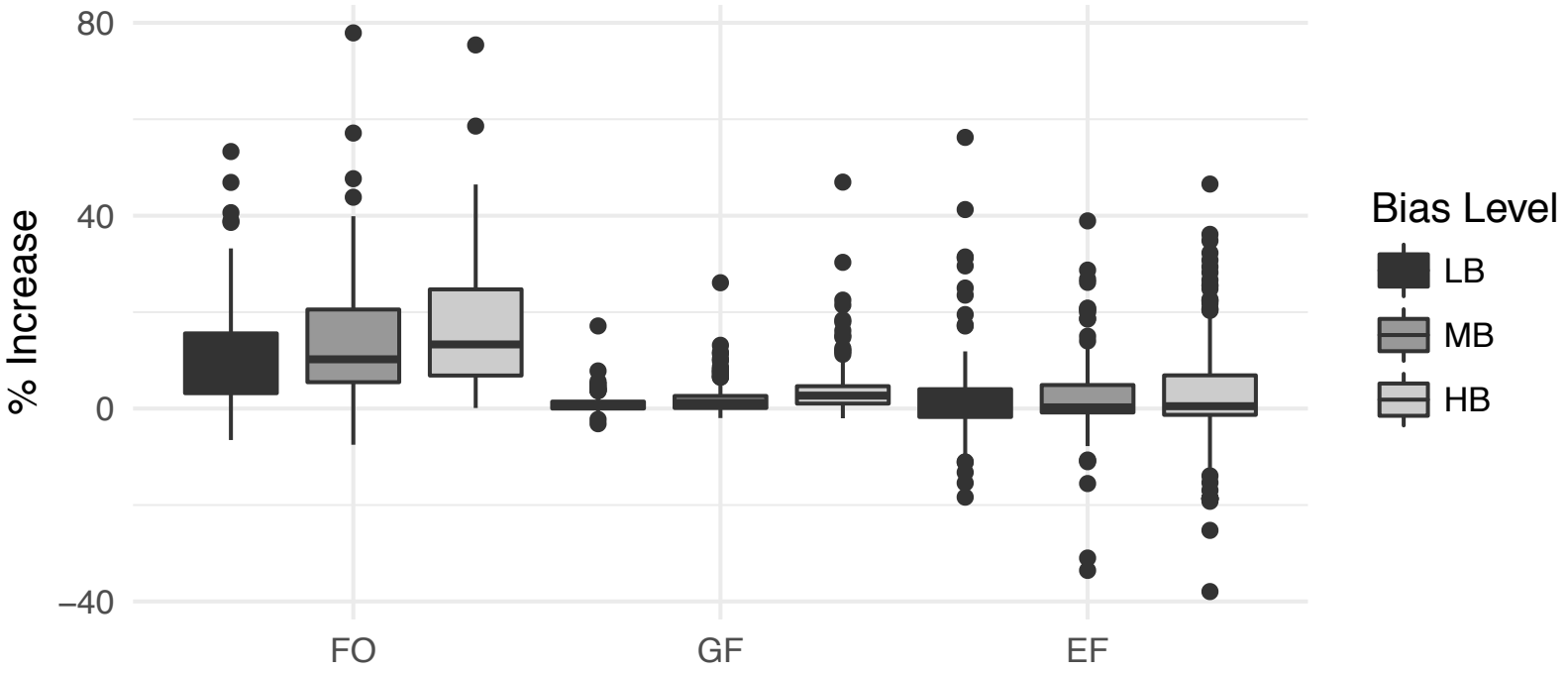

Figure 2.9. Improvement in Predicting Habitat Potential. All three correction methods were able to increase prediction ability in most species, though the FactorBiasOut correction method showed the greatest improvement across the board with an average 11% greater increase in ESP than the other two methods. The E-Filter method resulted in lower of ESP scores 43% of the time.

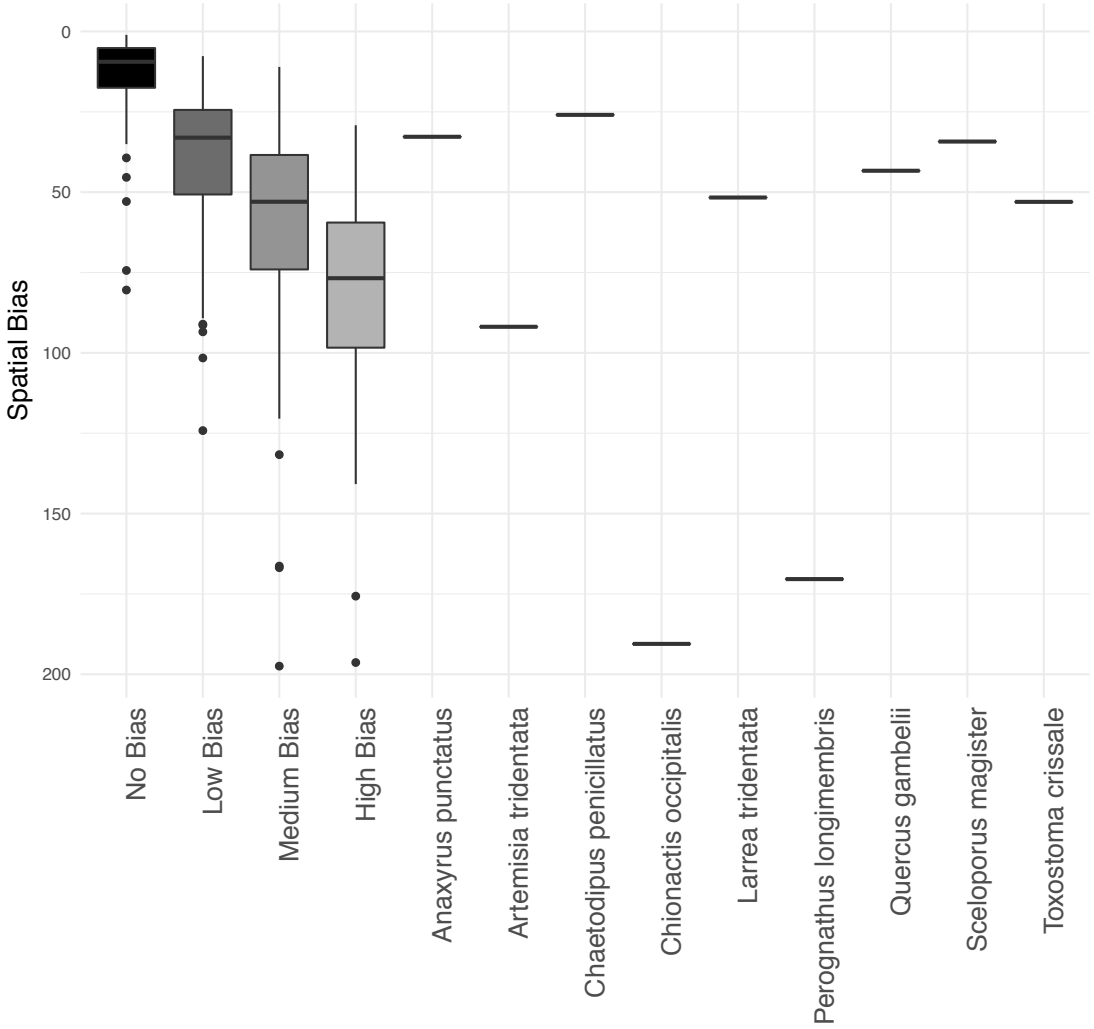

Figure 2.10. Geographic Sampling Bias in Selected Species. Geographic sampling bias in 9 observation datasets obtained from the Global Biodiversity Information Facility give context to the No, Low, Medium and High Bias observation datasets used for all virtual species. Geographic sampling bias was measured as the mean difference between t theoretical K(r) and border-corrected K(r) Ripley's K density function for inhomogeneous point processes of the spatial point pattern for each biased dataset out to a maximum distance of 350 km.

CHAPTER 3

SPATIAL SAMPLING BIAS IN NEOTOMA MIDDEN ARCHIVES AFFECTS SPECIES PALEO-DISTRIBUTION MODELS

ABSTRACT

Aim: Quantification of the spatial sampling bias in a North American packrat midden archive and its impact on species distribution modeling (SDM) of plant paleo-distributions. I test whether (1) spatial sampling bias inherent in this plant macrofossil record can influence estimates of paleo-distributions, (2) any bias can alter the ability to measure shifts in distributions and climatic niche breadth from the early/mid Holocene (11.5 ka – 5 ka) to present day (1950 – present), and (3) bias correction methods can improve paleo-distribution models and analyses of range shifts and niche breadth.

Location: Western North America

Methods: I estimate spatial sampling bias in a packrat midden archive for the early/mid Holocene period with a three-stage statistical model, each representing a hypothesized source of bias: fossil site availability, preservation and accessibility. This approach enables us to use SDM to evaluate three separate paleo-distributions calibrated on the packrat midden archive: those without bias correction (σ-naïve), those created with a standard method (σ-standard), and those created with a novel alternative (σ-modeled) incorporating the three-stage model of bias. I compare these paleo-distributions to a set of 'true' paleo-distributions created by hindcasting present-day models of 6 species well represented in the packrat midden archive, and to independent locations identified in pollen records from lake sediment cores. I measure niche breadth using a generalized dissimilarity matrix of Mahalanobis distance.

Results: I find that paleo-distributions modelled for the early/mid Holocene without bias correction (σ-naïve) provided poor estimates of hindcast paleo-distributions, and that the σ-modeled correction method improved paleo-distributions for my six species with, on average, 91% higher overlap to hindcast distributions than σ-naïve paleo-distributions (σ-standard results fell between σ-naïve and σ-modeled). These improvements were confirmed at independent locations from lake sediment pollen records.

Main Conclusions: I suggest that this approach can be applied to finer time slices using the Neotoma record, and more generally, can be adapted for other paleoecological archives as a framework for estimating spatial sampling bias.

INTRODUCTION

A core focus of biogeography rests in understanding the determinants of species distributions and the processes by which they change. Towards that goal, rapid development of ecological archives and analytical tools over the past 20 years has enable investigations of broad macro-ecological, evolutionary and conservation questions about the mechanisms and forces altering patterns of biodiversity throughout the history of our planet (Swetnam and Allen 1999, Brewer et al. 2012). A dominant methodological tool in biogeographic studies is species distribution modeling (SDM), a quantitative modeling approach that relates environmental conditions at locations where a species has been observed to locations where it has not (Franklin 2010a). However, confirming locations where organisms are absent is far more difficult than identifying where they are present (MacKenzie et al. 2002, Brotons et al. 2004, MacKenzie 2005); as a result, presence-background (PB) modeling methods that compare environmental conditions of the entire

study area (background) to locations where a species has been observed have been developed. These methods do not rely on knowledge of species absence, and as such, software for PB methods (e.g. Phillips et al. 2006) have become primary tools for paleobiogeography research in recent years (Moreno-Amat et al. 2017).

The ability to infer paleo-distributions with limited knowledge of absence has propelled SDM's use as an analytical method for addressing paleobiogeographic questions of niche stability (e.g. Stigall 2012), range dynamics (e.g. Nogués-Bravo et al. 2008), speciation (e.g. Peterson and Nyári 2008), and extinction (e.g. Lorenzen et al. 2011), among many others. When used to investigate paleo-distributions, SDM offers two analytical opportunities to use paleoecological archives: 1) validation of models calibrated on extant species that have been 'hindcast' to past environmental conditions, and 2) direct calibration with past environmental conditions. The former has been used most often, driven by the wealth of spatially explicit ecological archives available for extent species (Moreno-Amat et al. 2017). In this approach, models are developed using modern observations of species and their environment and are applied to environmental data representing paleoclimatic conditions to create spatial predictions of biotic distributions for the historic period of interest. Paleoecological archives are then used to quantitatively assess the accuracy of these hindcast projections (e.g. Martinez-Meyer et al. 2004, Franklin et al. 2015) or to qualitatively evaluate the congruence between hindcast projections and fossil localities (e.g. Carnaval and Moritz 2008). I refer to these predictions of paleo-distributions as 'hindcast' distributions. In paleo-SDM, paleoecological archives are used directly for calibrating models under past environmental conditions. Rather than using species-environment parameters from

modern distributions to hindcast, paleo-SDM estimates species-environment parameters directly from locations obtained from paleoecological archives and reconstructions of environmental conditions. Paleo-SDM is likely used less often because paleo-distribution data are usually sparse in time and space and can be poorly resolved chronologically and taxonomically (Moreno-Amat et al. 2017). However, paleo-SDM allows a key assumption of hindcasting to be relaxed, namely, the requisite of niche conservation through time. Under niche conservation, species-environment model parameters are maintained through time, even with environmental change (Wiens and Graham 2005); this is a key assumption of hindcasting. In hindcasting, one might expect to see a species track preferred habitats and exhibit geographic shifts instead of niche changes (Nogués-Bravo 2009).

Paleo-SDM, directly calibrating on fossil archives, can estimate new species-environment parameters for different chronological sequences. Each different set of species-environment model parameters may provide evidence of a changed niche, and in conjunction with spatial predictions of habitat potential, can be compared across different time slices to evaluate change in habitat. Often, these studies primarily rely on the spatial predictions of habitat potential because many clear metrics exist for evaluating overlap in spatial distributions such as the Sorenson's similarity index (Sørensen 1948), Schoener's D (Schoener 1968) or Godsoe's ESP (Godsoe 2013). These metrics, among others, allow for simple comparisons of spatial predictions rather than complex assessments of niche complexity, dimensionality, or breadth. And when coupled with hindcasting, direct tests of niche conservation can be made between distributions derived from hindcasting (or projections forward) and those from paleo-SDM (e.g. Walls and Stigall 2011). These

coupled approaches have been used often, contributing evidence that niches evolve slowly (e.g. Peterson et al. 1999, Peterson 2011, Malizia and Stigall 2011, Stigall 2012, 2014). In the vast majority of studies, reliance on paleoecological archives for paleo-SDM equates to using small sample sizes, which can be biased in space and time (Varela et al. 2011). If adequate paleo-distribution and paleoenvironmental data were available in time and space, it would be preferable to develop paleo-distribution models using contemporaneous observations rather than hindcasting, and with expanding paleoecological databases this may be possible (e.g. Blois et al. 2013). However, because paleo-SDM often necessitates a PB framework, the issue of small sample sizes and sampling bias needs to be addressed.

Explored extensively since the 1970's, sampling bias in terrestrial and marine paleoecological archives can be introduced due to 1) substrate exposure (erosion processes), 2) substrate material type, and 3) substrate volume; each represented by the age of the substrate (e.g. Raup 1972, Signor 1982, Varela et al. 2011). In general, areas with more recent deposits will have greater prevalence of fossils due to the larger volume of sedimentary material, and because more recent deposits are often less eroded (Raup 1972). The biases introduced to paleoecological archives span taxonomic, temporal and spatial bias, and may hinder a model's ability to accurately represent historic distributions. Taxonomic bias affects estimated changes in biodiversity and occurs when certain species are preserved better than others in the fossil record (Allison and Bottjer 2010). The fossil pollen record suffers from taxonomic bias resulting from differences among species in pollen production and dispersal levels, as well as differences in deposition and preservation (Birks and Birks 2000, Goring et al. 2013). Temporal bias is

most evident when evaluating chronosequences through deep time, and results in some time periods being better represented than others due to differential fossilization through time (Allison and Bottjer 2010). Spatial bias is very common in the fossil record (Varela et al. 2011), though frequently unquantified or unaccounted for in analyses of Phanerozoic biodiversity (Vilhena and Smith 2013, Moreno-Amat et al. 2017).

Spatial bias is problematic for PB SDM because these methods assume that any sampling bias is proportional to the background distribution of environmental covariates (Araújo and Guisan 2006), and that a species' niche is sampled over the full range of environmental conditions in which they occur (Phillips et al. 2009). These assumptions are not often met with paleoecological archives due to spatial variation of taphonomic conditions in different deposits (Allison and Bottjer 2010, Varela et al. 2011, Vilhena and Smith 2013, Moreno-Amat et al. 2017), and results in spatial bias where more fossils are found in certain areas due not to a greater prevalence of an organism, but instead to a lack of fossils in other areas. Spatial bias in biodiversity data for extant species is often addressed with one or more bias correction methods that have been developed for PB frameworks. These methods stem from careful filtering of observation data (Varela et al. 2014, Boria et al. 2014) or from estimating the biased sampling distribution (σ) and manipulating background selection weights to result in proportional background samples (Phillips et al. 2009). In order be effective, these bias correction methods require large sample sizes. Paleoecological archives, however, rarely offer large samples (Svenning et al. 2011, Moreno-Amat et al. 2017), and the ability to estimate σ from them is not often tested. An alternative method to estimate σ that does not rely on large sample sizes usually unavailable in paleoecological archives may improve estimates of paleo-

distributions, thereby allowing analyses of range shifts and niche characteristics through time.

Here I explore potential effects of sampling bias on paleo-SDM and investigate an alternative for estimating σ with a focal group of extant plant species. Specifically, I test whether (1) spatial sampling bias inherent in a commonly used paleoecological archive, the North American Neotoma packrat plant macrofossil record (Strickland et al. 2013, Williams et al. 2018), can influence estimates of paleo-distributions, (2) this bias can alter our ability to measure shifts in distributions and niche breadth from the early/mid Holocene (11.5 ka – 5 ka) to present day (1950 – present), and (3) bias correction methods can improve paleo-distributions and analyses of range shifts and niche breadth. I do this by comparing paleo-distributions created by hindcasting present-day models to three separate paleo-SDMs calibrated on the fossil record: those without bias correction (σ-naïve), those created with a standard method (σ-standard), and those created with a novel alternative (σ-modeled). Using hindcast distributions for paleo-SDM evaluation assumes that the hindcast distribution is valid, and so to independently verify the paleo-SDM distributions I also used pollen records from lake sediment cores from the western USA not used in the modeling. I aim to identify an effective method for reducing sampling bias in paleo-SDM and to highlight how bias may affect analyses of range shifts and niche breadth.

METHODS

Study Area and Environmental Gradients

My study region covered 3,171,335 km^2 of the western USA (Figure 3.1) encompassing the locations of packrat middens represented in the Neotoma database. I

assembled raster data describing 11 climatic and physiographic environmental conditions to characterize present-day (1950 – 2000 yr) and early/mid Holocene (11.5 ka – 5 ka) time periods and generalized each at a spatial scale of 1 km (Appendix 3.1). I assumed that most changes between the two periods were limited to climatic variables, and that any changes in surface physiographic conditions due to Holocene erosion or deposition were minimal and within 2x the maximum vertical error of the terrain elevation data; 10 m (Danielson and Gesch 2011).

Species Distribution Modeling

I developed present-day and paleo-distributions for 6 extant species well represented in the North American Packrat midden archive that occur in a range of habitat types, including two small perennial shrubs inhabiting cold desert habitats (*Artemisia tridentata*, *Coleogyne ramosissima*), a small deciduous tree inhabiting foothills and low mountain elevations (*Quercus gambelli*), a small conifer tree confined to northern latitudes (*Juniperus communis*), and two large conifers occurring in high elevation mountain habitat (*Abies concolor*, *Pinus ponderosa*). The Neotoma database has been used extensively since the 1960's to assess regional vegetation community shifts (e.g. Phillips et al. 1974, Cole and Webb 1985, Spaulding 1990, McAuliffe and Van Devender 1998, Thompson and Anderson 2000, Jackson et al. 2005) paleoclimate (e.g. Jacobson 1991, Arundel 2002, Coats et al. 2008, Thompson et al. 2012) and faunal community composition (e.g. Van Devender et al. 1977, Van Devender and Mead 1978, Mead 1981) during the late Pleistocene and throughout the Holocene. More recently, packrat midden archives have been used to estimate spatially explicit paleo-distributions for some species (e.g. Angulo et al. 2017), though few studies have used paleo-SDM

methods. The paucity of studies using paleo-SDM is likely due to the spatial bias inherent in the packrat midden archive (Webb and Betancourt 1990). I develop a novel approach to estimate and correct for this bias (σ) so that paleo-SDM may be used to create spatially explicit paleo-distributions from the packrat midden database.

I obtained macrofossil observations from the USGS/NOAA North American Packrat Midden database (Strickland et al. 2013) for the early/mid Holocene period based on radiocarbon ages and used them to create paleo-distributions with each of the three paleo-SDM methods. A species was considered present at the reported midden location if any of the ^{14}C ages associated with that species were dated to the early/mid Holocene, resulting in sample sizes ranging from 21 – 129 (Table 3.1). Extant locations from 1950 to present-day for the 6 species were obtained from the Geographic Biodiversity Information Facility (www.GBIF.org) in October, 2017 (Appendix 3.2).

Present-day Distributions

I used MaxEnt version 3.4.0 (Phillips et al. 2006), a widely-used PB SDM, to create distribution models for present-day conditions. For each species, I created a model with all 11 environmental explanatory variables and sequentially removed those contributing the least to model fit using a step-wise jackknife test of training gain (Phillips and Dudik 2008, Elith et al. 2011). I stopped removing variables when a noticeable drop in the Area Under the receiver operating characteristic Curve (AUC; Fielding and Bell 1997) was observed with 20% withheld test data. In theory, the AUC metric provides a robust measure of a model's ability to discriminate between presence and absence localities, independent of an arbitrary cutoff threshold (Cumming 2000) - though it has been criticized for its sensitivity to areal extent, among other factors (Lobo

et al. 2008). However, because my models were evaluated under the same geographic extent, and because I was attempting to select a single model with which to evaluate the differences between bias correction methods, I used AUC rather than incorporating a multi-model inference perspective (e.g. Warren and Seifert 2011). The resulting present-day model for each species contained three to five explanatory variables. The Maxent software implements a transformation function to estimate of occurrence probability: the complementary log-log function (Phillips et al. 2017). I used this function, allowed inclusion of each feature class (linear, quadratic, product, threshold and hinge) in a bootstrap framework with 100 iterations, and saved the standard deviation across all iterations to approximate model error at each grid cell.

I use the FactorBiasOut (hereafter, σ-standard) algorithm (Dudik et al. 2005, Phillips et al. 2009) for reducing spatial sampling bias inherent in present-day GBIF observations. The σ-standard method estimates the true species distribution (π) by deriving the combined distribution of π and biased sampling distribution (σ), and then factoring σ out. This method relies on knowledge of σ, which, in practice, is rarely known. However, because the biased observation dataset is a sample of σ (i.e. the observations are sampled with the same biased sampling distribution), σ can be estimated when the observation dataset is large (Phillips et al. 2009). In these cases, σ is represented as an auxiliary variable, often in the form of a sampling intensity bias grid (Elith et al. 2011). The σ-standard method has been shown to be more effective at reducing bias than filtering methods in studies using simulated and actual species (Phillips et al. 2009, Syfert et al. 2013), especially with large sample sizes. My sample

sizes for extant observations ranged from 496 to 3007 (Table 3.1). I develop a bias grid to estimate σ by creating a kernel density raster of each biased observation dataset, and estimate the bandwidth for each kernel with a cross-validated selection method to minimize mean-square error (Baddeley et al. 2015). The resulting bias grid was rescaled to 1-20, to give greater selection probability to areas with higher densities of observations as recommended by Elith et al. (2011).

Early/Mid Holocene Distributions

Paleo-distributions were created with 4 methods: 1) hindcasting from present-day conditions, 2) paleo-SDM without bias correction (σ-naïve), 3) paleo-SDM with standard correction (σ-standard), and 4) paleo-SDM with model correction (σ-modeled). The hindcast paleo-distribution was created by projecting present-day distributions with the same explanatory variables, but with climate values representing the mid Holocene. I used the default options in Maxent for this, but disabled clamping to allow extrapolation of projections into potentially novel climate conditions. In contrast, the three paleo-SDM methods relied on calibrating new models with the same explanatory variables specified in the present-day distributions (but with climate values representing the mid Holocene) and the macrofossil records obtained from the USGS/NOAA North American Packrat Midden database dated to the early/mid Holocene period. For each of the paleo-SDM methods, I used the same bootstrap framework in MaxEnt with 100 iterations and 20% withheld test data, and I saved the standard deviation across all iterations to approximate model error at each grid cell. The σ-naïve paleo-distributions were created without any bias correction, while the σ-standard used the FactorBiasOut algorithm (described above)

with a kernel density bias grid estimated from the macrofossils to approximate the biased sampling distribution of the North American Packrat Midden archive.

Because macrofossil sample sizes can be relatively small, I expected that the σ-standard method would not sufficiently reduce spatial sampling bias and therefore developed an alternative approach, σ-modeled, to reduce model bias. I hypothesized that the macrofossils obtained from the North American Packrat Midden archive would be biased towards areas that 1) were suitable for *Neotoma* (packrat) populations during the early/mid Holocene, and 2) have been suitable for fossil preservation since the early/mid Holocene. These processes describe the conditions necessary for macrofossils to be 'sampled' in the Packrat midden archive, and are therefore the processes that describe the taxonomic, temporal and spatial biases that may hinder paleo-SDM from accurately representing paleo-distributions.

A new approach to paleo-SDM bias correction: σ-modeled

My σ-modeled approach draws on three separate statistical models to estimate σ, each representing a hypothesized source of bias in fossil data: availability, preservation and accessibility. The first statistical model, *availability*, accounts for the prerequisite of *Neotoma* species being present at a midden location during the early/mid Holocene. This component was modeled with paleo-SDM using macrofossil locations of *N. albigula* obtained from FAUNMAP (FAUNMAP Working Group 1994) dated to the early/mid Holocene. Biased sampling distributions were accounted for using the σ-standard bias correction method because the sampling distribution is suitable to support this approach; the FAUNMAP repository contains over 5000 sampling sites in the continental USA

from a wide range of paleontological sites beyond those containing packrat middens (FAUNMAP Working Group 1994), and the sample size for FAUNMAP records of *Neotoma* for the early/mid Holocene was 1195, equivalent to sample sizes for extant species. As with other implementations of Maxent in this study, I use a bootstrap framework with 100 iterations and 20% of sample observations withheld for testing with AUC. Environmental explanatory variables consisted of the same datasets described in Appendix 3.1 but were extended to include the conterminous USA to include the full range of *Neotoma*. Variable selection was conducted with a jackknife test of gain.

The second component, *preservation*, accounts for the physical conditions needed to create a well-preserved midden, which are limited to certain physiographic and substrate conditions such as rocky hillsides, cliff faces, or talus slopes, and are usually on north, northeast, south or southwest facing slopes (Webb and Betancourt 1990). Arid conditions are also needed for midden preservation, such that locations with high soil moisture or dense vegetation canopy cover are not very suitable (Webb and Betancourt 1990). I considered explanatory variables representing climate (e.g. aridity and temperature), physiography (e.g. solar exposure, drainage, ruggedness, slope and aspect), underlying material composition (e.g. consolidated and unconsolidated), and geologic characteristics (e.g. sedimentary-, metamorphic-, and igneous- rock types) for the conterminous USA (Appendix 3.3). I calibrated this model on locations of middens containing records of *any* plant species dated to the early/mid Holocene. Again, I use a bootstrap framework with 100 iterations and 20% of observations withheld for testing the Maxent model based on AUC, and variables selected using a jackknife test of gain.

Background samples were selected randomly from the conterminous USA to create a probability map for macrofossil preservation potential since the early/mid Holocene.

The third component, *discovery*, represented the potential for macrofossils to be discovered, and was therefore calibrated on all known midden sites in North America. I considered explanatory variables hypothesized to influence fossil discovery, such as erosional proxies and human accessibility (Appendix 3.3). The three statistical models for availability, discovery, and preservation components had AUC scores of 0.931, 0.891, and 0.950, respectively, and are mapped in Appendix 3.4. The product of these three probability models was used to represent σ in the σ-modeled paleo-distributions for each species and was used to select background records with a probability equal to σ.

Paleo-SDM validation with hindcast distributions: permutation tests

I hypothesized that the σ-modeled paleo-distributions would show higher congruence to the hindcast paleo-distributions than would either the σ-naïve or σ-standard methods. This hypothesis relies on the assumption that hindcast distributions, calibrated on large samples from present-day conditions, should represent true paleo-distributions better than the paleo-SDM models (which are calibrated on biased and small sample sizes). It is reasonable to assume that very little niche evolution occurred since the early/mid Holocene (Peterson 2011, Stigall 2012), especially when a species' niche is characterized in climatic and environmental space (Wiens et al. 2009, 2010, Araújo et al. 2013). Therefore, hindcast distributions over short intervals present opportunities for assessing the effectiveness of multiple bias correction methods.

To assess congruences between hindcast and the σ-naïve, σ-standard and

σ-modeled paleo-distributions, I used the Expected fraction of Shared Presences overlap metric (ESP; Godsoe 2013) by comparing the estimated habitat potential of each across all cells with the equation:

$$ESP = \frac{2\sum_j P_{1j}P_{2j}}{\sum_j (P_{1j}P_{2j})} \quad (3.1)$$

Where P_{1j} denotes the habitat potential for the hindcast paleo-distribution at location j, and P_{2j} denotes the prediction generated from either the σ-naïve, σ-standard or σ-modeled paleo-distributions at location j. This index is a modified Sørenson similarity index used to compare two maps of predicted probabilities that each species is present in a given cell rather than relying on presence/absence information (Godsoe 2013). Scores of 1 indicate perfect agreement between the two maps, while an ESP value of 0 indicates complete geographic separation (Godsoe 2013). I incorporated the uncertainty of each model by randomly permuting the value of each cell 100 times according to the standard deviation obtained from model calibration. I use a Mann-Whitney test of univariate distribution shifts to test if the permutated ESP scores were greater for any of the σ-naïve, σ-standard or σ-modeled paleo-distributions, and mixed-models with repeated measures to assess differences in overlap scores to hindcast paleo-distributions. I report marginal F-tests for significance.

Validation with Pollen

I also compared the four paleo-distributions of each species to pollen records from lake sediment cores taken in the western conterminous USA obtained from Pangea (https://www.pangaea.de) in January 2018 (Appendix 3.5). I selected pollen count data for the genus of each of my focal species with ^{14}C radiocarbon dates spanning the

early/mid Holocene. For each sediment core location, I calculated the mean habitat potential value within a 100 km radius for each of the four paleo-distributions to account for short-distance wind transport (King and Van Devender 1977, Broadhurst 2015). I hypothesized that habitat potential from the σ-modeled bias correction method would be higher in the areas surrounding each sediment core containing pollen (and dated to the early/mid Holocene) than habitat potential from the σ-naïve or σ-standard methods and would be more similar to the hindcast distributions.

Geographic Distribution Shifts and Niche Breadth

I assumed that dominant niche characteristics have remained stable since the early/mid Holocene, and that any changes due to climate would result in distribution shifts only. I therefore investigated how sampling bias could affect estimates of geographic range shifts by measuring changes the spatial predictions of habitat potential between the present-day and early/mid Holocene derived from the σ-naïve, σ-standard, σ-modeled paleo-distributions. I identified areas where habitat potential either increased or decreased significantly as those where the difference was greater than twice the combined standard error from the two time periods to capture ~ 95% of the potential variability due to model error. I report the total area where habitat potential either significantly increased or decreased for each species as estimates of range shifts. I hypothesized that the estimated net change for each species would be most similar between the hindcast and σ-modeled paleo-distributions. I also posited that not all significant changes in habitat potential would be substantial. For example, areas with habitat potential of 0.95 during the early/mid Holocene that changed to 0.85 in the

present-day should not constitute substantial changes because these two values are high, even if the marginal change (0.1) was greater than two times the standard error of each model. I therefore identify areas where habitat potential switched from being below 0.5 to above 0.5 (substantial increase), or from being above 0.5 to being below 0.5 (substantial decrease).

To test that niche characteristics have remained stable, I measured a primary niche trait, environmental niche breadth, by deriving estimates for present-day and early/mid Holocene for each of the four paleo-distributions. My metric for niche breadth measures the uniqueness of the environmental conditions defining each species' geographic distribution, and was defined as the median of the squared Mahalanobis distance of all occupied cells:

$$\widetilde{D^2} = (X - \mu)' \Sigma^{-1} (X - \mu) \tag{3.2}$$

Where X is the matrix of explanatory variables used to define the species' niche over all occupied cells, and Σ is the covariance matrix of X. I determined occupied cells probabilistically, with the equation:

$$P_i = \frac{1}{1 + e^{\frac{x_i - 0.65}{-0.05}}} \tag{3.3}$$

Where x_i is the habitat potential for cell i. Niche breadth values can range from near 4 (the most generalist species, or organism that has an ability to live in a wide variety of habitats in a wide range of environmental conditions) to over 400, a completely unrealistic value representing the most specialist of species (an organism capable of tolerating a narrow range of environmental conditions) possible in my study area; namely a species occurring on a single grid cell with the most unique environmental conditions. I

use the same permutation test described above to check if niche breadths under current-day distributions were different from those calculated under each of the four paleo-distributions, and I use a Mann-Whitney test to identify if the permutated niche breadth scores for the present-day were not significantly different from any of the four paleo-distributions.

Climate novelty

I hypothesized that areas with novel climate in the present-day relative to early/mid Holocene would also be areas where distributions have retreated from and would therefore show a decline in habitat potential. I calculated univariate and multivariate climatic novelty by incorporating the correlation structure among climatic variables with Mahalanobis distances following the procedures for Type 1 and Type 2 novelty proposed by Mesgaran et al. (2014). Type 1 novelty identifies areas where climate becomes novel because they are beyond the range of any individual covariate, and scores can range from 0 (no univariate novelty) to negative infinity (high univariate novelty). In contrast, Type 2 novelty identifies areas that are within the univariate range but represent novel combinations between covariates and can range from 0 to positive infinity, with values under 1 indicating no multivariate novelty (Mesgaran et al. 2014). I calculate both types of climate novelty across my study area and compare each using Pearson's correlation with rasters of habitat potential change from the early/mid Holocene to present-day conditions under the hindcast, the σ-naïve, σ-standard and σ-modeled paleo-distributions.

RESULTS

Present-day and early/mid Holocene Distributions

Among the three bias correction methods, the σ-modeled correction method resulted in paleo-distributions that best matched actual distributions when compared to hindcast models and independent pollen data. The geographic means of habitat potential scores for present-day conditions in the study area ranged from 0.173 (sd=0.226; *C. ramosissima*) to 0.543 (sd=0.163; *A. tridentata*), while hindcast paleo-distribution scores ranged from 0.159 (sd=0.242; *C. ramosissima*) to 0.552 (sd=0.156; *A. tridentata*), indicating that the relative amount of habitat remained consistent between periods (Table 3.2). Of the three bias-correction methods (σ-naïve, σ-standard and σ-modeled), σ-naïve resulted in the lowest habitat potential scores across the study region and were substantially lower than hindcast paleo-distributions (Table 3.2). ESP overlap scores between hindcast paleo-distributions and the three fossil calibrated methods (σ-naïve, σ-standard and σ-modeled) were significantly different from one another ($F_{2,10}$=19.6414, $p<0.0001$), with σ-naïve paleo-distributions showing the lowest ESP scores (Figure 3.2); thereby indicating that without bias correction, sampling bias caused paleo-distributions to be far from their (assumed) true values. In contrast, the σ-modeled paleo-distributions yielded ESP overlap scores that were significantly higher than either the σ-naïve or σ-standard paleo-distributions for all species except *C. ramosissima* (Figure 3.2), suggesting that the model of σ was able to overcome some of the bias inherent in the packrat midden fossil record and bring paleo-distributions closer to their (assumed) true value. Improvements ranged from 26 to 157% with the σ-modeled bias correction method (Figure 3.2). I provide mean overlap between hindcast and the three paleo-SDM methods (σ-naïve, σ-standard and σ-modeled) in Appendix 3.6. Independent pollen

locations yielded insight consistent with this improvement, with four of five taxa showing higher habitat potential estimated with the σ-modeled method at sites where the pollen record indicated presence of the genera during the early/mid Holocene (Figure 3.3). The sixth species, *C. ramosissima*, did not have any corresponding pollen records and was excluded. The σ-standard method also predicted increased habitat potential (over the σ-naïve method) at these sites, but increases were not as great as with the σ-modeled method.

Relationship of model improvement to sampling bias, σ

The ability to infer paleo-distributions with limited knowledge of true absence locations has propelled PB SDM to become the method of choice for addressing paleobiogeographical questions of extinction (McKinney 1997, Lorenzen et al. 2011), speciation (Wiens and Harrison 2004, Graham et al. 2004b) and niche conservation through time (Stigall 2012). However, a key assumption of PB frameworks is that any sampling bias (σ) is proportional to the background distribution of environmental covariates (Araújo and Guisan 2006), and that species' niches are equally sampled over the full range of environmental conditions in which they occur (Phillips et al. 2009). The degree to which this bias may affect paleo-SDM is the degree to which σ can be quantified and separated from the true species distribution (π). In species where σ and π are similar, there may be less need to precisely quantify σ because their combined distribution may sufficiently represent the true species' distribution (π). I might then expect that species with similar σ and π would show limited improvement from a σ-modeled approach. I found some evidence for this; species with high correlation between

π (hindcast) and the estimate of σ showed lower improvements in spatial overlap of σ-modeled and hindcast distributions ($F_{1,4}$=4.9267, p=0.09065; Figure 3.4). But even in the case of *C. ramosissima*, which showed the highest degree of overlap between σ and π (Figure 3.5), I found that σ-modeled paleo-distributions were 25% better than σ-naïve estimates, and that spatial overlap scores of σ-modeled paleo-distributions were within 1% of σ-standard paleo-distributions. I therefore found little evidence that paleo-distribution predictions were made worse by the σ-modeled correction method.

Geographic Distribution Shifts and Niche Breadth

Estimates of range area shifts between the early/mid Holocene and present-day varied dramatically among the methods of estimating paleo-distributions. Projections of areas with significant increases in habitat potential from the early/mid Holocene to present-day with σ-modeled paleo-distributions provided the closest estimates to changes in habitat potential from hindcast distributions for all species except *C. ramosissima* (Table 3.3), where the σ-standard paleo-distribution provided the better estimate. However, when assessing significant reductions in habitat potential, the σ-modeled paleo-distributions did not improve estimates over the σ-naïve paleo-distributions (Table 3.4). This suggests that while the σ-modeled paleo-distributions provided higher spatial congruence with hindcast distributions than the σ-naïve or σ-standard paleo-distributions, they likely overestimate habitat potential in the early/mid Holocene and result in elevated estimates of habitat potential decrease from the mid-Holocene to the present. I found a similar pattern when I identified substantial increases (range expansions) and decreases (range contractions) in habitat potential: the σ-modeled paleo-distributions provided the

closest estimates to hindcast distributions for all species except *C. ramosissima* (Tables 3.3 and 3.4).

Niche breadths for the 6 species ranged from 5.74 to 10.02 (Table 3.5), with *A. concolor* and *J. communis* being the most specialized, and *A. tridentata* and *Q. gambelii* the most generalist species within my study area. Niche breadths estimated with the σ-modeled paleo-distributions most closely replicated those from hindcast distributions for four species but not *C. ramosissima* and *Q. gambelii*. The σ-naïve paleo-distributions provided the least accurate representations of niche breadth, with differences ranging from 10 to 50%.

Climate novelty

Type 1 novelty scores ranged from 0 to -0.0337, indicating no univariate novelty between the mid-Holocene and present-day datasets. I also found no multivariate novelty, with Type 2 novelty scores ranging from 0 to 0.9177 (scores <1 indicate no novelty). With minimal climatic novelty between the two periods, I expected little, if any, evidence of a relationship between climatic novelty and changes in climatic habitat potential. Pearson's correlation coefficients between Type 2 climate novelty and the change in habitat potential between the early/mid Holocene and present-day period were negative for the hindcast paleo-distributions in five of the six species, though all correlation coefficients were below 0.5. *J. communis* was an outlier with a very low positive correlation coefficient (Table 3.6). Negative correlation coefficients are indicative of an association between habitat potential loss and Type 2 climate novelty and provided only weak evidence that novel climates resulted in habitat loss, my expected association. The σ-modeled paleo-distributions most closely matched the relationship found with hindcast

paleo-distributions, but again, correlation coefficients were low, indicating a weak relationship at best. The σ-naïve, and σ-standard paleo-distributions suggested different relationships, with positive correlation coefficients for all species expect *C. ramosissima*. While all of these associations were weak, the estimation of any relationship between climate novelty and range shifts was reversed in the absence of bias correction or when the standard correction method was used. I had also hypothesized that areas with high model uncertainty during the early/mid Holocene would result in a loss of habitat potential projected by hindcasting using the model conditioned on present-day conditions. I found minimal support for this prediction, with correlation coefficients ranging from -0.07 to 0.51 (Table 3.6).

DISCUSSION

Packrat Midden Fossil Bias

Paleobiogeographers have studied fossilized packrat middens since the pioneering work of Philip Wells in the 1960s (Wells 1966, Wells and Berger 1967). In the last half-century, numerous researchers have contributed to the packrat midden archive, which has continued to grow taxonomically, temporally and spatially (Williams et al. 2018). This archive offers access to a wealth of macrofossil observations, many of which have species level taxonomic precision and can be geo-located to within 100 m of the midden site from which they were extracted (Vaughan 1990). This archive spans well into the Pleistocene at the limits of ^{14}C dating methods, making it ideally suited for investigating changes in recent north American floral (e.g. Cole and Webb 1985, Spaulding 1990, McAuliffe and Van Devender 1998, Thompson and Anderson 2000, Jackson et al. 2005), faunal (e.g. Van Devender et al. 1977, Van Devender and Mead 1978, Mead 1981) and

climatic (e.g. Jacobson 1991, Arundel 2002, Coats et al. 2008, Thompson et al. 2012) reconstructions. While the breadth of biogeographic inquiries using these data continues to grow (Williams et al. 2018), their use of paleo-SDM has been limited at best. The paucity of studies using paleo-SDM to estimate spatially explicit paleo-distributions is likely due to the spatial bias inherent in the Neotoma database (Webb and Betancourt 1990, Mensing et al. 2000). Here, I developed a statistical model of this bias, σ-modeled, for the Neotoma database, and use it to develop paleo-distributions of six species for the early/mid Holocene.

I found that paleo-distributions for the early/mid Holocene modeled without bias correction (σ-naïve) provided poor matches to hindcast paleo-distributions, my comparison measure of true early/mid Holocene distributions. The σ-modeled correction method improved paleo-distributions for my six species and showed, on average, 91% higher overlap with hindcast than σ-naïve paleo-distributions. These improvements were confirmed at independent locations from lake sediment pollen records, where I found habitat potential scores for σ-modeled paleo-distributions to be higher than the σ-naïve and σ-standard paleo-distributions.

I used hindcast paleo-distributions as my reference distributions because they can draw on a wealth of biogeographic repositories characterizing contemporary distributions of extant species. Hindcast distributions however, assume that a species niche has remained unchanged between the calibration and projection time periods. This assumption is reasonable for periods in the mid- to late Holocene, a time frame of only a few millennia when the world's climate has been relatively stable and evolutionary

change unlikely, but may be less so for paleobiogeographic studies of the Pleistocene or earlier (Peterson et al. 1999, Peterson 2011). In studies where hindcasting is less appropriate, paleo-SDM calibrated with paleo-ecological archives has shown to be useful (e.g. Walls and Stigall 2012, Saupe et al. 2014, Serra-Varela et al. 2015), although it still would benefit from correction measures to reduce the effects of biased sampling distributions (Svenning et al. 2011, Varela et al. 2011).

Niche Characteristics

Measuring niche characteristics is difficult, at best. My work confirms the subjectivity of niche breadth assessments and further suggests that fossil bias may cause even greater distortions in assessments of niche breadth and niche conservation. Niche conservation assumes that niche characteristics, such as niche breadth, remain stable through time (Wiens and Graham 2005) and that any changes in climate may instead cause shifts in geographic distributions. Formal tests, such as niche equivalency (Warren et al. 2008), have been developed and used extensively to investigate niche conservatism in related extant taxa (e.g. Strubbe et al. 2014, Kolanowska et al. 2017), but these tests compare spatial predictions of habitat potential to infer similarity in niche characteristics, and do not estimate niche properties directly. Properties such as niche breadth have often been assumed to be linked to extinction, with specialist species being more susceptible to extinction than generalist species (McKinney 1997, Hernández fernández and Vrba 2005, Nürnberg and Aberhan 2013), though this relationship is not universal; geographic range size is often given greater attribution to extinction risk (Kammer et al. 1997, Thuiller et al. 2005, Harnik et al. 2012, Saupe et al. 2015).

The contradictory evidence on the effect of niche breadth on extinction is no wonder; no unified metric with which to measure niche breadth exists. Metrics of niche breadth span volumetric measurements of the dominant principle component axes of presumed occupied regions of environmental space (e.g. Saupe et al. 2015), to counts of different habitat types presumed to be occupied (e.g. Harnik et al. 2012, Nürnberg and Aberhan 2013). These different metrics, including ours, are highly dependent on the environmental characteristics used to define an organism's niche, and as such, are often not comparable (Slatyer et al. 2013). In all six species, σ-naïve estimates of niche breadth were improved with σ-modeled paleo-distributions, though in two species (*C. ramosissima* and *Q. gambelii*), σ-standard paleo-distributions provided marginally improved estimates over σ-modeled. This suggests that the σ-modeled paleo-distributions did not always improve niche breadth estimates, and that estimates of niche breadth for species whose paleo-distributions align more closely with fossil bias may be reduced when calibrated on the fossil record.

Climate Novelty

I investigated potential relationships between climate change and range retraction under the assumption that habitat potential would decline in areas experiencing the greatest change in climate. I only found weak evidence of this, with negative Pearson's correlation coefficients for only five of my six species. The greatest changes in climate in the Holocene occurred during the early period of the Holocene, prior to approximately 9 ka (Viau et al. 2006), but the widely available paleoclimate data used here (Hijmans et al. 2005) characterize climate during the Mid-Holocene, at approximately 6 ka. Assessments

of climate novelty comparing present day climate to the Mid-Holocene based on these data would not capture the changes influencing distribution shifts that were occurring during the early Holocene, such as the dramatic warming occurring prior to 9 ka.

Access to paleoecological archives

The marked increase in online data storage and ease of establishing and maintaining web services has led to the proliferation of online, open access paleoecological databases well suited for paleo-SDM. Such resources include broad data repositories like PANGAEA (https://pangaea.de), and the NOAA/World Data Service for Paleoclimatology (https://www.ncdc.noaa.gov), as well as curated databases such as the USGS/NOAA North American Packrat Midden database (https://geochange.er.usgs.gov/midden/; Strickland et al. 2013), the Neotoma Paleocology Database (Williams et al. 2018), FAUNMAP and MIOMAP (Carrasco et al. 2005), among others. These databases offer spatially referenced fossil archives that extend well into the Miocene. When species paleo-distribution records are combined with the Coupled Modelling Intercomparison Project (CMIP5: http://cmip-pcmdi.llnl.gov/cmip5/) and the Paleoclimate Modelling Intercomparison Project (PMIP3: https://pmip3.lsce.ipsl.fr/) that provide modeled and reconstructed spatial paleo-climates (e.g. Lima-Ribeiro et al. 2015, Lorenz et al. 2016, Fordham et al. 2017), paleo-SDM offers biogeographers new tools for exploring paleo-distributions well beyond the early/mid Holocene addressed here. Moreover, improvements in the temporal resolution of gridded climate data offer opportunities to investigate many time slices of recent history (Pearman et al. 2008, Blois et al. 2013). I suggest that the approach described here to model sampling bias can be applied to finer time slices using the Neotoma database,

and more generally, can be adapted for other paleoecological archives as a framework for estimating spatial sampling bias, σ.

TABLES

Table 3.1. Sample Sizes. Sample size of geo-referenced observations obtained from the Geographic Biodiversity Information Facility (extant) and the USGS/NOAA North American Packrat Midden database (early/mid Holocene).

species	sample size extant	sample size early/mid Holocene
Abies concolor	1359	59
Artemisia tridentata	3007	129
Coleogyne ramosissima	496	56
Juniperus communis	732	76
Pinus ponderosa	1687	82
Quercus gambelii	529	21

Table 3.2. Habitat Potential Values. Mean (and standard deviation) of habitat potential values in the study area for Present-day (1950 – 2000 yr) and early/mid Holocene (11.5 ka – 5 ka) conditions. Habitat potential for the early/mid Holocene conditions was estimated using 4 methods: hindcasting from present day conditions (Hindcast), paleo-SDM without bias correction (σ-naïve), paleo-SDM with standard correction (σ-standard), and paleo-SDM with model correction (σ-modeled).

	Present-Day		early/mid Holocene							
Species			Hindcast		σ-naïve		σ-standard		σ-modeled	
Abies concolor	0.304	(0.224)	0.273	(0.228)	0.113	(0.181)	0.164	(0.215)	0.416	(0.332)
Artemisia tridentata	0.543	(0.163)	0.552	(0.156)	0.133	(0.206)	0.185	(0.237)	0.347	(0.232)
Coleogyne ramosissima	0.173	(0.226)	0.159	(0.242)	0.050	(0.136)	0.083	(0.173)	0.108	(0.189)
Juniperus communis	0.232	(0.265)	0.244	(0.275)	0.138	(0.194)	0.262	(0.242)	0.483	(0.256)
Pinus ponderosa	0.332	(0.256)	0.354	(0.268)	0.184	(0.215)	0.262	(0.242)	0.566	(0.316)
Quercus gambelii	0.318	(0.278)	0.282	(0.258)	0.494	(0.176)	0.540	(0.143)	0.764	(0.205)

Table 3.3. Range Expansion. Total area (km^2) with significant increase in habitat potential between early/mid Holocene and present-day conditions. Areas with a significant increase in habitat potential were defined as areas where the difference was greater than twice the combined standard error of the paleo-distributions from the two time periods. Areas with substantial increase in habitat potential were identified as areas where habitat potential switched from being below 0.5 to above 0.5 (substantial increase).

		Range Expansion (Increase)							
		significant				substantial			
species	Total	Hindcast	σ-naïve	σ-standard	σ-modeled	Hindcast	σ-naïve	σ-standard	σ-modeled
Abies concolor	3,162,474	360,035	1,716,853	1,552,253	419,966	79,818	457,183	444,537	67,806
Artemisia tridentata		10,819	2,637,177	2,465,774	2,050,502	456	1,611,433	1,493,410	1,348,343
Coleogyne ramosissima		240,286	1,936,083	1,243,322	1,503,453	28,653	215,272	139,440	169,305
Juniperus communis		11,933	1,233,631	679,739	9,099	4,091	523,764	390,323	4,140
Pinus ponderosa		11,699	1,303,959	878,375	64,370	4,257	660,325	572,172	22,063
Quercus gambelii		109,392	248,897	174,506	11,359	33,186	202,509	84,211	31

Table 3.4. Range Contraction. Total area (km^2) with significant decrease in habitat potential between early/mid Holocene and present-day conditions. Areas with a significant decrease in habitat potential were defined as areas where the difference was less than the negative of twice the combined standard error of the paleo-distributions from the two time periods. Areas with substantial decrease in habitat potential were identified as areas where habitat potential switched from being above 0.5 to below 0.5 (substantial decrease).

	Range Contraction (Decrease)							
	significant				substantial			
species	Hindcast	σ-naïve	σ-standard	σ-modeled	Hindcast	σ-naïve	σ-standard	σ-modeled
Abies concolor	45,006	39,486	155,928	1,156,777	5,828	28,669	125,814	542,522
Artemisia tridentata	85,029	49,354	102,444	385,328	19,144	10,595	17,492	260,398
Coleogyne ramosissima	59,402	37	2,750	155,850	21,048	7	1,864	52,759
Juniperus communis	105,601	186,426	999,505	2,428,090	9,453	149,562	288,986	593,964
Pinus ponderosa	227,459	134,341	248,719	2,591,410	93,143	115,228	201,074	778,419
Quercus gambelii	10,189	1,205,203	1,472,827	2,887,400	3,664	939,497	1,265,042	1,873,854

Table 3.5. Niche Breadths. Niche breadth as estimated by each of the 4 methods: hindcasting from present day conditions (Hindcast), paleo-SDM without bias correction (σ-naïve), paleo-SDM with standard correction (σ-standard), and paleo-SDM with model correction (σ-modeled). Niche breadth used here measures the uniqueness of the environmental conditions defining each species' geographic distribution and was defined as the median of the squared Mahalanobis distance of all occupied cells.

	Hindcast	σ-naïve		σ-standard		σ-modeled	
species	mean	mean	% Diff	mean	% Diff	mean	% Diff
Abies concolor	10.02	7.79	22.254	7.19	28.275	9.01	10.069
Artemisia tridentata	5.59	5.04	9.807	4.35	22.212	5.55	0.777
Coleogyne ramosissima	6.27	9.63	-53.613	8.29	-32.299	9.21	-46.972
Juniperus communis	9.52	5.55	41.664	5.73	39.837	7.71	18.986
Pinus ponderosa	7.74	6.15	20.501	5.64	27.135	7.26	6.146
Quercus gambelii	5.74	4.54	20.989	4.60	19.905	4.55	20.779

Table 3.6. Climatic Novelty. Pearson's correlation coefficients and p-values as estimates of Type 2 novelty and paleo-distributions from each of the four methods: hindcasting from present day conditions (Hindcast), paleo-SDM without bias correction (σ-naïve), paleo-SDM with standard correction (σ-standard), and paleo-SDM with model correction (σ-modeled). Type 2 novelty identifies areas that are within the univariate range but represent novel combinations between covariates and can range from 0 to positive infinity, with values under 1 indicating no multivariate novelty.

			early/mid Holocene paleo-distributions							
	Hindcast Error		Hindcast		σ-naïve		σ-standard		σ-modeled	
Species	r	p	r	p	r	p	r	p	r	p
Abies concolor	0.24	0.00	-0.34	0.00	0.20	0.00	0.22	0.00	-0.28	0.00
Artemisia tridentata	0.51	0.00	-0.34	0.00	0.05	0.00	0.11	0.00	-0.04	0.00
Coleogyne ramosissima	-0.07	0.00	-0.18	0.00	-0.21	0.00	-0.23	0.00	-0.37	0.00
Juniperus communis	0.25	0.00	0.04	0.00	0.31	0.00	0.38	0.00	0.15	0.00
Pinus ponderosa	0.17	0.00	-0.15	0.00	0.24	0.00	0.28	0.00	-0.23	0.00
Quercus gambelii	-0.03	0.00	-0.05	0.00	0.05	0.00	0.02	0.00	-0.37	0.00

FIGURES

Figure 3.1. Study Area. Study area (thick black line) encompassed the greater western conterminous USA where the majority of Neotoma database records have been identified.

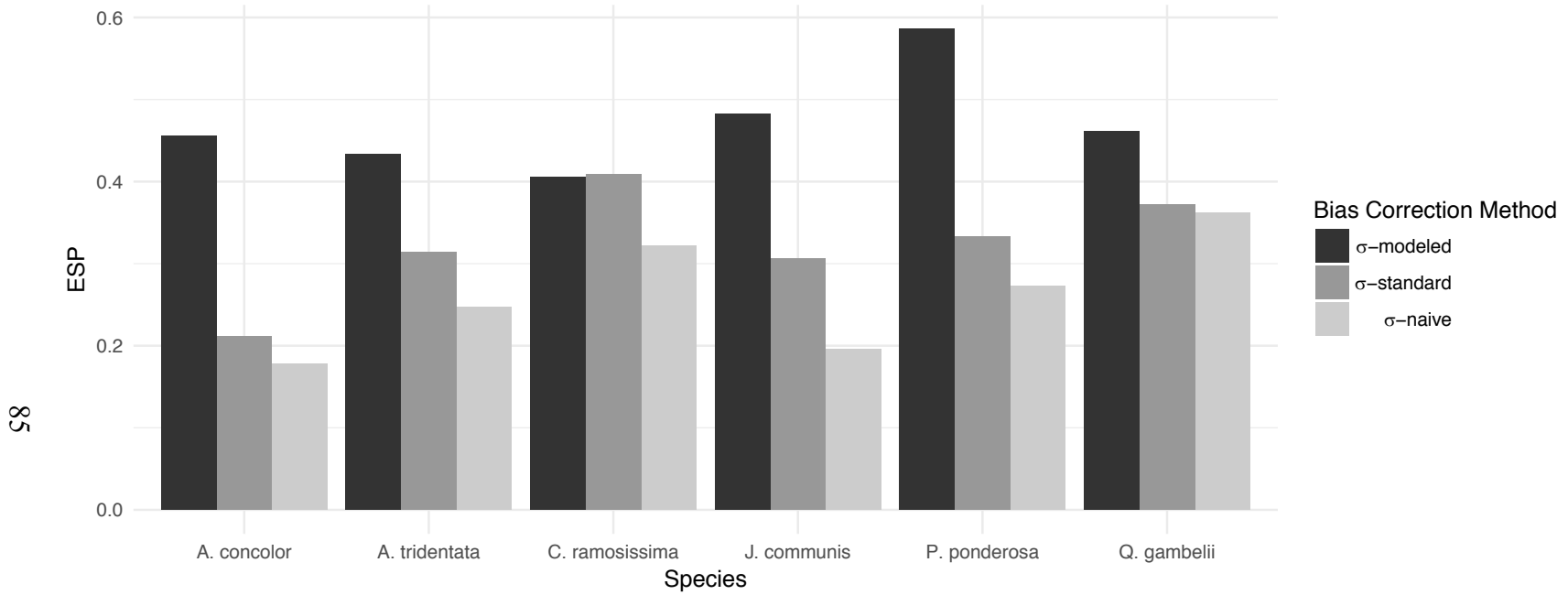

Figure 3.2. Overlap between Hindcast and Paleo-SDM. Mean Expected fraction of Shared Presences (ESP) scores for overlap between hindcasting from present day conditions to paleo-SDM without bias correction (σ-naïve), paleo-SDM with standard correction (σ-standard), and paleo-SDM with model correction (σ-modeled). ESP measures overlap between σ-modeled paleo-distribution and hindcast paleo-distribution.

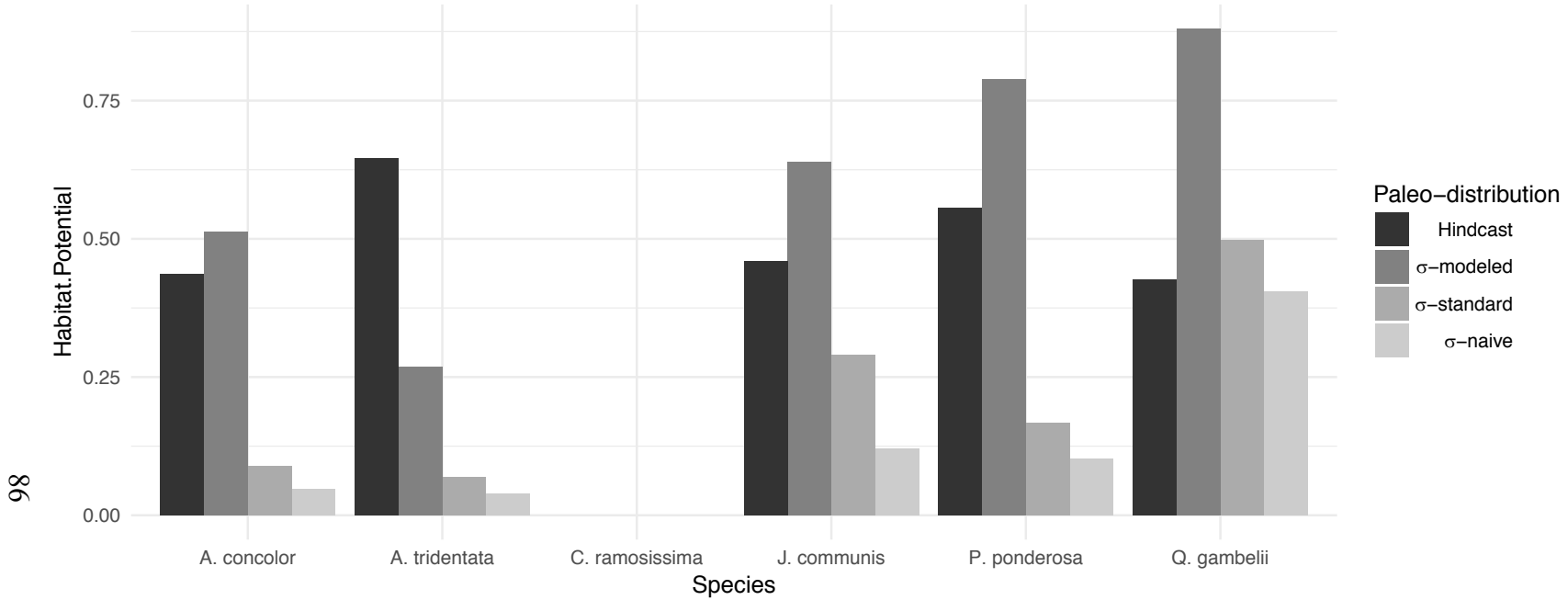

Figure 3.3. Independent Pollen Assessment. Mean habitat potential values within 100 km radius of sites where the pollen record indicated presence of the genera during the early/mid Holocene for each of the 4 paleo-distributions: hindcasting from present day conditions (Hindcast), paleo-SDM without bias correction (σ-naïve), paleo-SDM with standard correction (σ-standard), and paleo-SDM with model correction (σ-modeled).

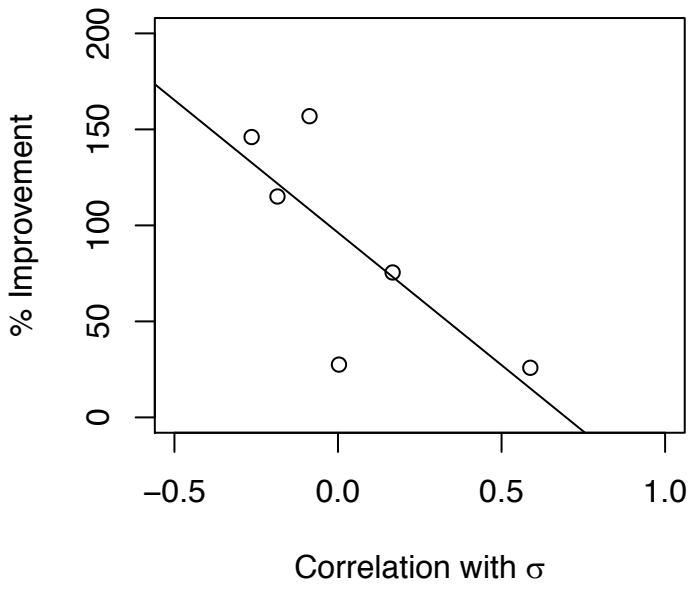

Figure 3.4. Relationship between total improvement in Expected Fraction of Shared Presences (ESP) score (y-axis) and Pearson's correlation coefficient (r; x-axis) between hindcast paleo-distribution models and the estimate of spatial sampling bias (σ) from the midden potential model. ESP measures overlap between σ-modeled paleo-distribution and hindcast paleo-distribution.

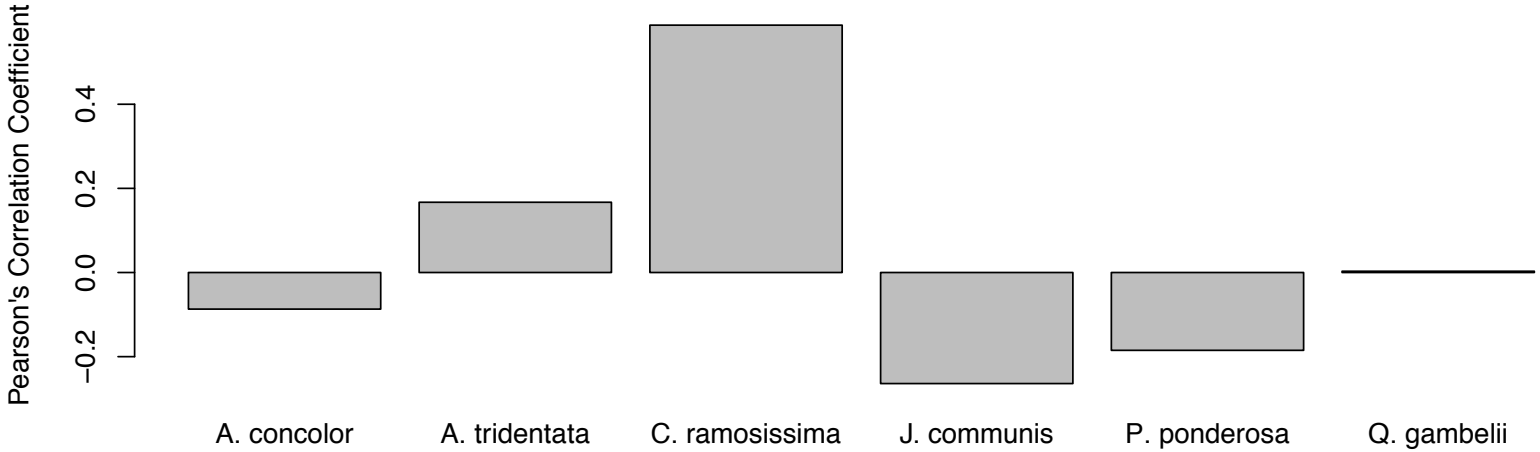

Figure 3.5. Habitat Potential Overlap with Estimated Sampling Bias. Pearson's correlation coefficient between hindcast paleo-distribution and the estimate of spatial sampling bias (σ). The hindcast paleo-distribution for *C. ramosissima* showed the highest correlation to of spatial sampling bias (σ), while *J. communis* was most negatively correlated.

CHAPTER 4

USING MULTISCALE GEOGRAPHICALLY WEIGHTED REGRESSION TO INVESTIGATE ECOLOGICAL NICHE SEPARATION: THE CASE OF MOJAVE AND SONORAN TORTOISES

ABSTRACT

Aims: To investigate spatial congruence between genotype and ecological niche separation in spatially adjacent sister taxa of desert tortoise using multiscale geographically weighted regression.

Location: Mojave and Sonoran Desert ecoregions; California, Nevada, Arizona, Utah, USA.

Methods: I designate two areas of ecological niche separation using a novel approach coupling species distribution modeling and multiscale geographically weighted regression (MGWR). This approach uses a new extension to GWR to estimate parameters at separate spatial scales for each explanatory variable and explores non-stationarity in the spatial residuals of a pooled-taxa distribution model. I predicted ecological niche separation with multivariate clustering of the MGWR parameter surfaces. Using an index of phylogenetic diversity, I compare models of (i) a geographically-based taxonomic designation for two sister species, (ii) an environmental ecoregion designation, and (iii) an ecological niche separation from local habitat selection.

Results: A model of ecological niche separation that was based on local parameter estimates of habitat selection better explained an index of phylogenetic diversity for two sister taxa than did either the geographically based taxonomic designation or an environmental ecoregion designation. A novel approach coupling SDM and MGWR

improved computation time by enabling smaller regions of interest to be analyzed with GWR while still incorporating the entire species range in SDM.

Main Conclusions: Exploring spatial non-stationary with local regression can benefit studies of biogeography and conservation by coupling SDM and GWR. I find that niche separation in habitat selection conforms to genotypic differences between two sister taxa of tortoise in a recent secondary contact zone and highlights the need for special protection of individuals currently not covered by the geographic distribution defined under the US Endangered Species Act.

INTRODUCTION

Conservation biologists increasingly rely on metrics beyond taxonomic diversity to inform conservation priorities. The push towards a better understanding of the importance of functional (Cadotte and Jonathan Davies 2010, Flynn et al. 2011, Cadotte et al. 2011) and phylogenetic diversity (Crozier 1997, Helmus et al. 2007, Scoble and Lowe 2010, Vandergast et al. 2013, Wood et al. 2013) for conservation planning has led to an increased recognition that geographic patterns of multiple facets of diversity are required for managing biological resources (Myers et al. 2000, Naeem et al. 2012, Winter et al. 2013). Spatially structured variation in the different dimensions of diversity, especially phylogenetic variation, may foster ecosystem resilience to global change (Tews et al. 2004, Legendre et al. 2005, Devictor et al. 2010, Flynn et al. 2011), and long-term preservation of diversity may require protection of areas that span wide phylogenetic gradients (Moritz 2002, Scoble and Lowe 2010, Winter et al. 2013). Identifying the processes and conditions under which taxa have diverged can illuminate areas where inter-population divergence and intra-population genetic diversity sustain

adaptation to changing environments (Crandall et al. 2000, Moritz 2002). Moreover, identifying local variation in genetic divergence and diversity may also contribute to a biogeographical understanding of the conditions that influence speciation, their distributions, and their relationships to local environmental conditions.

Spatial non-stationarity and species distribution modeling

One hypothesis that often goes untested is the presence of spatial non-stationarity in species-environment relationships. In its application to conservation biogeography, spatial non-stationarity suggests that a single set of coefficients may not adequately represent species-environment relationships across space (Foody 2004) and that coefficients may covary with location (Fotheringham 1997, Atkinson 2001). Spatial non-stationarity may be apparent when ecological processes operate at multiple scales (Legendre 1993), when key variables are omitted, or when the model functional form is mis-specified (Fotheringham 1997, Fotheringham et al. 2003). Variable omission is likely when proxies are used instead of predictor variables that measure mechanistic causal factors (Kearney and Porter 2009). For example, 'mean annual temperature' may serve as a proxy for the more proximal limiting factor of hourly surface substrate temperature (Kearney et al. 2014), and as such, may show a varying relationship across a species' range as a function of another unmeasured variable such as substrate type. Spatial non-stationarity may also be apparent at the limits of a species' range or in areas with high phylogenetic diversity, especially if recent secondary contact between vicariant populations has highlighted gradients of niche differentiation (Endler 1977, Jiggins and Mallet 2000, Gay et al. 2008). Here, geographic gradients in habitat use (species-

environment relationships) could be driven by parapatric speciation, though this hypothesis has rarely been tested.

Species distribution modelling (SDM) comprises a suite of analytical methods used to test and explore habitat use by relating locations of species occurrences to environmental explanatory variables hypothesized to influence species limitations and habitat associations (Franklin 2010b). SDM characterizes relationships between environmental conditions at locations where species occur and where they do not in order to make predictions about their likelihood of occurring at un-sampled locations. A common form of SDM draws on ordinary least squares (OLS) regression methods such as generalized linear modeling (GLM) (Guisan and Zimmermann 2000), which rely on the assumption that species-environment relationships remain constant across a species' geographic distribution. In this common form of SDM, a single (i.e. 'global') parameter representing each relationship is estimated, and any local residual variation is explored post-hoc. Often, the residuals of traditional, non-spatial regression are spatially auto-correlated (Austin 2002); this non-independence violates a key assumption of standard regression and affects the significance and values of model parameters (Anselin and Rey 2009). Moreover, the use of global parameters precludes the possibility of incorporating spatial non-stationarity directly into the model specification.

Geographically weighted regression

Geographically weighted regression (GWR; Fotheringham et al. 2003) has become a dominant method to incorporate spatial non-stationarity in a regression framework, and uses local statistics to characterize spatially varying relationships between predictors and response variables. GWR also enables the exploration of local

variation in processes that span borders (Cheng and Fotheringham 2013). Identifying spatially varying relationships across boundaries can provide inference about the nature of a boundary in terms of its permeability and history, and can draw attention to differences in data quality spanning those borders (Cheng and Fotheringham 2013). In a conservation biogeography context, borders and the gradients spanning them are key concepts that give context to phylogenetic diversity and the conditions that influence speciation (Hoffmann and Blows 1994). GWR is an underutilized tool for exploring the drivers of these biogeographical patterns, which are increasingly important to conservation planning and land management. Few studies have explored spatial non-stationarity in context of biogeographical patterns (but see Foody 2004, Bickford and Laffan 2006, Holloway and Miller 2015), and even fewer have incorporated spatial non-stationarity with SDM (e.g. Kupfer and Farris 2006, Miller 2012). Incorporating GWR into SDM provides the capacity to account for spatial autocorrelation in residuals and to explore spatial non-stationarity in habitat use. While the former has been addressed in SDM through model structures with spatial dependence terms such as Spatial Auto-Regressive and Conditional Auto-Regressive models (Diggle et al. 1998, Miller et al. 2007, Miller 2012) and hierarchical Bayesian models (Wikle 2003, Chakraborty et al. 2010, Aderhold et al. 2012), spatial non-stationarity has rarely been addressed (but see Miller 2012).

Many ecological processes have an implicit spatial scale (e.g. McIntyre and Lavorel 1994) and may become less important or non-significant at another spatial scale (Turner et al. 1989). Often, biodiversity studies incorporate multiscale approaches to investigate the additional dimension of spatial scale (e.g. Rahbek and Graves 2001, Willis

and Whittaker 2002, Seo et al. 2009). In GWR, spatial scale is represented with a bandwidth parameter that, in conjunction with adaptive spatial kernels, determines how nearby observations are given higher weights than more distance ones (Fotheringham et al. 2003). Large bandwidths approximate global models, while small bandwidths result in highly local models. However, previous GWR analyses have used a single bandwidth for all explanatory variables, regardless of the spatial scale at which they may affect the response variable. A recent development in GWR is the capacity to estimate separate bandwidths for each explanatory variable specified in the model: Multiscale Geographically Weighted Regression (MGWR; Fotheringham et al. 2017). Here I use MGWR to investigate whether non-stationarity in habitat use may be apparent for some, but possibly not all, explanatory variables.

Some of the key features that have facilitated the widespread use of SDM have also hindered its integration with GWR. One of these features is the use of georeferenced observations of species occurrences (presence), or presence and absence. These data are not easily incorporated into GWR frameworks due to their sparse nature and often biased sampling; at fine local scales with few observations, calibration of local logistic regression models cannot converge due to complete separation of response classes (zeros and ones; Fotheringham et al. 2003). The biased sampling distributions problematic to SDM and GWR stem from two primary types of bias: 1) incomplete sampling, and 2) over-sampling. Both of these sources of bias result in spatial heterogeneity in sampling intensity, and both are common in geographically referenced biodiversity data (Ponder et al., 2001; Graham et al., 2004; Frey, 2009; Newbold, 2010). The use of biased species occurrence data in GWR is problematic and generally requires the use large bandwidths

approximating global models (Miller 2012), though this precludes exploration of local patterns and negates one of the primary benefits of GWR.

Niche Differences in Sister Species

In this study, I propose a novel method to overcome biased sampling when using GWR by coupling SDM *with* GWR, thereby drawing on the strengths of both approaches. To avoid convergence failure in logistic GWR, I first use occurrence localities obtained from biased sampling to develop global predictions of habitat suitability with SDM. By using SDM, I am also able to apply bias correction measures recently developed to reduce the effects of biased sampling (e.g. Phillips et al. 2009, Varela et al. 2014, Boria et al. 2014). I then apply MGWR to the residuals (unexplained variance), resulting from global SDM predictions, to explore local variability in habitat use (species-environment relationships). This shifts the role of GWR from prediction to exploration, for which GWR is more suited (Fotheringham et al. 2011).

I develop a case study of two closely related sister-taxa that are found in the deserts of southwestern North America that suffer from 1) extreme sampling bias in occurrence observations, 2) differing legal conservation and protection status, and 3) distribution uncertainty. These two species, *Gopherus agassizii* (Agassiz's desert tortoise) and *Gopherus morafkai* (Morafka's desert tortoise) diverged approximately 6 Ma due to geographic isolation by the Bouse embayment, a putative marine transgression of the ancestral Gulf of California along the lower Colorado River, resulting in allopatric speciation (Murphy et al. 2011). These two cryptic species were only recently distinguished as phylogenetically and taxonomically separate due to differences in genetics, reproductive ecology, and seasonal activity (McLuckie et al. 1999, Murphy et

al. 2011), but are not readily distinguished morphologically. Prior to the taxonomic split, a Distinct Population Segment defined as the Mojave population (Figure 4.1; tortoises west and north of the Colorado river) was listed as threatened (given legal protection) under the US Endangered Species Act (ESA) (Department of the Interior 1990) and has received extensive monitoring resulting in a wealth of georeferenced observations (Anderson and Burham 1996). The remaining "Sonoran Population", later elevated as a distinct species, *G. morafkai*, is not afforded the same protection or monitoring (Murphy et al. 2011, Service 2015). The Colorado River defines the geographic division between the two species, however, recent genetic work has identified a secondary contact zone where *G. agassizii* (the western species) occurs in a small population east of the Colorado River (McLuckie et al. 1999, Edwards et al. 2015). This secondary contact zone likely emerged only 2.5 ka as a result of fluctuations in the Colorado River, but now *G. agassizii* in this zone are isolated from individuals occurring on the other side of the Colorado River. This small, isolated population of *G. agassizii* east of the Colorado faces threats from increasing development in this region - but does not receive federal protection under the ESA due to the geographic delineation of the two species. This is further complicated by recent evidence of natural hybridization between *G. agassizii* and *G. morafkai* occurring in the secondary contact zone (Edwards et al. 2015), and by the lack of a clear definition of suitable habitat for this population of *G. agassizii* east of the River. The careful application of SDM for conservation management is particularly important where species boundaries are not easy determined (Barrowclough et al. 2011).

Here, I use SDM and MGWR to investigate differences in habitat use by *G. agassizii* and *G. morafkai* in the recent secondary contact zone. Specifically, I aim to 1)

identify geographical boundaries in habitat use between the two species, and 2) determine which of three delineations better describes landscape patterns of genotypic variation. These delineations include A) the Colorado River, the current geographic boundary defining each species, B) the Mojave and Sonoran Basin and Range ecotone, and C) geographic similarities in local habitat use identified in this study. The results of this study will inform conservation planning in the secondary contact zone of these two species.

METHODS

Study Area

My study area included the known range of *G. agassizii and G. morafkai* across 68,323 km^2 in the southwestern United States encompassing parts of California, Arizona, Nevada and Utah (Figure 4.1). This region is characterized as the Mojave Basin and Range Level III Ecoregion and Sonoran Basin and Range Level III Ecoregion (Commission for Environmental Cooperation Working Group 1997); hereafter the Mojave Desert and Sonoran Desert, respectively. The subregion encompassing the genetic sampling locations used by Edwards et al. (2015) offered an opportunity to explore habitat selection across the ecotone between the Mojave and Sonoran deserts, and the secondary contact zone between *G. agassizii and G. morafkai*.

Modeling Overview

I incorporate a 2-stage modeling approach drawing on the strengths of both SDM and MGWR to explore spatial non-stationarity in the species-environment relationships of *G. agassizii* and *G. morafkai* across this secondary contact zone. I treat the mapped *residuals* of SDM predictions as measures of local deviation from habitat preference of

the pooled-species and use MGWR of those residuals to explore non-stationarity in relationships to hypothesized environmental explanatory variables that may enumerate differences between the two species and their hybrids. While the interpretation of residuals is perhaps less intuitive than of global regression coefficients, residuals offer a local measure of SDM error that can be linked to explanatory variables with MGWR. This allows MGWR to illuminate landscape gradients in habitat selection in areas where logistic MGWR models with biased observation data would fail to converge.

Species Distribution Modeling

I developed pooled species distribution models for *G. agassizii* and *G. morafkai* using Generalized Additive Models (GAM) with the package *mgcv* (Wood 2011) in R (R Core Team 2016) in a presence/pseudo-absence framework. I treated *G. agassizii* and *G. morafkai* as a single taxon and pooled over 25,000 observations of both from 1970 through 2013 from over 23 separate datasets spanning the US portions of the two species' known ranges. Observations with spatial precision of less than 1 km were discarded, and the remainder were limited to one per each 1-km^2 grid cell resulting in 8728 observations available for model calibration. Pseudo-absence data (Zarnetske et al. 2007) were generated for each species by taking equally sized random samples of grid cells without observations but excluding areas within 2 km of an observation. To reduce the effects of sample bias caused by aggregated observations, I used a geographically weighted resampling method with 20 replications of sampling without replacement. This method assumes that geographically clustered calibration data result in environmental sampling bias (Boria et al. 2014) and that thinning observations from heavily sampled areas will reduce this bias. The resampling method used a grid (10 km cell size) placed across the

study area to identify areas where spatially aggregated observations occurred. In these cells, random selections of no more than three occurrences were used in each replication. A gamma control parameter of 1.3 was used in all GAM models to reduce over-fitting (Wood 2006).

Previous work modelling their habitat suitability has suggested a suite of physiographic, vegetative and climatic characteristics hypothesized to influence the distribution of *G. agassizii* and *G. morafkai* (Nussear et al. 2009, Inman et al. 2014, Edwards et al. 2015). I augmented these variables resulting in 18 explanatory variables available in this study (Table 4.1). I excluded pairs of variables from models with Pearson's correlation values greater than 0.6 to reduce multicollinearity. I evaluated model performance with a random sample of 20 percent of the calibration records withheld each of the 20 replicates. This dataset was used to derive the Area Under the receiver operating characteristic Curve (AUC; Fielding and Bell 1997, Cumming 2000) and Kullback-Leibler mean cross-entropy (MXE; Kullback and Leibler 1951) in the package *ROCR* (Sing et al. 2005) in R (R Core Team 2016). I report the mean and CV of these two measures across all iterations. While the AUC criterion has been used extensively in SDM for evaluating model performance (cf Franklin 2010a), it may be influenced by species prevalence ratios and may not always give a complete picture of model performance (McPherson et al. 2004, Lobo et al. 2008). I therefore also use MXE, a metric that has gained recognition in evaluating the performance of machine learning models (Byrne 1993, Georgiou and Lindquist 2003). I selected a candidate group of the top three models for each of the AUC and MXE performance criteria across the 20 replicates and used them to produce predictive maps; I averaged their outputs to create a

single model of habitat potential for the combined taxon of *G. agassizii* and *G. morafkai*. Residuals from the averaged model were calculated for all observations records and were centered to unit variance prior to use in MGWR.

Multiscale Geographically Weighted Regression

GWR uses spatially explicit kernel weighting schemes to create local parameter estimates (e.g. coefficients, t-values, standard errors and R^2) for each observation. The weighting schemes for classical GWR rely on a single bandwidth parameter, used to define the spatial weighting scheme for all explanatory variables. This parameter can be a fixed size or allowed to shrink and expand to include an optimal number of observations to accommodate variations in observation density. Classical GWR assumes that each explanatory variable interacts with the response vector at the same spatial scale. Here I use the new extension, Multiscale Geographically Weighted Regression, MGWR (Fotheringham et al. 2017), which relaxes this assumption by allowing the relationship for each explanatory variable to be fit at different spatial scales. This is implemented by estimating an optimal bandwidth vector indicating the spatial scale at which each explanatory variable is related to the response vector. A single MGWR model is an amalgamation of many separate regression models and results in locally varying estimates of the relationships between explanatory variables and response vector, and each may have a different spatial scale.

Rather than draw on the same environmental explanatory variables used to create the pooled SDM, I developed a reduced set of predictors for use in the MGWR analysis. MGWR can be more susceptible to multicollinearity than ordinary least squares regression (Fotheringham et al. 2003), and a carefully-chosen reduced set of explanatory

variables is less likely to exhibit multicollinearity. This reduced set of explanatory variables included the principal component axes summing to at least 80% of the component scores in four Principal Component Analyses (PCA) conducted separately for physiographic, climatic, soils and vegetation variables (Appendix 4.1). Principal components provide linearly uncorrelated explanatory variables representing the primary variation among multiple inputs (Abdi and Williams 2010), and offer straightforward methods for reducing the number of potential explanatory variables in an analysis. An additional variable representing highly unsuitable habitat in the form of impervious surfaces (such as paved roads and parking lots) and large water bodies (such as lakes and reservoirs) was created from the 2011 National Land Change Database (NLCD) Percent Developed Imperviousness layer (Fry et al. 2011) and the National Hydrography Dataset (Simley and Carswell 2010) and was quantified as the percent of each grid cell covered by impervious surfaces or water. All variables were centered to unit variance prior to PCA. I hypothesized that the bandwidths for the climate and land use explanatory variables would be larger than those for the vegetation or soil explanatory variables, because responses to climate and land use were not hypothesized to change across the landscape.

I selected a set of these variables for use in MGWR by regressing natural cubic splines with polynomial orders of 2 and 3 of each variable against the pooled SDM residuals. Natural cubic splines were considered due to the non-linear species-environment relationships found in the pooled SDM, and were compared using Bayesian Information Criterion (BIC; Sakamoto et al. 1986) to determine the optimal polynomial order for each variable. Variable selection was conducted using OLS regression with all

combinations of up to 10 variables. A single model was selected as the most parsimonious using the BIC to prevent including unnecessary variables. The set of variables included in this model were used in MGWR to explain the pattern of residuals from the pooled SDM in Python 2.7.10 (Python Software Foundation; http://www.python.org). MGWR uses an iterative back-fitting algorithm that is very computationally intensive (Fotheringham et al. 2017). I therefore thinned the calibration data to 3 per 10 km^2 in order to reduce computation time, resulting in a dataset with 2156 records. This thinning method created a near equal density of observations across the study areas to minimize bias towards the more heavily sampled species, *G. agassizii.* I used an adaptive bandwidth with a Gaussian spatial kernel for each explanatory variable, thereby allowing each explanatory variable to converge on a separate bandwidth with Akaike information criterion with small sample correction (AICc) selection (Fotheringham et al. 2017). Non-linear regression coefficients were not considered as they have not been implemented in MGWR, and because at fine local scales, response curves are expected to approximate linear responses due the limits in local range of each explanatory variable (Fotheringham et al. 2003). Bandwidths for each explanatory variable are reported along with the MGWR model R^2. I use an inverse distance weighted method to interpolate local regression coefficients and MGWR residuals to fill in areas that were thinned prior to running MGWR.

Comparison with Landscape Genetics

I hypothesized that landscape patterns in the interpolated regression coefficient surfaces (species-environment relationships) would be congruent with previously reported genotypes found among individuals in the secondary contact zone identified by

Edwards et al. (2015). I represented genotypes with an index of admixture proportion (Q) of a pure *G. agassizii* genotype from STRUCTURE 2.3.4 (Pritchard et al. 2000). This index represents the probability that an individual contained *G. agassizii* genotypes (Edwards et al. 2015), and was interpolated across my study area using inverse distance weighting to create a map of genotype association index for the Mojave geneotype. I used Kendall's rank correlation coefficient (tau) for paired samples to assess agreement of each explanatory variable's local regression coefficient with the genotype association index and I report tau for each explanatory variable.

I then asked if natural divisions (regions) in the interpolated local regression coefficients exist, and if present, do they coincide with the genotypes highlighted by Edwards et al. (2015). I identify any divisions with a K-mediods optimal partitioning in multi-variate space of the interpolated local regression coefficients for all interpolated local regression coefficients with the package *cluster* (Maechler et al. 2016) in R (R Core Team 2016). The optimal number of clusters was estimated by minimizing within-cluster variance (Hennig and Liao 2013). Cluster assignments were mapped back to geographic space and compared to the taxonomic (geographic) boundary for *G. agassizii* and *G. morafkai* as well as the genotypes of the sampled populations reported by Edwards et al. (2015). Here I used a spatial simultaneous autoregressive lag model (SSAR lag; Anselin 2001) to determine if the current taxonomic division between the two species better explains the genotype association index than does my mapped clusters. The SSAR lag model is well suited for making spatial predictions when dependencies exist among the values of the dependent variable, as is the case for the genotype association index. Three SSAR lag models, each with a single explanatory variable of either the taxonomic

division or mapped cluster, were calibrated with a random subset of 2000 locations to reduce processing time, and were compared using AIC with the package *spdep* (Bivand and Piras 2015) in R (R Core Team 2016).

Finally, I report the area of overlap between the clusters and the two taxonomic (geographic) ranges of the two species, and the mean of the genotype association index for each mapped cluster. I also compare the mapped clusters to the geographic division between the Mojave and Sonoran Deserts as defined by the U.S. EPA Level III Ecoregions to assess any spatial congruence between local regression coefficients and the ecotone between the two ecoregions and report the area of overlap.

RESULTS

Species Distribution Modeling

A total of 20,838 models were considered to represent pooled habitat for *G. agassizii* and *G. morafkai*. The top 6 models had AUC scores that ranged from 0.848 to 0.850 and MXE scores ranging from 0.463 to 0.466 (Appendix 4.2). Thirteen explanatory variables (descriptions found in Table 4.1) were included among these models: ten (PCPsmRt, SMCdiff, SMCs, SurfMat1, SurfMat2, TDIFF, TPX, TWMN, VEG1 and VEG2) were included in all 6 models, while three (SRF, SurfMat3 and VEG3) were included in only 3 of the 6 models (Appendix 4.2). Habitat potential from the average of the top 6 models is shown in Figure 4.2A.

MGWR

I included the first 3 components of each PCA as potential variables in the MGWR. The top performing OLS model predicting the residuals from the pooled SDM included 9 explanatory variables, incorporated 2nd or 3rd order cubic splines for 6 of the

explanatory variables (Appendix 4.3) and had an R^2 of 0.301. Explanatory variables included the 1st and 3rd components of the physiographic PCA, the 1st and 3rd components of the climate PCA, the 2nd and 3rd components of the soils PCA, the 1st and 3rd components of the vegetation PCA and the land use variable (Appendix 4.3). The resulting MGWR model based on these 9 explanatory variables had an R^2 of 0.722 and showed local R^2 values that ranged from near 0 to 0.999 (Figure 4.2B). Local R^2 values were highest in areas where habitat potential was either very low or very high (Figure 4.3). This MGWR model converged on bandwidths of 87 (PHYS1), 110 (PHYS2), 44 (CLIM1), 2154 (CLIM3), 44 (SOIL2), 44 (SOIL3), 2092 (LU2), 137 (VEG1) and 183 (VEG3) nearest neighbors for each explanatory variable. I estimated approximate effect distances as the product of the average distance between nearest neighbors (3 km) and the bandwidths for the explanatory variables, and these effect distances ranged from 49 km to 342 km (Table 4.2). Physiographic (PHYS1 and PHYS2) and soils (SOIL2, SOIL3) explanatory variables were optimized with short effect distances, indicating that their species-environment relationships varied at fine spatial scales across the study area. The vegetation explanatory variables (VEG1, VEG3) showed slightly larger bandwidths with effect distances approaching 100 km, which did not support my hypothesis that vegetation explanatory variables would exhibit the smallest bandwidths. As expected, the explanatory variable representing land use was optimized with the largest bandwidths (effect size = 336 km), indicating a near global species-environment relationship. Interestingly, the two climate explanatory variables showed different bandwidths, with CLIM1 optimizing with an effect size of 48 km, and CLIM3 optimizing at a near global bandwidth with an effect size of 342 km. The CLIM3 climate PCA component was

dominated by the annual temperature range and winter temperature, suggesting little differences between the two species in their response to either. In contrast, the CLIM1 climate PCA component was dominated by annual precipitation and maximum temperatures, suggesting local differences in population responses to regional climate. Parameter surfaces and mapped outputs are provided in Appendix 4.4.

Comparison with Landscape Genetics

Kendall's tau values representing the degree to which local parameter estimates were correlated with my genotype association index ranged from -0.43 to 0.40 (Table 4.3), indicating a low overall agreement between any given parameter estimate and genotype. However, when I identified clusters within the local parameter estimates, the optimum number of clusters in the explanatory variable coefficient surfaces was two when evaluated by average silhouette width. The silhouette width for each partition was 0.18 and 0.46, with isolation values of 1.46 and 1.18 respectively. When mapped back to geographic space, the two partitions were largely characterized by the Mojave and Sonoran deserts (Figure 4.4) with one cluster (Mojave) primarily west of the Colorado River and the other (Sonoran) primarily to the east. The division between the two regions was not directly along the Colorado River, however, and suggested a boundary approximately 40 km to the east of the Colorado River (Figure 4.4). The mean genotype association index for the two clusters was 0.98 and 0.15 for the Mojave and Sonoran clusters, respectively, indicating that the Mojave cluster was strongly associated with the Mojave genotype and the Sonoran cluster was not. The mapped categories of habitat use were better able to predict the genotype association index than either the ecoregions or the taxonomic (geographic) delineation between the species with a ΔAIC score of 51

between the top two models (Table 4.4). Each SSAR lag model had significant spatial terms with the Wald statistic (Rho: 0.984, 0.986, 0.988 for the habitat use, ecoregion and geographic delineation models, respectively). Overlaps between the mapped categories of habitat use and the current geographic delineations of the two species as well as to the Mojave and Sonoran ecoregions, suggested that the Mojave cluster most closely aligned with the Mojave ecoregion (93.1%) and not the current geographic delineation of the Mojave population of *G. agassizii* (Table 4.5). In contrast, the Sonoran cluster most closely aligned with the current geographic delineation of *G. morafkai* (96.6%), indicating that the current geographic delineation of *G. morafkai* is a better representation of Sonoran habitat use than the Sonoran ecoregion alone (Table 4.5). This is likely due to the presence of two additional ecoregion types in the Sonoran habitat use cluster: Arizona and New Mexico Mountains, and Arizona and New Mexico Plateaus.

DISCUSSION

I introduce a novel implementation of SDM to explore locally varying species-environment relationships by coupling SDM with a new extension of Geographically Weighted Regression; MGWR (Fotheringham et al. 2017). My investigation of non-stationarity in species-environment relationships for two sister taxa in a recent secondary contact zone has shown that local variation in habitat selection provides greater support for the phylogenetic differences among individuals than does the current geographic delineation between the two species. My results and recommendations lend additional evidence for the need to consider *G. agassizii* east of the Colorado River and west of Kingman AZ for species protection under the ESA. Here, I also find that habitat barriers such as water and developed surfaces (e.g. roads and cities) have consistently negative

effects on habitat regardless of location, while soil conditions and certain physiographic characteristics exhibit local effects that vary within the recent secondary contact zone.

In support of phylogenetic boundaries

I found evidence for two, but not three, categories (clusters) of habitat selection in the local species-environment parameter estimates. A third category, if it coincided with individuals showing a mixture of genotypes, might suggest that hybrid individuals select habitat in ways that are locally different than either of the two pure genotypes. Previous work did show that hybrid individuals exhibiting a mixture of genotypes also occupied a range of characteristics spanning Mojave and Sonoran habitats in terms of topographic, surface textural, and vegetation characteristics (Edwards et al. 2015). My enumeration of only two categories does not necessarily contradict this finding because I explored habitat selection, i.e. local species-environment relationships, and not differences in occupied habitat. Organisms located in different habitats may exhibit similar species-environment relationships when the local availability of habitat differs from one geographic region to another.

For example, consider individuals in one area that occupy habitats with values near 10 on a hypothetical environmental gradient. If the surrounding habitat has values near 5, these individuals will exhibit positive local species-environment relationships because the locally available habitat is lower on the hypothetical gradient. However, in another region, individuals occupying habitats with values near 5 may also show positive local species-environment relationships if nearby environments show values of 1. In this simple example, the two groups may show similar positive local species-environment parameter estimates even though they occupy different regions of this hypothetical

environmental gradient (i.e. 10 vs 5). This is where coupling SDM with MGWR differs from traditional habitat assessments: local differences in habitat *selection* are uncovered rather than differences in *occupied* habitat.

In the case of *G. agassizii* and *G. morafkai*, regional differences in occupied habitat are clearly evident. Differences span climate, vegetation, physiography, and geology (Nussear and Tuberville 2014), yet I found similar habitat selection (and avoidance) for characteristics such as land use disturbance (e.g. developed surfaces, agriculture and surface water), annual temperature range and winter minimum temperature throughout the secondary contact zone. This suggests that while the two species occupy different habitats, they exhibit similar habitat selection for certain environmental conditions. For example, both *G. agassizii* and *G. morafkai* appear to have range limits defined by cold winter temperatures, and each can tolerate extreme summer temperatures through behavioral aestivation (Nussear and Tuberville 2014). Similarly, disturbed areas such as road, cities and other developed surfaces have consistent negative effects on habitat regardless of location.

In contrast, I found differences in local habitat selection on characteristics such as summer and winter precipitation, terrain (e.g. slope and rockiness), soil (e.g. soil moisture and evapotranspiration) and vegetation (e.g. phenology and canopy growth). Differences in environmental conditions may drive local adaptation and help maintain population structure of genotypes for *G. agassizii* and *G. morafkai*. Ongoing work suggests that genotypic structure within the Mojave population of desert tortoise (those west of the Colorado River) may be maintained by selective pressure on key genes from local environmental differences (T. Edwards, *personal communication*, February 2018). Such

environmental differences include a pronounced precipitation seasonality gradient across the combined ranges of *G. agassizii* and *G. morafkai*, with the most western regions exhibiting high winter (November to March) precipitation and few summer monsoonal storms, whereas eastern and southern areas are more prone to intense monsoonal storms but little winter precipitation. Local adaptation resulting in local habitat selection to these environmental characteristics may help maintain population structure and may provide an opportunity for selective pressure to result in speciation. My results with the genotype association index lend additional support for this hypothesis. Here, I found that the most parsimonious spatial model explaining the landscape pattern of genotype association was the two mapped categories (clusters) of habitat selection in the local species-environment parameter estimates rather than the Mojave and Sonoran ecoregions or the current geographic protection status of the two species.

A novel SDM-MGWR coupled approach

The use of local regression to explore non-stationarity in regression coefficients is not new to SDM but has had limited success given the widespread reliance on binary (presence-absence or presence-background) calibration data necessitating logistic GWR. Logistic GWR suffers from complete separation of response classes at fine spatial scales (Fotheringham et al. 2003), forcing models to use large bandwidths approximating global models (Miller 2012). This is especially problematic when calibration datasets exhibit extreme sampling bias. I avoided this problem by calibrating a MGWR model on the residuals of a pooled SDM for both taxa to explore local deviation in species-environment relationships. Modeling residuals enables the use of Gaussian MGWR models and offers advantages for investigating non-stationarity in species-environment

relationships. By using SDM methods to create predictions of habitat potential, biogeographers can draw on the wealth of species occurrence data in biodiversity archives and SDM methods that have been developed over the past few decades (e.g. Phillips et al. 2006, Franklin 2010b, Elith and Leathwick 2015). These predictions can then be used to investigate non-stationarity with local regression tools such as MGWR.

This coupled approach supports exploration of spatial non-stationarity within small regions of interest, which is necessary when computationally intensive MGWR models require extreme processing times due to their use of an iterative back-fitting algorithm to fit optimal bandwidth vectors (Fotheringham et al. 2017). Additionally, presence-background SDM methods assume that the entirety of a species' range is sampled (Elith and Leathwick 2009, Franklin 2010a) and therefore local regression SDM would also need to include the entirety of a species' range; this would require processing times on the order of months or more for large datasets. However, by using global SDM to create predictions for the entire range, MGWR can be used in a smaller subset of the species' distribution to explore non-stationarity in deviations from these predictions, i.e. residuals.

Importance for conservation

Efforts to preserve biodiversity have placed new emphasis on quantifying and understanding geographic patterns in measures of biodiversity beyond simple taxonomic diversity. Understanding landscape patterns in phylogenetic diversity is especially important to conservation goals aimed at maximizing the resilience of the world's biodiversity in the face of rapid global change (Legendre et al. 2005, Flynn et al. 2011) and identifying conditions where recent lineage divergence has contributed to local

differences in habitat selection that may aid in adapting to changing environments (Crandall et al. 2000, Moritz 2002, Ackerly et al. 2010). Identifying spatially structured variation in habitat association, coupled with an understanding of landscape genetics, is therefore important for predicting potential outcomes from land management conservation decisions (Whittaker et al. 2005, Ferrier and Drielsma 2010). Often, conservation priorities focus on hot spots (Myers et al. 2000, Naeem et al. 2012, Winter et al. 2013) delineated on the basis of taxonomic diversity (Myers et al. 2000, Ferrier et al. 2004), phylogenetic diversity (Crozier 1997, Helmus et al. 2007, Scoble and Lowe 2010, Vandergast et al. 2013, Wood et al. 2013) or measures of evolutionary potential, such as sequence diversity (Tamura and Nei 1993) or divergence (Nei and Li 1979). However, the ability to compare these landscape measures of genetic diversity to landscape patterns of habitat selection (e.g. species-environment relationships) presents new opportunities to investigate the confluence of genetics and ecology in context of conservation biogeography.

Conservation managers tasked as stewards of healthy and sustainable ecosystems often need recommendations for spatially-explicit information that supports management objectives. Lake Mead National Recreation Area, for example, is the agency responsible for stewardship of ~1.5 million acres of southern Nevada and northwest Arizona. Park managers need information on tortoise distributions and lineages in order to prioritize protection and restoration of tortoise habitat impacted by invasive weeds, fire, and road disturbance, recreation and development (Books and Esque 2002, Esque et al. 2010, Lovich et al. 2011). My work lends evidence that the current geographic boundary of the Mojave distinct population segment (Department of the Interior 1990) does not capture

the full extent of *G. agassizii*, and further suggests that local habitat use in and around the secondary contact zone may contribute to uniqueness of *G. agassizii* currently residing on the eastern side of the Colorado River. Protection and restoration of these areas would further park goals of managing and maintaining suitable tortoise habitat.

TABLES

Table 4.1. Explanatory variable Descriptions. Names, abbreviations and general description of 18 explanatory variables considered for modeling the pooled distribution of two desert tortoises, *Gopherus agassizii* (Agassiz's tortoise) and *Gopherus morafkai* (Morafkai's tortoise). Explanatory variables spanned climate, physiographic, vegetation and surface hydrology environmental characteristics. Geographic mean and standard deviation are reported.

Abbreviation	Name	Description	Mean	SD
ST	surface texture	An index of apparent thermal inertia, the heat holding capacity of the surface substrate.	1.371	0.383
SRF	surface roughness	Ratio of surface to planar area, calculated from dem.	1.018	0.031
TPX	topographic position index	Index of surface drainage potential. ln(a/tan(beta)), where a: the area of the hillslope per unit contour length that drains through any point, tan(beta): the local surface topographic slope (delta vertical) / (delta horizontal).	10.848	2.153
SurfMat1	surface material index 1	Component 1 from PCA of 5 emissivity and land surface temperature MODIS data products.	98.018	34.376
SurfMat2	surface material index 2	Component 2 from PCA of 5 emissivity and land surface temperature MODIS data products.	128.547	28.756
SurfMat3	surface material index 3	Component 3 from PCA of 5 emissivity and land surface temperature MODIS data products.	120.262	17.179
TDIFF	seasonal temperature difference	TSMX - TWMN	21.384	2.686
TSMX	maximum summer temperature	Maximum of average temperature of each month during summer season	300.678	4.857
TWMN	minimum winter temperature	Minimum of average temperature for each month during winter season	279.290	4.433
PCPwnt	winter precipitation	Total of monthly precipitation for winter months	182.678	146.388
PCPsmRt	seasonal precipitation difference	(Summer Precipitation +Winter Precipitation)/(Summer precipitation -Winter precipitation)	-0.306	0.268
ETs	summer evapotranspiration	actual evapotranspiration for summer, is moisture limited and summed over all vegetation classes and also over all snow bands, mm	31.151	18.505

Abbreviation	Name	Description	Mean	SD
ETdiff	seasonal evapotranspiration difference	seasonal in actual evapotranspiration for summer, is moisture limited and summed over all vegetation classes and also over all snow bands, mm	19.791	16.051
SMCs	summer soil moisture content	summer soil moisture, mm (state, 1st day of month, summed across the three VIC soil layers)	201.090	65.713
SMCdiff	seasonal soil moisture content difference	seasonal difference soil in moisture, mm (state, 1st day of month, summed across the three VIC soil layers)	1.982	23.920
VEG1	vegetation index 1	Component 1 from PCA of 9 phonological vegetation layers	147.149	
VEG2	vegetation index 2	Component 2 from PCA of 9 phonological vegetation layers	131.959	
VEG3	vegetation index 3	Component 3 from PCA of 9 phonological vegetation layers	149.859	

Table 4.2. Bandwidths and Effective Distances. Multiscale geographically weighted regression summary. Explanatory variable names, bandwidths (BW) and spatial scale (effective distances; km) are given along with the region of interest mean and standard deviation for each species of desert tortoise, *Gopherus agassizii* (Agassiz's tortoise) and *Gopherus morafkai* (Morafkai's tortoise).

NAMES	BW	Effective Distance (km)
SOIL2n	44	48.8
SOIL3n	44	48.8
CLIM1n	44	48.8
VEG1n	137	86.2
CLIM3n	2154	341.6
PHYS2n	110	77.2
VEG3n	183	99.6
LU2n	2092	336.7
PHYS1n	87	68.7

Table 4.3 Correlation to Genotype Association Index. Kendall's rank correlation value for each local parameter surface of the multiscale geographically weighted regression model with the genotype association index. None of the local parameter surfaces showed correlations greater than 0.43, suggesting no direct relationship between any explanatory variables and the genotype association index.

Variable	Tau	p
SOIL2	0.169	p<0.001
SOIL3	0.406	p<0.001
VEG3n	-0.411	p<0.001
PHYS1	-0.437	p<0.001
PHYS2	-0.030	p<0.001
CLIM1	0.048	p<0.001
CLIM3	0.065	p<0.001

Table 4.4. Spatial Model Summary. Spatial simultaneous autoregressive lag models were used to explain the spatial variation in the genotype association index. Each model used one of three explanatory variables and were compared with AIC.

SSAR Lag Model	ΔAIC	AIC	Rho	Rho p	Wald Statistic	Wald p
Mapped Cluster	0	-10121	0.98407	< 0.001	585320	< 0.001
Ecoregion	37	-10084	0.98608	< 0.001	720030	< 0.001
Geographic (taxonomic)	51	-10070	0.98777	< 0.001	872040	< 0.001

Table 4.5. Spatial Overlap between Geographic Clusters. Overlap between each mapped category (cluster) of habitat use with the 1) current geographic delineations between *Gopherus agassizii* (Agassiz's desert tortoise) and *Gopherus morafkai* (Morafka's desert tortoise), and 2) the Mojave and Sonoran Basin and Range U.S. EPA Level III Ecoregions.

	Mojave Cluster	%	Sonoran Cluster	%
G. agassizii (geographic)	21,769	91.2	1,523	3.4
G. morafkai (geographic)	2,091	8.8	42,956	96.6
Mojave Ecoregion	22,215	93.1	4,818	10.8
Sonoran Ecoregion	1,645	6.9	33,521	75.4

FIGURES

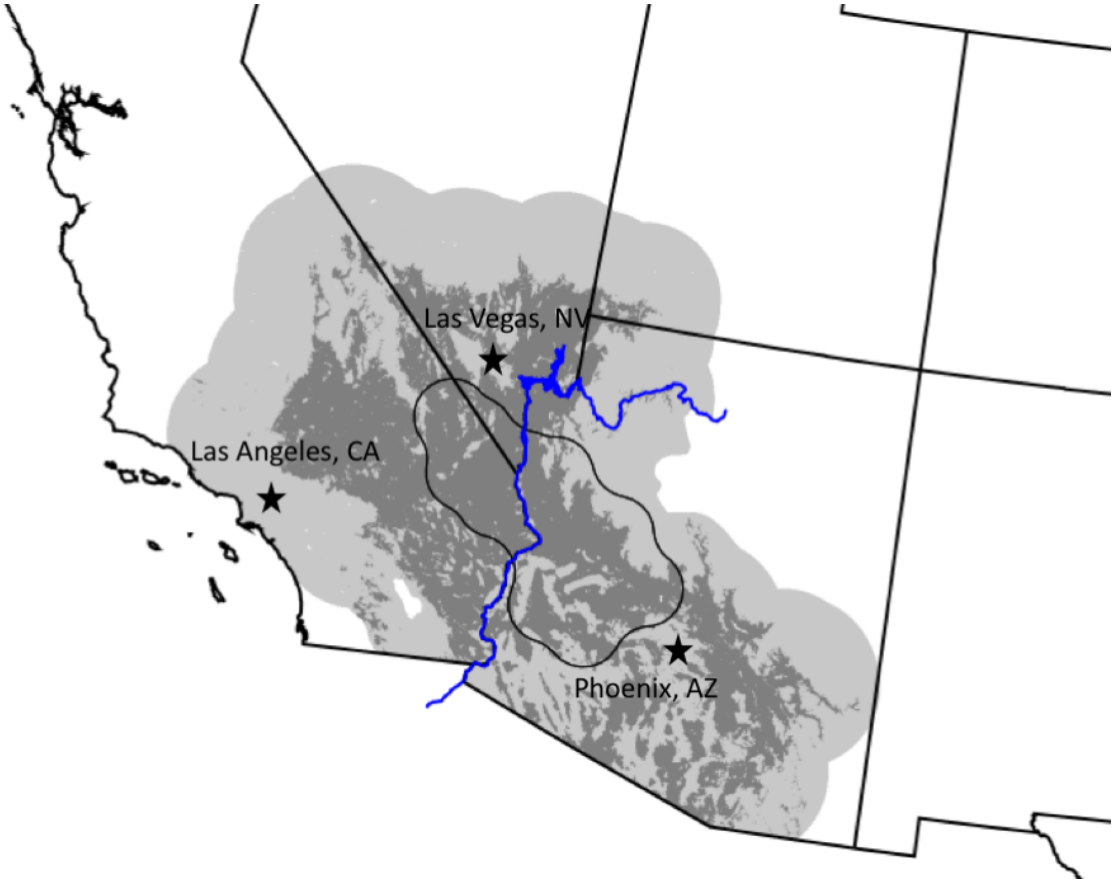

Figure 4.1. Study Area. Study area used to create pooled-taxa species distribution models (light grey) and region of habitat for the two species of desert tortoise, *Gopherus agassizii* (Agassiz's tortoise) and *Gopherus morafkai* (Morafkai's tortoise) in dark grey. Smaller region of interest (black outline) for multiscale geographically weighted regression and genotype assessment. The Colorado River (blue) separates California and Arizona and creates the division between the two species of desert tortoise. A Distinct Population Segment defined as the Mojave population includes individuals located west of the Colorado River.

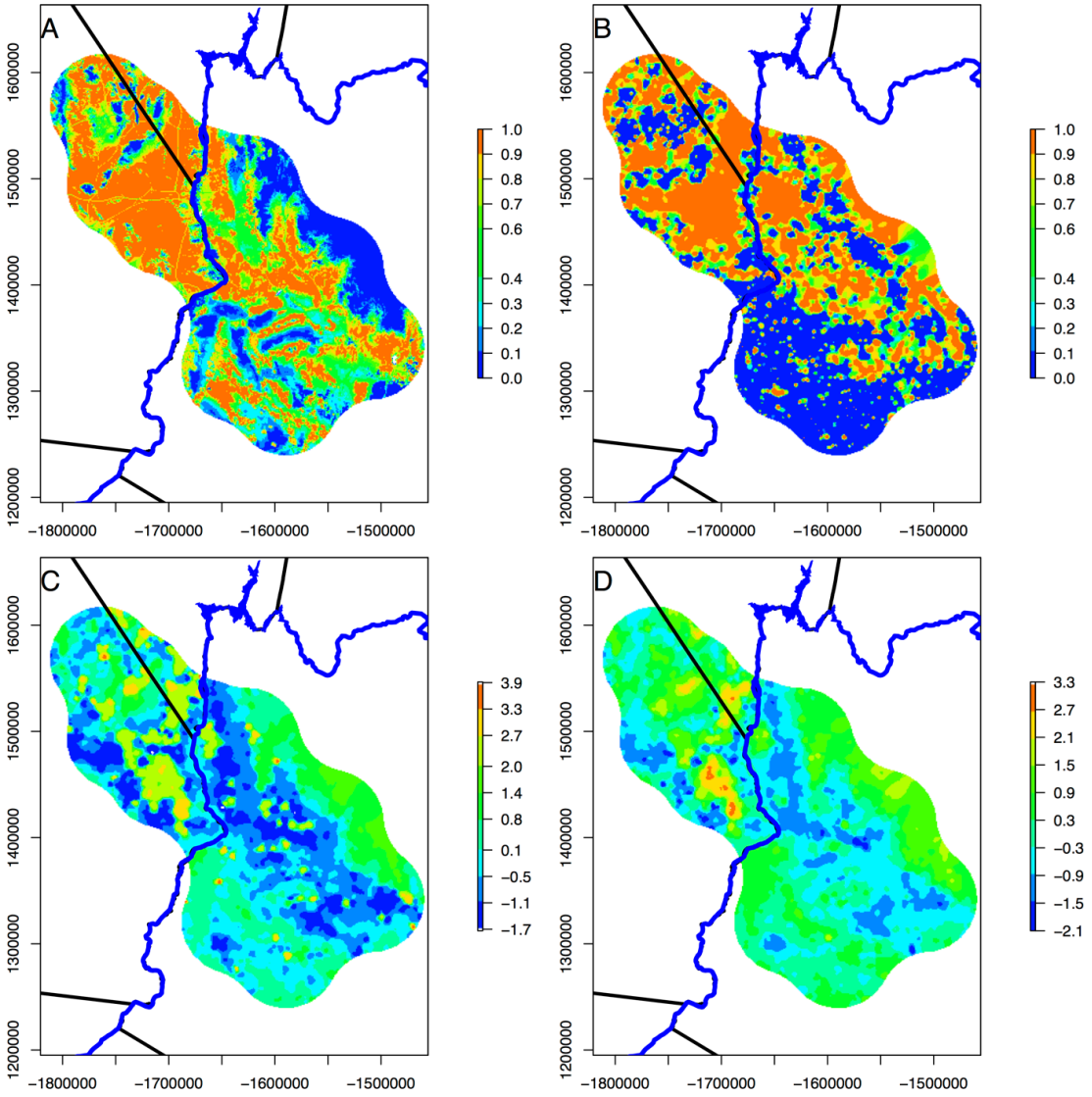

Figure 4.2. Habitat potential and MWGR Predictions. (A) Habitat potential resulting from the average of 6 pooled distribution models. (B) Local R^2 from selected Multiscale Geographically Weighted Regression model of SDM residuals. (C) Standardized residuals from pooled distribution models, and (D) predicted y-hat values from selected Multiscale Geographically Weighted Regression model. The Colorado River (blue) separates California and Arizona and creates the division between the two species of desert tortoise.

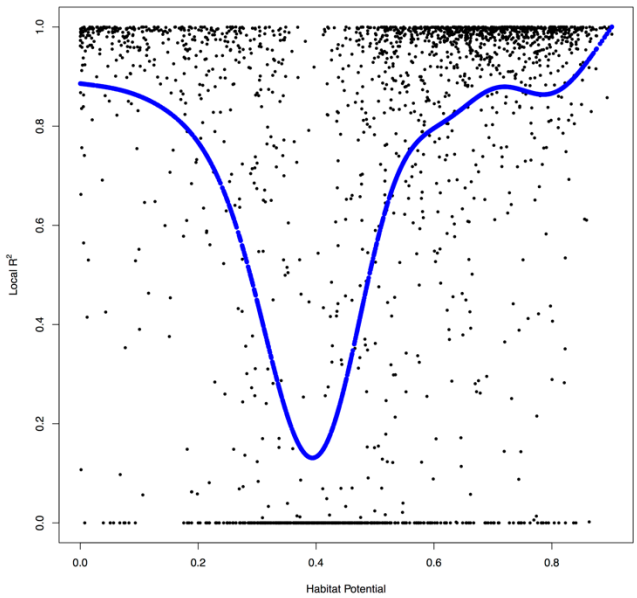

Figure 4.3. Relationship between Habitat Potential and Local R^2. Local R^2 from selected Multiscale Geographically Weighted Regression model was highest for low and high values of habitat potential from the pooled distribution model. A spline regression line (blue) shown for emphasis of low local R^2 values at mediocre habitat potential values.

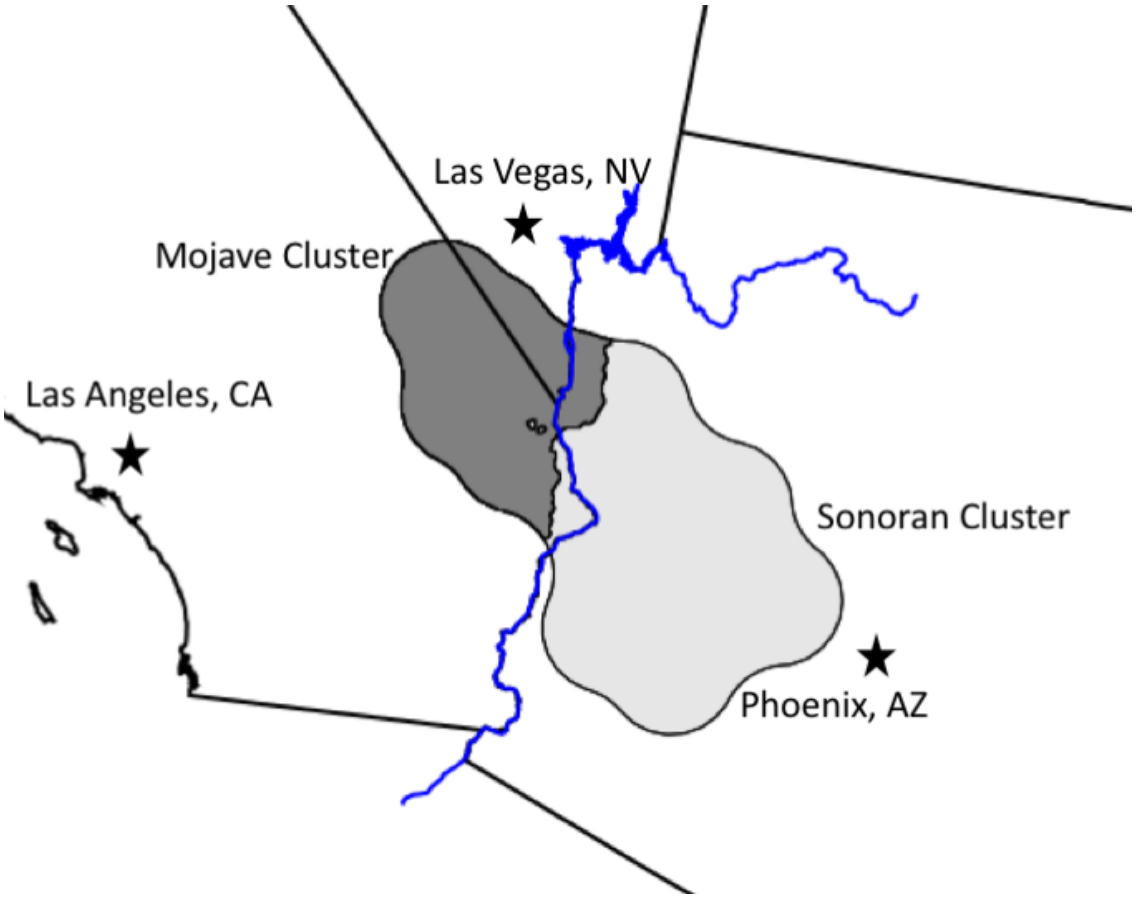

Figure 4.4. Mapped Clusters of Local Habitat Use Parameters. Two categories (clusters) of habitat use identified from local parameter estimates of species-environment relationships. The Mojave cluster (dark grey) includes a region 40 km east of the Colorado River (blue) where *Gopherus agassizii* (Agassiz's tortoise) individuals have been identified but are not protected under the US Endangered Species Act. The Sonoran cluster (light grey), includes a small region west of the Colorado River, though this area contains only marginal habitat.

CHAPTER 5

CONCLUSIONS

In the work presented here, I have investigated how sampling bias can degrade species distribution modelling (SDM), and in each chapter I have presented methods – some novel and new; others familiar and oft-used – to mitigate against biased observations.

The three methods I contrast in Chapter 2 had not previously been systematically evaluated with a robust set of simulated species spanning generalist to specialist niche characteristics. The insight I have provided will benefit biogeographers and spatial ecologists investigating patterns of biodiversity, and those interested in conserving our planet's biota. Researchers and practitioners in these fields have adopted SDM as a primary tool for quantifying the spatial configuration of biodiversity, and for uncovering the processes that have led to – and are changing – those patterns. The issue of sampling bias, then, has far reaching implications for understanding the biodiversity of our earth's history and its future. This is more important than ever if humanity wishes to place some governance on the current loss of biodiversity that is ongoing and expected to worsen in years to come as our earth's climate continues to be destabilized by anthropogenic activities. In Chapter 2, I have shown that even in the presence of low levels of bias, SDM results can be skewed, and that common methods to mitigate against bias did not improve the ability to correctly identify explanatory variables or recreate species-environment relationships. The low levels of bias I used for the simulation studies in Chapter 2 were even lower than the lowest level of bias found in a survey of nine taxonomically diverse species occurring in the southwestern continental USA. Moreover, two of these species exhibited levels of geographic bias rivaling my most biased virtual

species. It seems that identifying true drivers of distributions may be difficult, at best. This is unfortunate since SDM can be used to infer niche characteristics from the explanatory variables and species-environment relationships identified during the calibration process. More often, however, studies using SDM are focused on the spatial predictions of habitat potential. When they do, bias correction methods become important: I found improvements in the accuracy of mapped predictions of habitat potential with the easily implemented FactorBiasOut method for Maxent (Phillips et al. 2006) software. The insight I have provided about bias correction methods and their failure to improve niche variable selection and species-environment relationships further reinforces the need for SDM to be grounded in sound ecological theory prior to model calibration.

While the bias correction methods I compare are most often used, they are not an exhaustive list of available techniques. I was unable to include some recent methods that use changes in model structure to statistically account for sampling bias by representing the variable of interest as a distribution conditional on latent processes (i.e. unmeasured factors affecting the response variable of interest; Wikle 2003). These process models estimate an unknown latent parameter (i.e. biased sampling distribution) from additional covariates that are believed to influence the response variable (Cressie et al. 2009). When cast in a Bayesian framework, these models assume that each process can be nested in a hierarchy and represented as a random variable modeled through posterior-predictive distributions (Banerjee et al. 2014). These models can also use additional covariates to model the underlying environmental sampling bias, such as sampling accessibility due to road proximity or land ownership (Gelfand et al. 2006). Due to logistical constraints, I

was unable to include these additional methods for incorporating sampling bias into SDM. Their use in SDM has been limited, with some authors implementing these methods as hierarchical Bayesian models (HBMs; e.g. Hooten et al. 2003, Gelfand et al. 2006, Chakraborty et al. 2010, Aderhold et al. 2012, Hefley and Hooten 2016) with varying success. These HBMs have many theoretical benefits over other SDM methods, including the capacity to overcome the assumption of spatial independence by using a spatial random effects parameter modeled as conditionally dependent on its neighbors in a Conditional AutoRegressive specification (e.g. Besag et al. 1991). Another substantial benefit of the Bayesian approach is the clarity with which they can represent and quantify uncertainty in the modeling process (Cressie et al. 2009), which is often ignored in many implementations of SDMs (Rocchini et al. 2011). However, these methods are extremely computationally intensive and prohibitive for large datasets and species assemblies.

Instead of using HBMs, I adopt a similar approach in Chapter 3 with a three stage statistical model of the theoretical biased sampling distribution in a paleoecological archive. This novel method represented the biased sampling distribution with a process model, but instead of estimating it as part of a nested hierarchical Bayesian model, I adapted the commonly used Maxent software to use background samples that I selected with a probability equal to that identified in my three stage statistical model of the bias in the Packrat midden archive. Here I found that estimates of paleo-distributions were improved, but that not all species were improved equally. Those with distributions more closely aligned to the hypothesized biased sampling distribution were improved the least, suggesting that this novel method may be less useful for correcting paleo-distribution of species like *Coleogyne ramosissima*, which are restricted to regions where fossilized

middens are most likely to occur. The benefit for numerous other species is improved estimates of historical habitat potential, which advances our understanding of how biodiversity patterns have changed in recent history.

However, the analytical resolution of paleo-SDM is limited to the temporal resolution of available paleoclimate data. In Chapter 3, I used gridded climate reconstructions of the mid-Holocene because they are readily available for geographic analyses at 1 km resolution spatial scales; but they do not represent the temporal variation that has occurred since the start of the Holocene. Instead, these data (and many other modeled paleoclimate data) are the result of simulations run for limited time windows according to prescribed experimental protocols; the result is gridded climate data for periods such as the middle Pliocene (3.3 to 3.0 Ma), last interglacial (125 ka), last glacial maximum (21 ka), mid-Holocene (6 ka), and last millennium (Braconnot et al. 2012). The periods between these prescribed windows of analysis contain immense biological change in our earth's history, and efforts to model and reconstruct climate at finer time slices (e.g. Lorenz et al. 2016, Fordham et al. 2017) offer an exciting opportunity leverage paleo-SDM and the wealth of paleoecological archives for exploring the biodiversity of our earth's history.

The results from chapter 4 shed light on two taxa that diverged approximately 6 mya due to geographic isolation by the Bouse embayment resulting in allopatric speciation (Murphy et al. 2011). Conservation of desert tortoises is particularly important to federal agencies, especially because the Mojave desert tortoise (*Gopherus agassizii*) is protected under the US federal Endangered Species Act (ESA) while its sister species, the Sonoran desert tortoise (*Gopherus morafkai*), is not. Hybridization between the two

species is evident, yet land managers have little guidance on how to protect hybrids or *G. agassizii* in the secondary contact zone. If additional populations of *G. agassizii* and hybrids in Arizona are given formal protection under the ESA (i.e. "listed"), land managers would likely be tasked with new habitat conservation goals. I explore local differences in present-day habitat use and niche separation between these two species and find spatial patterns of habitat use that match genotypic differences between the species; lending further evidence that individuals in Arizona need unique habitat protection.

This novel work has also shown how multiscale geographically weighted regression (MGWR) can be used to identify natural groupings in mapped habitat-use parameters, and that these groupings can be tied back to genetic differences resulting from allopatric speciation. Chapter 4 also demonstrates a key advantage of MGWR over classical GWR, that of unique bandwidths for each model covariate. Bandwidths, in conjunction with adaptive spatial kernels, determine how nearby observations are given higher weights than more distance ones (Fotheringham et al. 2003). Large bandwidths approximate global functions, while small bandwidths result in highly local functions. Some ecologists have struggled with the concept of spatial non-stationarity, because many patterns observed in ecology are assumed to be the result of biophysical processes, which are by definition, stationary due to their foundation in first principles (e.g. an organism's thermodynamic exchange with its proximal environment; Porter and Gates 1969). These relationships (such as an organism's rate of water loss) are governed by physical properties such as an organism's size, shape, solar reflectance, insulation, metabolic rate and so forth, and do not vary as a function of an individual's location on the landscape. With MGWR, these global relationships can remain fixed across

geographic space, while other parameters exhibiting spatial non-stationarity can become locally different; such as the preference for sandy soils or alluvial fans that I have explored in Chapter 4.

The work presented in this dissertation contributes to our broader understanding of spatial and ecological theory by building on the diverse fields of quantitative geography, macro- and evolutionary-ecology and conservation biology, motivated by improving our understanding of geographic distributions and environmental niches of desert adapted species of conservation concern. The contributions made here will not only benefit the conservation of these unique desert adapted organisms but will also benefit the broad fields of spatial ecology, paleobiogeography, landscape ecology and conservation biogeography by contributing new insights on how sampling bias affects SDM.

REFERENCES

Abdi, H., and L. J. Williams. 2010. Principal component analysis. Wiley Interdisciplinary Reviews: Computational Statistics 2:433–459.

Ackerly, D. D., S. R. Loarie, W. K. Cornwell, S. B. Weiss, H. Hamilton, R. Branciforte, and N. J. B. Kraft. 2010. The geography of climate change: implications for conservation biogeography. Diversity and Distributions 16:476–487.

Aderhold, A., D. Husmeier, J. J. Lennon, C. M. Beale, and V. A. Smith. 2012. Hierarchical Bayesian models in ecology: Reconstructing species interaction networks from non-homogeneous species abundance data. Ecological Informatics 11:55–64.

Aiello-Lammens, M. E., R. A. Boria, A. Radosavljevic, B. Vilela, and R. P. Anderson. 2015. spThin: an R package for spatial thinning of species occurrence records for use in ecological niche models. Ecography 38:541–545.

Allison, P. A., and D. J. Bottjer. 2010. Taphonomy. Springer.

Anderson, D. R., and K. P. Burham. 1996. A monitoring program for the desert tortoise. Report to the Desert Tortoise Management ….

Anderson, R. P., and A. Raza. 2010. The effect of the extent of the study region on GIS models of species geographic distributions and estimates of niche evolution: Preliminary tests with montane rodents (genus Nephelomys) in Venezuela. Journal of Biogeography 37:1378–1393.

Angulo, D. F., L. D. Amarilla, A. M. Anton, and V. Sosa. 2017. Colonization in North American Arid Lands: The Journey of Agarito (Berberis trifoliolata) Revealed by Multilocus Molecular Data and Packrat Midden Fossil Remains. Plos One 12:e0168933–25.

Anselin, L. 2001. Spatial econometrics, Chapter 14 in B. Baltagi, ed. A Companion to Theoretical Econometrics.

Anselin, L. 2003. Spatial Econometrics. Pages 310–330 *in* A Companion to Theoretical Econometrics. Blackwell Publishing Ltd, Malden, MA, USA.

Anselin, L., and S. J. Rey. 2009. Perspectives on Spatial Data Analysis. Springer Science & Business Media.

Araújo, M. B., and A. Guisan. 2006. Five (or so) challenges for species distribution modelling. Journal of Biogeography 33:1677–1688.

Araújo, M. B., F. Ferri-Yáñez, F. Bozinovic, P. A. Marquet, F. Valladares, and S. L. Chown. 2013. Heat freezes niche evolution. Ecology Letters 16:1206–1219.

Arundel, S. T. 2002. Modeling Climate Limits of Plants Found in Sonoran Desert Packrat Middens. Quaternary Research 58:112–121.

Atkinson, P. M. 2001. Progress reports, Geographical information science: GeoComputation and nonstationarity. Progress in Physical Geography 25:111–124.

Austin, M. 2002. Spatial prediction of species distribution: an interface between ecological theory and statistical modelling. Ecological Modelling 157:101–118.

Baddeley, A., E. Rubak, and R. Turner. 2015. Spatial Point Patterns: Methodology and Applications with R. Chapman and Hall/CRC Press, London.

Baddeley, A., J. Moller, and R. Waagepetersen. 2000. Non- and semi-parametric estimation of interaction in inhomogeneous point patterns. Statistica Neerlandica 54:329–350.

Banerjee, S., B. P. Carlin, and A. E. Gelfand. 2014. Hierarchical Modeling and Analysis for Spatial Data, Second Edition. CRC Press.

Barrowclough, G. F., R. J. Gutiérrez, J. G. Groth, J. E. Lai, and D. F. Rock. 2011. The Hybrid Zone Between Northern and California Spotted Owls in the Cascade–Sierran Suture Zone. The Condor 113:581–589.

Bell, D. M., and D. R. Schlaepfer. 2016. On the dangers of model complexity without ecological justification in species distribution modeling. Ecological Modelling 330:50–59.

Besag, J., and J. Newell. 1991. The Detection of Clusters in Rare Diseases. Journal of the Royal Statistical Society: Series A (Statistics in Society) 154:143.

Besag, J., J. York, and A. Mollié. 1991. Bayesian image restoration, with two applications in spatial statistics. Annals of the Institute of Statistical Mathematics 43:1–59.

Bickford, S. A., and S. W. Laffan. 2006. Multi-extent analysis of the relationship between pteridophyte species richness and climate. Global Ecology and Biogeography 0:060811081017003–???

Birks, H. H., and H. J. B. Birks. 2000. Future uses of pollen analysis must include plant macrofossils. Journal of Biogeography 27:31–35.

Bivand, R., and G. Piras. 2015. Comparing Implementations of Estimation Methods for Spatial Econometrics. Journal of Statistical Software 63:1–36.

Blois, J. L., J. W. Williams, M. C. Fitzpatrick, S. T. Jackson, and S. Ferrier. 2013. Space can substitute for time in predicting climate-change effects on biodiversity. Proceedings of the National Academy of Sciences 110:9374–9379.

Blonder, B., C. Lamanna, C. Violle, and B. J. Enquist. 2014. The n-dimensional hypervolume. Global Ecology and Biogeography 23:595–609.

Books, M. L., and T. Esque. 2002. Alien Plants and Fire in Desert Tortoise (Gopherus agassizii) Habitat and of the Mojave and Colorado Deserts. Chelonian Conservation and Biology 4:330–340.

Boria, R. A., L. E. Olson, S. M. Goodman, and R. P. Anderson. 2014. Spatial filtering to reduce sampling bias can improve the performance of ecological niche models. Ecological Modelling 275:73–77.

Braconnot, P., S. P. Harrison, M. Kageyama, P. J. Bartlein, V. Masson-Delmotte, A. Abe-Ouchi, B. Otto-Bliesner, and Y. Zhao. 2012. Evaluation of climate models using palaeoclimatic data. Nature Climate Change 2:417–424.

Brewer, S., S. T. Jackson, and J. W. Williams. 2012. Paleoecoinformatics: applying geohistorical data to ecological questions. Trends in ecology & evolution (Personal edition) 27:104–112.

Broadhurst, L. 2015. Pollen Dispersal in Fragmented Populations of the Dioecious Wind-Pollinated Tree, Allocasuarina verticillata (Drooping Sheoak, Drooping She-Oak; Allocasuarinaceae). Plos One 10:e0119498–17.

Brotons, L., W. Thuiller, M. Araujo, and A. Hirzel. 2004. Presence-absence versus presence-only modelling methods for predicting bird habitat suitability. Ecography 27:437–448.

Brown, J. H. 1984. On the Relationship between Abundance and Distribution of Species. The American Naturalist 124:255–279.

Byrne, C. L. 1993. Iterative image reconstruction algorithms based on cross-entropy minimization. Image Processing, IEEE Transactions on 2:96–103.

Cadotte, M. W., and T. Jonathan Davies. 2010. Rarest of the rare: advances in combining evolutionary distinctiveness and scarcity to inform conservation at biogeographical scales. Diversity and Distributions 16:376–385.

Cadotte, M. W., K. Carscadden, and N. Mirotchnick. 2011. Beyond species: functional diversity and the maintenance of ecological processes and services. Journal of Applied Ecology 48:1079–1087.

Carnaval, A. C., and C. Moritz. 2008. Historical climate modelling predicts patterns of current biodiversity in the Brazilian Atlantic forest. Journal of Biogeography 35:1187–1201.

Carrasco, M. A., E. B. Kraatz, E. B. Davis, and A. D. Barnosky. 2005. Miocene Mammal Mapping Project (MIOMAP). University of California Museum of Paleontology.

Chakraborty, A., A. E. Gelfand, A. M. Wilson, A. M. Latimer, and J. A. Silander Jr. 2010. Modeling large scale species abundance with latent spatial processes 4:1403–1429.

Cheng, J., and A. S. Fotheringham. 2013. Multi-scale issues in cross-border comparative analysis 46:138–148.

Cheverud, J. M. 1996. Quantitative genetic analysis of cranial morphology in the cotton-top (Saguinus oedipus) and saddle-back (S. fuscicollis) tamarins. Journal of Evolutionary Biology 9:5–42.

Cheverud, J. M., and G. Marroig. 2007. Research Article Comparing covariance matrices: random skewers method compared to the common principal components model. Genetics and Molecular Biology 30:461–469.

Coats, L. L., K. L. Cole, and J. I. Mead. 2008. 50,000 years of vegetation and climate history on the Colorado Plateau, Utah and Arizona, USA. Quaternary Research 70:322–338.

Cole, K. L., and R. H. Webb. 1985. Late Holocene Vegetation Changes in Greenwater Valley, Mojave Desert, California. Quaternary Research 23:227–235.

Commission for Environmental Cooperation Working Group. (n.d.). Ecological regions of North America—Toward a common perspective: Montreal, Quebec, Commission for Environmental Cooperation. Page 71.

Crandall, K. A., O. Bininda-Emonds, G. M. Mace, and R. K. Wayne. 2000. Considering evolutionary processes in conservation biology. Trends in ecology & evolution (Personal edition) 15:290–295.

Cressie, N., C. A. Calder, J. S. Clark, J. M. Ver Hoef, and C. K. Wikle. 2009. Accounting for uncertainty in ecological analysis: the strengths and limitations of hierarchical statistical modeling. Ecological applications : a publication of the Ecological Society of America 19:553–570.

Crozier, R. H. 1997. Preserving the information content of species: Genetic diversity, phylogeny, and conservation worth. Annual Review of Ecology and Systematics 28:243–268.

Cumming, G. S. 2000. Using between-model comparisons to fine-tune linear models of species ranges. Journal of Biogeography 27:441–455.

Danielson, J. J., and D. B. Gesch. 2011. Global Multi-resolution Terrain Elevation Data 2010 (GMTED2010). U.S. Geological Survey Open-File Report 2011–1073.

Department of the Interior. 1990. *Fish and Wildlife Service, 50 CFR part 17, RIN 1018-AB35. Endangered and threatened wildlife and plants; determination of threatened status for the Mojave population of the desert tortoise (final rule)*. Pages 12178–12191. Federal Register.

Devictor, V., D. Mouillot, C. Meynard, F. Jiguet, W. Thuiller, and N. Mouquet. 2010. Spatial mismatch and congruence between taxonomic, phylogenetic and functional diversity: The need for integrative conservation strategies in a changing world. Ecology Letters 13:1030–1040.

Diggle, P. J., J. A. Tawn, and R. A. Moyeed. 1998. Model-based geostatistics. Applied Statistics-Journal of the Royal Statistical Society Series C 47:299–326.

Dormann, C. F. 2007. Assessing the validity of autologistic regression. Ecological Modelling 207:234–242.

Dudik, M., S. J. Phillips, and R. E. Schapire. 2005. Correcting sample selection bias in maximum entropy density estimation:1–8.

Edwards, T. C., D. R. Cutler, N. E. Zimmermann, L. Geiser, and G. G. Moisen. 2006. Effects of sample survey design on the accuracy of classification tree models in species distribution models. Ecological Modelling 199:132–141.

Edwards, T., K. H. Berry, R. D. Inman, T. C. Esque, K. E. Nussear, C. A. Jones, and M. Culver. 2015. Testing Taxon Tenacity of Tortoises: Evidence for a geographical selection gradient at a secondary contact zone. Ecology and Evolution 5:2095–2114.

Elith, J., and J. Leathwick. 2007. Predicting species distributions from museum and herbarium records using multiresponse models fitted with multivariate adaptive regression splines. Diversity and Distributions 13:265–275.

Elith, J., and J. Leathwick. 2015. Boosted Regression Trees for ecological modeling:1–22.

Elith, J., and J. R. Leathwick. 2009. Species Distribution Models: Ecological Explanation and Prediction Across Space and Time. Annual Review of Ecology, Evolution, and Systematics 40:677–697.

Elith, J., C. Graham, R. P. Anderson, M. Dudik, S. Ferrier, A. Guisan, R. J. Hijmans, F. Huettmann, J. R. Leathwick, A. Lehmann, J. Li, L. G. Lohmann, B. A. Loiselle, G. Manion, C. Moritz, M. Nakamura, Y. Nakazawa, J. M. M. Overton, A. T. Peterson,

S. J. Phillips, K. Richardson, R. Scachetti-Pereira, R. E. Schapire, J. Soberón, S. Williams, M. S. Wisz, and N. E. Zimmermann. 2006. Novel methods improve prediction of species' distributions from occurrence data. Ecography 29:129–151.

Elith, J., M. Kearney, and S. Phillips. 2010. The art of modelling range-shifting species. Methods in Ecology and Evolution 1:330–342.

Elith, J., S. J. Phillips, T. Hastie, M. Dudik, Y. E. Chee, and C. J. Yates. 2011. A statistical explanation of MaxEnt for ecologists. Diversity Distributions 17:43–57.

Endler, J. A. 1977. Geographic Variation, Speciation, and Clines. Princeton University Press.

Esque, T. C., K. E. Nussear, K. K. Drake, A. D. Walde, K. H. Berry, R. C. Averill-Murray, A. P. Woodman, W. I. Boarman, P. A. Medica, J. Mack, and J. S. Heaton. 2010. Effects of subsidized predators, resource variability, and human population density on desert tortoise populations in the Mojave Desert, USA. Endangered Species Research 12:167–177.

Ferrier, S., and M. Drielsma. 2010. Synthesis of pattern and process in biodiversity conservation assessment: a flexible whole-landscape modelling framework. Diversity and Distributions 16:386–402.

Ferrier, S., G. Powell, K. Richardson, G. Manion, J. Overton, T. Allnutt, S. Cameron, K. Mantle, N. Burgess, D. Faith, J. Lamoreux, G. Kier, R. Hijmans, V. Funk, G. Cassis, B. Fisher, P. Flemons, D. Lees, J. Lovett, and R. Van Rompaey. 2004. Mapping more of terrestrial biodiversity for global conservation assessment. Bioscience 54:1101–1109.

Fielding, A., and J. Bell. 1997. A review of methods for the assessment of prediction errors in conservation presence/absence models. Environmental Conservation 24:38–49.

Flynn, D. F. B., N. Mirotchnick, M. Jain, M. I. Palmer, and S. Naeem. 2011. Functional and phylogenetic diversity as predictors of biodiversity-ecosystem-function relationships. Ecology 92:1573–1581.

Foody, G. M. 2004. Spatial nonstationarity and scale-dependency in the relationship between species richness and environmental determinants for the sub-Saharan endemic avifauna. Global Ecology and Biogeography 13:315–320.

Foody, G. M. 2008. GIS: biodiversity applications. Progress in Physical Geography 32:223–235.

Fordham, D. A., F. Saltré, S. Haythorne, T. M. L. Wigley, B. L. Otto-Bliesner, K. C. Chan, and B. W. Brook. 2017. PaleoView: A tool for generating continuous climate

projections spanning the last 21,000 years at regional and global scales. Ecography:1–29.

Fotheringham, A. S. 1997. Trends in quantitative methods 1: stressing the local. Progress in Human Geography 21:88–96.

Fotheringham, A. S., C. Brunsdon, and M. Charlton. 2000. Quantitative Geography. SAGE.

Fotheringham, A. S., C. Brunsdon, and M. Charlton. 2003. Geographically Weighted Regression. John Wiley & Sons.

Fotheringham, A. S., W. Yang, and W. Kang. 2017. Multiscale Geographically Weighted Regression (MGWR). Annals of the American Association of Geographers 107:1247–1265.

Fotheringham, A., C. Brunsdon, and M. Charlton. 2011. Quantitative Geography: Spatial Modelling and the Evolution of Spatial Theory

. Pages 1–23. SAGE Publications Ltd, 1 Oliver's Yard, 55 City Road, London England EC1Y 1SP United Kingdom.

Fourcade, Y. 2016. Comparing species distributions modelled from occurrence data and from expert-based range maps. Implication for predicting range shifts with climate change. Ecological Informatics 36:8–14.

Fourcade, Y., J. O. Engler, D. Rödder, and J. Secondi. 2014. Mapping Species Distributions with MAXENT Using a Geographically Biased Sample of Presence Data: A Performance Assessment of Methods for Correcting Sampling Bias. Plos One 9:e97122–13.

Franklin, J. 2010a. Mapping Species Distributions. Cambridge University Press.

Franklin, J. 2010b. Moving beyond static species distribution models in support of conservation biogeography. Diversity and Distributions 16:321–330.

Franklin, J. 2013. Species distribution models in conservation biogeography: developments and challenges. Diversity and Distributions 19:1217–1223.

Franklin, J., A. J. Potts, E. C. Fisher, R. M. Cowling, and C. W. Marean. 2015. Paleodistribution modeling in archaeology and paleoanthropology. Quaternary Science Reviews 110:1–14.

Franklin, J., K. E. Wejnert, S. A. Hathaway, C. J. Rochester, and R. N. Fisher. 2009. Effect of species rarity on the accuracy of species distribution models for reptiles and amphibians in southern California. Diversity and Distributions 15:167–177.

Frey, J. K. 2009. Distinguishing range expansions from previously undocumented populations using background data from museum records. Diversity and Distributions 15:183–187.

Fry, J., G. Z. Xian, S. Jin, J. Dewitz, C. G. Homer, L. Yang, C. A. Barnes, N. D. Herold, and J. D. Wickham. 2011. Completion of the 2006 national land cover database for the conterminous united states. Photogrammetric Engineering and Remote Sensing 77:858–864.

Gay, L., P. A. Crochet, D. A. Bell, and T. Lenormand. 2008. Comparing clines on molecular and phenotypic traits in hybrid zones: A window on tension zone models. Evolution 62:2789–2806.

Gelfand, A. E., J. A. J. Silander, S. Wu, A. Latimer, P. O. Lewis, A. G. Rebelo, and M. Holder. 2006. Explaining Species Distribution Patterns through Hierarchical Modeling. Bayesian Analysis 1:41–91.

Georgiou, T. T., and A. Lindquist. 2003. Kullback-leibler approximation of spectral density functions. IEEE Transactions on Information Theory 49:2910–2917.

Godsoe, W. 2013. Inferring the similarity of species distributions using Species' Distribution Models. Ecography 37:130–136.

Goring, S., T. Lacourse, M. G. Pellatt, and R. W. Mathewes. 2013. Pollen assemblage richness does not reflect regional plant species richness: a cautionary tale. Journal of Ecology 101:1137–1145.

Graham, C. H., S. Ferrier, F. Huettman, C. Moritz, and A. T. Peterson. 2004a. New developments in museum-based informatics and applications in biodiversity analysis. Trends in ecology & evolution (Personal edition) 19:497–503.

Graham, C. H., S. R. Ron, J. C. Santos, C. J. Schneider, and C. Moritz. 2004b. Integrating phylogenetics and environmental niche models to explore speciation mechanisms in dendrobatid frogs. Evolution 58:1781–1793.

Graham, C., and R. J. Hijmans. 2006. A comparison of methods for mapping species ranges and species richness. Global Ecology and Biogeography 15:578–587.

Guillera-Arroita, G., J. J. Lahoz-Monfort, J. Elith, A. Gordon, H. Kujala, P. E. Lentini, M. A. McCarthy, R. Tingley, and B. A. Wintle. 2015. Is my species distribution model fit for purpose? Matching data and models to applications. Global Ecology and Biogeography 24:276–292.

Guisan, A., and N. Zimmermann. 2000. Predictive habitat distribution models in ecology. Ecological Modelling 135:147–186.

Harnik, P. G., C. Simpson, and J. L. Payne. 2012. Long-term differences in extinction risk among the seven forms of rarity. Proceedings: Biological Sciences 279:4969–4976.

Hefley, T. J., and M. B. Hooten. 2016. Hierarchical Species Distribution Models. Current Landscape Ecology Reports 1:1–11.

Helmus, M. R., T. J. Bland, C. K. Williams, and A. R. Ives. 2007. Phylogenetic measures of biodiversity. American Naturalist 169:E68–E83.

Hennig, C. 2015. fpc: Flexible Procedures for Clustering. R package.

Hennig, C., and T. F. Liao. 2013. How to find an appropriate clustering for mixed-type variables with application to socio-economic stratification. Journal of the Royal Statistical Society Series C-Applied Statistics 62:309–369.

Hernandez, P. A., C. Graham, L. L. Master, and D. L. Albert. 2006. The effect of sample size and species characteristics on performance of different species distribution modeling methods. Ecography 29:773–785.

Hernández fernández, M., and E. S. Vrba. 2005. Macroevolutionary Processes and Biomic Specialization: Testing the Resource-use Hypothesis. Evolutionary Ecology 19:199–219.

Higgins, S. I., R. B. O'Hara, O. Bykova, M. D. Cramer, I. Chuine, E.-M. Gerstner, T. Hickler, X. Morin, M. R. Kearney, G. F. Midgley, and S. Scheiter. 2012. A physiological analogy of the niche for projecting the potential distribution of plants. Journal of Biogeography 39:2132–2145.

Hijmans, R. J., S. E. Cameron, J. L. Parra, P. G. Jones, and A. Jarvis. 2005. Very high resolution interpolated climate surfaces for global land areas. International Journal of Climatology 25:1965–1978.

Hirzel, A. H., V. Helfer, and F. Metral. 2001. Assessing habitat-suitability models with a virtual species. Ecological Modelling 145:111–121.

Hirzel, A., and A. Guisan. 2002. Which is the optimal sampling strategy for habitat suitability modelling. Ecological Modelling 157:331–341.

Hoffmann, A. A., and M. W. Blows. 1994. Species borders: ecological and evolutionary perspectives. Trends in Ecology & Evolution 9:223–227.

Holloway, P., and J. Miller. 2015. Exploring Spatial Scale, Autocorrelation and Nonstationarity of Bird Species Richness Patterns 4:783–798.

Hooten, M. B., D. R. Larsen, and C. K. Wikle. 2003. Predicting the spatial distribution of ground flora on large domains using a hierarchical Bayesian model. Landscape Ecology 18:487–502.

Hortal, J., A. Jiménez-Valverde, J. F. Gómez, J. M. Lobo, and A. Baselga. 2008. Historical bias in biodiversity inventories affects the observed environmental niche of the species. Oikos 117:847–858.

Inman, R. D., K. E. Nussear, T. C. Esque, A. G. Vandergast, S. A. Hathaway, D. A. Wood, K. R. Barr, and R. N. Fisher. 2014. Mapping habitat for multiple species in the Desert Southwest. US Geological Survey.

Jackson, S. T., J. L. Betancourt, M. E. Lyford, S. T. Gray, and K. A. Rylander. 2005. A 40,000-year woodrat-midden record of vegetational and biogeographical dynamics in north-eastern Utah, USA. Journal of Biogeography 32:1085–1106.

Jacobson, G. L. 1991. Packrat Middens and Climate Change. Ecology 72:760–760.

Jiggins, C. D., and J. Mallet. 2000. Bimodal hybrid zones and speciation. Trends in ecology & evolution (Personal edition) 15:250–255.

Kadmon, R., O. Farber, and A. Danin. 2004. Effect of roadside bias on the accuracy of predictive maps produced by bioclimatic models. Ecological applications : a publication of the Ecological Society of America 14:401–413.

Kammer, T. W., T. K. Baumiller, and W. I. Ausich. 1997. Species longevity as a function of niche breadth: Evidence from fossil crinoids. Geology 25:219–222.

Kaufman, L., and P. J. Rousseeuw. 2008. Finding Groups in Data: An Introduction to Cluster Analysis. John Wiley & Sons, Inc., Hoboken, NJ, USA.

Kearney, M. R., A. P. Isaac, and W. P. Porter. 2014. microclim: Global estimates of hourly microclimate based on long-term monthly climate averages. Scientific Data 1.

Kearney, M. R., B. A. Wintle, and W. P. Porter. 2010. Correlative and mechanistic models of species distribution provide congruent forecasts under climate change. Conservation Letters 3:203–213.

Kearney, M., and W. Porter. 2009. Mechanistic niche modelling: combining physiological and spatial data to predict species' ranges. Ecology Letters 12:334–350.

King, J. E., and T. R. Van Devender. 1977. Pollen analysis of fossil packrat middens from the Sonoran Desert. Quaternary Research 8:191–204.

Kolanowska, M., E. Grochocka, and K. Konowalik. 2017. Phylogenetic climatic niche conservatism and evolution of climatic suitability in Neotropical Angraecinae (Vandeae, Orchidaceae) and their closest African relatives. PeerJ 5:e3328–22.

Kramer-Schadt, S., J. Niedballa, J. D. Pilgrim, B. Schröder, J. Lindenborn, V. Reinfelder, M. Stillfried, I. Heckmann, A. K. Scharf, D. M. Augeri, S. M. Cheyne, A. J. Hearn, J. Ross, D. W. Macdonald, J. Mathai, J. Eaton, A. J. Marshall, G. Semiadi, R. Rustam, H. Bernard, R. Alfred, H. Samejima, J. W. Duckworth, C. Breitenmoser-Wuersten, J. L. Belant, H. Hofer, and A. Wilting. 2013. The importance of correcting for sampling bias in MaxEnt species distribution models. Diversity and Distributions 19:1366–1379.

Kullback, S., and R. A. Leibler. 1951. On Information and Sufficiency. The Annals of Mathematical Statistics 22:79–86.

Kupfer, J. A., and C. A. Farris. 2006. Incorporating spatial non-stationarity of regression coefficients into predictive vegetation models. Landscape Ecology 22:837–852.

Legendre, P. 1993. Spatial Autocorrelation - Trouble or New Paradigm 74:1659–1673.

Legendre, P., D. Borcard, and P. R. Peres-Neto. 2005. Analyzing beta diversity: Partitioning the spatial variation of community composition data. Ecological Monographs 75:435–450.

Leroy, B., C. N. Meynard, C. Bellard, and F. Courchamp. 2015. virtualspecies, an R package to generate virtual species distributions. Ecography 39:599–607.

Lima-Ribeiro, M. S., S. Varela, J. González-Hernández, G. de Oliveira, J. A. F. Diniz-Filho, and L. C. Terribile. 2015. EcoClimate: a database of climate data from multiple models for past, present, and future for macroecologists and biogeographers. Biodiversity Informatics 10.

Lobo, J. M., A. Jiménez-Valverde, and R. Real. 2008. AUC: a misleading measure of the performance of predictive distribution models. Global Ecology and Biogeography 17:145–151.

Loiselle, B. A., P. M. Jørgensen, T. Consiglio, I. Jiménez, J. G. Blake, L. G. Lohmann, and O. M. Montiel. 2007. Predicting species distributions from herbarium collections: does climate bias in collection sampling influence model outcomes? Journal of Biogeography 0:070908043732003–???

Lorenz, D. J., D. Nieto-Lugilde, J. L. Blois, M. C. Fitzpatrick, and J. W. Williams. 2016. Downscaled and debiased climate simulations for North America from 21,000 years ago to 2100AD. Scientific Data 3:160048–19.

Lorenzen, E. D., D. Nogués-Bravo, L. Orlando, J. Weinstock, J. Binladen, K. A. Marske, A. Ugan, M. K. Borregaard, M. T. P. Gilbert, R. Nielsen, S. Y. W. Ho, T. Goebel, K. E. Graf, D. Byers, J. T. Stenderup, M. Rasmussen, P. F. Campos, J. A. Leonard, K.-P. Koepfli, D. Froese, G. Zazula, T. W. Stafford, K. Aaris-Sørensen, P. Batra, A. M. Haywood, J. S. Singarayer, P. J. Valdes, G. Boeskorov, J. A. Burns, S. P. Davydov, J. Haile, D. L. Jenkins, P. Kosintsev, T. Kuznetsova, X. Lai, L. D. Martin, H. G. McDonald, D. Mol, M. Meldgaard, K. Munch, E. Stephan, M. Sablin, R. S. Sommer, T. Sipko, E. Scott, M. A. Suchard, A. Tikhonov, R. Willerslev, R. K. Wayne, A. Cooper, M. Hofreiter, A. Sher, B. Shapiro, C. Rahbek, and E. Willerslev. 2011. Species-specific responses of Late Quaternary megafauna to climate and humans. Nature 479:359–364.

Lovich, J. E., J. R. Ennen, K. Meyer, C. Loughran, C. Bjurlin, T. Arundel, W. Turner, C. Jones, and G. M. Groenendaal. 2011. Effects of Wind Energy Production on Growth, Demography, and Survivorship of a Desert Tortoise (Gopherus Agassizii) Population in Southern California with Comparisons to Natural Populations. Herpetological Conservation and Biology 6:161–174.

Luoto, M., J. Pöyry, R. K. Heikkinen, and K. Saarinen. 2005. Uncertainty of bioclimate envelope models based on the geographical distribution of species. Global Ecology and Biogeography 14:575–584.

MacKenzie, D. I. 2005. What are the issues with presence-absence data for wildlife managers? The Journal of Wildlife Management 69:849–860.

MacKenzie, D. I., J. D. Nichols, G. B. Lachman, S. Droege, J. A. Royle, and C. A. Langtimm. 2002. Estimating site occupancy rates when detection probabilities are less than one. Ecology 83:2248–2255.

Maechler, M., P. Rousseeuw, A. Struyf, M. Hubert, and K. Hornik. 2016. cluster: Cluster Analysis Basics and

Malizia, R. W., and A. L. Stigall. 2011. Niche stability in Late Ordovician articulated brachiopod species before, during, and after the Richmondian Invasion. Palaeogeography, Palaeoclimatology, Palaeoecology 311:154–170.

Marmion, M., M. Luoto, R. K. Heikkinen, and W. Thuiller. 2008. The performance of state-of-the-art modelling techniques depends on geographical distribution of species. Ecological Modelling:1–11.

Martinez-Meyer, E., A. Townsend Peterson, and W. W. Hargrove. 2004. Ecological niches as stable distributional constraints on mammal species, with implications for Pleistocene extinctions and climate change projections for biodiversity. Global Ecology and Biogeography 13:305–314.

Mateo, R. G., T. B. Croat, Á. M. Felicísimo, and J. Muñoz. 2010. Profile or group discriminative techniques? Generating reliable species distribution models using pseudo-absences and target-group absences from natural history collections. Diversity and Distributions 16:84–94.

McAuliffe, J. R., and T. R. Van Devender. 1998. A 22,000-year record of vegetation change in the north-central Sonoran Desert. Palaeogeography, Palaeoclimatology, Palaeoecology 141:253–275.

McIntyre, S., and S. Lavorel. 1994. Predicting Richness of Native, Rare, and Exotic Plants in Response to Habitat and Disturbance Variables across a Variegated Landscape. Conservation Biology 8:521–531.

McKinney, M. L. 1997. Extinction vulnerability and selectivity: Combining ecological and paleontological views. Annual Review of Ecology and Systematics 28:495–516.

McLuckie, A. M., T. Lamb, C. R. Schwalbe, and R. D. McCord. 1999. Genetic and Morphometric Assessment of an Unusual Tortoise (Gopherus agassizii) Population in the Black Mountains of Arizona. Journal of Herpetology 33:36.

McPherson, J., W. Jetz, and D. J. Rogers. 2004. The effects of species' range sizes on the accuracy of distribution models: ecological phenomenon or statistical artefact? Journal of Applied Ecology 41:811–823.

Mead, J. I. 1981. The Last 30,000 Years of Faunal History Within the Grand-Canyon, Arizona. Quaternary Research 15:311–326.

Mensing, S. A., R. G. Elston Jr, G. L. Raines, and R. J. Tausch. 2000. A GIS model to predict the location of fossil packrat (Neotoma) middens in central Nevada. Western North American ….

Merow, C., M. J. Smith, T. C. Edwards, A. Guisan, S. M. McMahon, S. Normand, W. Thuiller, R. O. Wüest, N. E. Zimmermann, and J. Elith. 2014. What do we gain from simplicity versus complexity in species distribution models? Ecography 37:1267–1281.

Mesgaran, M. B., R. D. Cousens, and B. L. Webber. 2014. Here be dragons: a tool for quantifying novelty due to covariate range and correlation change when projecting species distribution models. Diversity and Distributions 20:1147–1159.

Meynard, C. N., and D. M. Kaplan. 2012. Using virtual species to study species distributions and model performance. Journal of Biogeography:n/a–n/a.

Miller, J. A. 2012. Species distribution models: Spatial autocorrelation and non-stationarity. Progress in Physical Geography 36:681–692.

Miller, J. A. 2014. Virtual species distribution models: Using simulated data to evaluate aspects of model performance. Progress in Physical Geography 38:117–128.

Miller, J. A., and R. Q. Hanham. 2011. Spatial nonstationarity and the scale of species–environment relationships in the Mojave Desert, California, USA. International Journal of Geographical Information Science 25:423–438.

Miller, J., J. Franklin, and R. Aspinall. 2007. Incorporating spatial dependence in predictive vegetation models. Ecological Modelling 202:225–242.

Moreno-Amat, E., J. M. Rubiales, C. Morales-Molino, and I. García-Amorena. 2017. Incorporating plant fossil data into species distribution models is not straightforward: Pitfalls and possible solutions. Quaternary Science Reviews 170:56–68.

Moritz, C. 2002. Strategies to protect biological diversity and the evolutionary processes that sustain it. Systematic Biology 51:238–254.

Moudrý, V. 2015. Modelling species distributions with simulated virtual species. Journal of Biogeography 42:1365–1366.

Murphy, R., K. Berry, T. Edwards, A. Leviton, A. Lathrop, and J. D. Riedle. 2011. The dazed and confused identity of Agassiz's land tortoise, Gopherus agassizii (Testudines: Testudinidae) with the description of a new species and its consequences for conservation. ZooKeys 113:39.

Myers, N., R. Mittermeier, C. Mittermeier, G. da Fonseca, and J. Kent. 2000. Biodiversity hotspots for conservation priorities 403:853–858.

Naeem, S., J. E. Duffy, and E. Zavaleta. 2012. The Functions of Biological Diversity in an Age of Extinction. Science 336:1401–1406.

Nei, M., and W. H. Li. 1979. Mathematical model for studying genetic variation in terms of restriction endonucleases. Proceedings of the National Academy of Sciences 76:5269–5273.

Neteler, M., M. H. Bowman, M. Landa, and M. Metz. 2012. GRASS GIS: A multi-purpose open source GIS. Environmental Modelling and Software 31:124–130.

Newbold, T. 2010. Applications and limitations of museum data for conservation and ecology, with particular attention to species distribution models. Progress in Physical Geography 34:3–22.

Nogués-Bravo, D. 2009. Predicting the past distribution of species climatic niches. Global Ecology and Biogeography 18:521–531.

Nogués-Bravo, D., J. Rodríguez, J. Hortal, P. Batra, and M. B. Araújo. 2008. Climate Change, Humans, and the Extinction of the Woolly Mammoth. PLoS Biology 6:e79.

Nussear, K. E., and T. D. Tuberville. 2014. Habitat characteristics of North American tortoises: chapter 9.

Nussear, K. E., T. C. Esque, R. D. Inman, L. Gass, and K. A. Thomas. 2009. Modeling habitat of the desert tortoise (Gopherus agassizii) in the Mojave and parts of the Sonoran Deserts of California, Nevada, Utah, and Arizona. US Geological Survey.

Nürnberg, S., and M. Aberhan. 2013. Habitat breadth and geographic range predict diversity dynamics in marine Mesozoic bivalves. Paleobiology 39:360–372.

Okabe, A., T. Satoh, and K. Sugihara. 2009. A kernel density estimation method for networks, its computational method and a GIS-based tool. International Journal of Geographical Information Science 23:7–32.

Pearman, P. B., C. F. Randin, O. Broennimann, P. Vittoz, W. O. van der Knaap, R. Engler, G. Le Lay, N. E. Zimmermann, and A. Guisan. 2008. Prediction of plant species distributions across six millennia. Ecology Letters 11:357–369.

Pearson, R. G., and T. P. Dawson. 2003. Predicting the impacts of climate change on the distribution of species: are bioclimate envelope models useful? Global Ecology and Biogeography 12:361–371.

Peterson, A. T. 2011. Ecological niche conservatism: a time-structured review of evidence. Journal of Biogeography 38:817–827.

Peterson, A. T., and Á. S. Nyári. 2008. Ecological niche conservatism and pleistocene refugia in the thrush-like Mourner, Schiffornis sp., in the neotropics. Evolution 62:173–183.

Peterson, A. T., J. Soberón, and V. Sanchez-Cordero. 1999. Conservatism of ecological niches in evolutionary time. Science 285:1265–1267.

Phillips, A. M., T. R. Van Devender, and T. R. Van Deveneer. 1974. Pleistocene Packrat Middens from the Lower Grand Canyon of Arizona. Journal of the Arizona Academy of Science 9:117.

Phillips, S. J., and M. Dudik. 2008. Modeling of species distributions with Maxent: New extensions and a comprehensive evaluation. Ecography 31:161–175.

Phillips, S. J., M. Dudik, and R. E. Schapire. 2018. Maxent software for modeling species niches and distributions (Version 3.4.1).

Phillips, S. J., M. Dudik, J. Elith, C. Graham, A. Lehmann, J. Leathwick, and S. Ferrier. 2009. Sample selection bias and presence-only distribution models: Implications for background and pseudo-absence data. Ecological Applications 19:181–197.

Phillips, S. J., R. P. Anderson, and R. E. Schapire. 2006. Maximum entropy modeling of species geographic distributions. Ecological Modelling 190:231–259.

Phillips, S. J., R. P. Anderson, M. Dudik, R. E. Schapire, and M. E. Blair. 2017. Opening the black box: an open-source release of Maxent. Ecography 40:887–893.

Ponder, W. F., G. A. Carter, P. Flemons, and R. R. Chapman. 2001. Evaluation of Museum Collection Data for Use in Biodiversity Assessment. Conservation biology : the journal of the Society for Conservation Biology 15:648–657.

Porter, W. P., and D. M. Gates. 1969. Thermodynamic Equilibria of Animals with Environment 39:227.

Pritchard, J. K., M. Stephens, and P. Donnelly. 2000. Inference of population structure using multilocus genotype data. Genetics 155:945–959.

Pulliam, H. 2000. On the relationship between niche and distribution. Ecology Letters 3:349–361.

R Core Team. 2016. R: A language and environment for statistical computing. R Foundation for Statistical Computing, Vienna, Austria.

Rahbek, C., and G. R. Graves. 2001. Multiscale assessment of patterns of avian species richness. Proceedings of the National Academy of Sciences 98:4534–4539.

Ranc, N., L. Santini, C. Rondinini, L. Boitani, F. Poitevin, A. Angerbjörn, and L. Maiorano. 2016. Performance tradeoffs in target-group bias correction for species distribution models. Ecography 40:1076–1087.

Raup, D. M. 1972. Taxonomic Diversity during the Phanerozoic. Science 177:1065–1071.

Revell, L. J. 2012. phytools: an R package for phylogenetic comparative biology (and other things). Methods in Ecology and Evolution 3:217–223.

Rocchini, D., J. Hortal, S. Lengyel, J. M. Lobo, A. Jiménez-Valverde, C. Ricotta, G. Bacaro, and A. Chiarucci. 2011. Accounting for uncertainty when mapping species distributions: The need for maps of ignorance. Progress in Physical Geography 35:211–226.

Roff, D. A., J. M. Prokkola, I. Krams, and M. J. Rantala. 2012. There is more than one way to skin a G matrix. Journal of Evolutionary Biology 25:1113–1126.

Sakamoto, Y., M. Ishiguro, and G. Kitagawa. 1986. Akaike Information Criterion Statistics. D. Reidel Publishing Company.

Saupe, E. E., H. Qiao, J. R. Hendricks, R. W. Portell, S. J. Hunter, J. Soberón, and B. S. Lieberman. 2015. Niche breadth and geographic range size as determinants of species survival on geological time scales. Global Ecology and Biogeography 24:1159–1169.

Saupe, E. E., J. R. Hendricks, R. W. Portell, H. J. Dowsett, A. Haywood, S. J. Hunter, and B. S. Lieberman. 2014. Macroevolutionary consequences of profound climate change on niche evolution in marine molluscs over the past three million years. Proceedings of the Royal Society B: Biological Sciences 281:20141995–20141995.

Schoener, T. W. 1968. The Anolis Lizards of Bimini: Resource Partitioning in a Complex Fauna. Ecology 49:704–726.

Scoble, J., and A. J. Lowe. 2010. A case for incorporating phylogeography and landscape genetics into species distribution modelling approaches to improve climate adaptation and conservation planning. Diversity and Distributions 16:343–353.

Segurado, P., and M. Araujo. 2004. An evaluation of methods for modelling species distributions. Journal of Biogeography 31:1555–1568.

Seo, C., J. H. Thorne, L. Hannah, and W. Thuiller. 2009. Scale effects in species distribution models: implications for conservation planning under climate change. Biology Letters 5:39–43.

Serra-Varela, M. J., D. Grivet, L. Vincenot, O. Broennimann, J. Gonzalo-Jiménez, and N. E. Zimmermann. 2015. Does phylogeographical structure relate to climatic niche divergence? A test using maritime pine (Pinus pinasterAit.). Global Ecology and Biogeography 24:1302–1313.

Service, U. S. F. A. W. 2015. Species Status Assessment for the Sonoran Desert Tortoise:1–35.

Signor, P. 1982. Species richness in the Phanerozoic: Compensating for sampling bias. Geology 10:625–628.

Simley, J. D., and W. J. Carswell. 2010. *The National Map*—Hydrography: U.S. Geological Survey Fact Sheet 2009-3054:1–4.

Sinclair, S. J., M. D. White, and G. R. Newell. 2010. How useful are species distribution models for managing biodiversity under future climates. Ecology and Society 15.

Sing, T., O. Sander, N. Beerenwinkel, and T. Lengauer. 2005. ROCR: visualizing classifier performance in R. Bioinformatics 21:3940–3941.

Slatyer, R. A., M. Hirst, and J. P. Sexton. 2013. Niche breadth predicts geographical range size: a general ecological pattern. Ecology Letters 16:1104–1114.

Soultan, A., and K. Safi. 2017. The interplay of various sources of noise on reliability of species distribution models hinges on ecological specialisation. Plos One 12:e0187906–20.

Spaulding, W. G. 1990. Vegetation dynamics during the last deglaciation, southeastern Great Basin, U.S.A. Quaternary Research 33:188–203.

Stigall, A. L. 2012. Using ecological niche modelling to evaluate niche stability in deep time. Journal of Biogeography 39:772–781.

Stigall, A. L. 2014. When and how do species achieve niche stability over long time scales? Ecography 37:1123–1132.

Stolar, J., and S. E. Nielsen. 2015. Accounting for spatially biased sampling effort in presence-only species distribution modelling. Diversity and Distributions 21:595–608.

Strickland, L. E., R. S. Thompson, and K. H. Anderson. 2013. Usgs/Noaa North American Packrat Midden Database, Data Dictionary. BiblioGov.

Strubbe, D., O. Beauchard, and E. Matthysen. 2014. Niche conservatism among non-native vertebrates in Europe and North America. Ecography 38:321–329.

Svenning, J.-C., C. Fløjgaard, K. A. Marske, D. Nogués-Bravo, and S. Normand. 2011. Applications of species distribution modeling to paleobiology. Quaternary Science Reviews 30:2930–2947.

Swetnam, T. W., and C. D. Allen. 1999. Applied historical ecology: using the past to manage for the future. Ecological Applications 9:1189–1206.

Syfert, M. M., M. J. Smith, and D. A. Coomes. 2013. The Effects of Sampling Bias and Model Complexity on the Predictive Performance of MaxEnt Species Distribution Models. Plos One 8:e55158.

Sørensen, T. 1948. A Method of Establishing Groups of Equal Amplitude in Plant Sociology Based on Similarity of Species Content and Its Application to Analyses of the Vegetation on Danish Commons.

Tamura, K., and M. Nei. 1993. Estimation of the number of nucleotide substitutions in the control region of mitochondrial DNA in humans and chimpanzees. Molecular biology and evolution 10:512–526.

Tews, J., U. Brose, V. Grimm, K. Tielborger, M. C. Wichmann, M. Schwager, and F. Jeltsch. 2004. Animal species diversity driven by habitat heterogeneity/diversity: the importance of keystone structures. Journal of Biogeography 31:79–92.

Thompson, R. S., and K. H. Anderson. 2000. Biomes of western North America at 18,000, 6000 and 0 14C yr bp reconstructed from pollen and packrat midden data. Journal of Biogeography 27:555–584.

Thompson, R. S., K. H. Anderson, R. T. Pelltier, L. E. Strickland, P. J. Bartlein, and S. L. Shafer. 2012. Quantitative estimation of climatic parameters from vegetation data in North America by the mutual climatic range technique. Quaternary Science Reviews 51:18–39.

Thuiller, W., S. Lavorel, and M. B. Araújo. 2005. Niche properties and geographical extent as predictors of species sensitivity to climate change. Global Ecology and Biogeography 14:347–357.

Turner, M. G., R. V. O'Neill, R. H. Gardner, and B. T. Milne. 1989. Effects of changing spatial scale on the analysis of landscape pattern. Landscape Ecology 3:153–162.

Van Devender, T. R., A. M. Phillips, and J. I. Mead. 1977. Late Pleistocene Reptiles and Small Mammals from the Lower Grand Canyon of Arizona. The Southwestern Naturalist 22:49.

Van Devender, T. R., and J. I. Mead. 1978. Early Holocene and late Pleistocene amphibians and reptiles in Sonoran Desert packrat middens. Copeia 1978:464.

van Proosdij, A. S. J., M. S. M. Sosef, J. J. Wieringa, and N. Raes. 2015. Minimum required number of specimen records to develop accurate species distribution models. Ecography 39:542–552.

Vandergast, A., R. Inman, K. Barr, K. Nussear, T. Esque, S. Hathaway, D. Wood, P. Medica, J. Breinholt, C. Stephen, A. Gottscho, S. Marks, W. Jennings, and R. Fisher. 2013. Evolutionary Hotspots in the Mojave Desert 5:293–319.

Varela, S., J. M. Lobo, and J. Hortal. 2011. Using species distribution models in paleobiogeography: A matter of data, predictors and concepts. Palaeogeography, Palaeoclimatology, Palaeoecology 310:451–463.

Varela, S., R. P. Anderson, R. García-Valdés, and F. Fernández-González. 2014. Environmental filters reduce the effects of sampling bias and improve predictions of ecological niche models. Ecography 37:no–no.

Vaughan, T. A. 1990. Ecology of living packrats. *in* Packrat middens; the last 40,000 years of biotic change. University of Arizona Press, Tucson.

Veloz, S. D. 2009. Spatially autocorrelated sampling falsely inflates measures of accuracy for presence-only niche models. Journal of Biogeography 36:2290–2299.

Viau, A. E., K. Gajewski, M. C. Sawada, and P. Fines. 2006. Millennial-scale temperature variations in North America during the Holocene. Journal of Geophysical Research Atmospheres 111.

Vilhena, D. A., and A. B. Smith. 2013. Spatial Bias in the Marine Fossil Record. Plos One 8:e74470–8.

Walls, B. J., and A. L. Stigall. 2011. Analyzing niche stability and biogeography of Late Ordovician brachiopod species using ecological niche modeling. Palaeogeography, Palaeoclimatology, Palaeoecology 299:15–29.

Walls, B. J., and A. L. Stigall. 2012. A field-based analysis of the accuracy of niche models applied to the fossil record. Paleontological Contributions.

Warren, D. L., and S. N. Seifert. 2011. Ecological niche modeling in Maxent: the importance of model complexity and the performance of model selection criteria. Ecological applications : a publication of the Ecological Society of America 21:335–342.

Warren, D. L., R. E. Glor, and M. Turelli. 2008. Environmental niche equivalency versus conservatism: quantitative approaches to niche evolution. Evolution 62:2868–2883.

Webb, R. H., and J. L. Betancourt. 1990. The spatial and temporal distribution of radiocarbon ages from pack-rat middens. *in* Packrat middens; the last 40,000 years of biotic change. University of Arizona Press, Tucson.

Wells, P. V. 1966. Late Pleistocene Vegetation and Degree of Pluvial Climatic Change in the Chihuahuan Desert. Science 153:970–975.

Wells, P. V. 1976. Macrofossil Analysis of wood rat (Neotoma) Middens as a Key to the Quaternary Vegetational History of Arid America. Quaternary Research 6:223–248.

Wells, P. V., and R. Berger. 1967. Late Pleistocene History of Coniferous Woodland in the Mohave Desert. Science 155:1640–1647.

Whittaker, R. J., M. B. Araújo, J. Paul, R. J. Ladle, J. Watson, and K. J. Willis. 2005. Conservation Biogeography: assessment and prospect. Diversity and Distributions 11:3–23.

Wiens, J. A., D. Stralberg, D. Jongsomjit, C. A. Howell, and M. A. Snyder. 2009. Niches, models, and climate change: assessing the assumptions and uncertainties. PNAS 106 Suppl 2:19729–19736.

Wiens, J., and C. Graham. 2005. Niche Conservatism: Integrating Evolution, Ecology, and Conservation Biology. Annual Review of Ecology, Evolution, and Systematics 36:519–539.

Wiens, J., and R. Harrison. 2004. Speciation and ecology revisited: phylogenetic niche conservatism and the origin of species. Evolution 58:193.

Wiens, J., D. D. Ackerly, A. P. Allen, B. L. Anacker, L. B. Buckley, H. V. Cornell, E. I. Damschen, T. Jonathan Davies, J.-A. Grytnes, S. P. Harrison, B. A. Hawkins, R. D. Holt, C. M. McCain, and P. R. Stephens. 2010. Niche conservatism as an emerging principle in ecology and conservation biology. Ecology Letters 13:1310–1324.

Wikle, C. K. 2003. Hierarchical Bayesian Models for Predicting the Spread of Ecological Processes 84:1382–1394.

Williams, J. W., E. C. Grimm, J. L. Blois, D. F. Charles, E. B. Davis, S. J. Goring, R. W. Graham, A. J. Smith, M. Anderson, J. Arroyo-Cabrales, A. C. Ashworth, J. L. Betancourt, B. W. Bills, R. K. Booth, P. I. Buckland, B. B. Curry, T. Giesecke, S. T. Jackson, C. Latorre, J. Nichols, T. Purdum, R. E. Roth, M. Stryker, and H. Takahara. 2018. The Neotoma Paleoecology Database, a multiproxy, international, community-curated data resource. Quaternary Research (United States) 89:156–177.

Williams, K. J., L. Belbin, M. P. Austin, J. L. Stein, and S. Ferrier. 2012. Which environmental variables should I use in my biodiversity model? International Journal of Geographical Information Science 26:2009–2047.

Willis, K. J., and R. J. Whittaker. 2002. Ecology. Species diversity--scale matters. Science 295:1245–1248.

Winter, M., V. Devictor, and O. Schweiger. 2013. Phylogenetic diversity and nature conservation: where are we? Trends in ecology & evolution (Personal edition) 28:199–204.

Wisz, M. S., R. J. Hijmans, J. Li, A. T. Peterson, C. H. Graham, A. Guisan, NCEAS Predicting Species Distributions Working Group†. 2008. Effects of sample size on the performance of species distribution models. Diversity and Distributions 14:763–773.

Wood, D. A., A. G. Vandergast, K. R. Barr, R. D. Inman, T. C. Esque, K. E. Nussear, and R. N. Fisher. 2013. Comparative phylogeography reveals deep lineages and regional evolutionary hotspots in the Mojave and Sonoran Deserts. Diversity and Distributions 19:722–737.

Wood, S. 2006. Generalized Additive Models. CRC Press.

Wood, S. N. 2011. Fast stable restricted maximum likelihood and marginal likelihood estimation of semiparametric generalized linear models. Journal of the Royal Statistical Society Series B-Statistical Methodology 73:3–36.

Zarnetske, P. L., T. C. J. Edwards, and G. G. Moisen. 2007. Habitat classification modeling with incomplete data: Pushing the habitat envelope. Ecological applications : a publication of the Ecological Society of America 17:1714–1726.

APPENDIX A (2.1)

MAPPED ENVIRONMENTAL EXPLANATORY VARIABLES

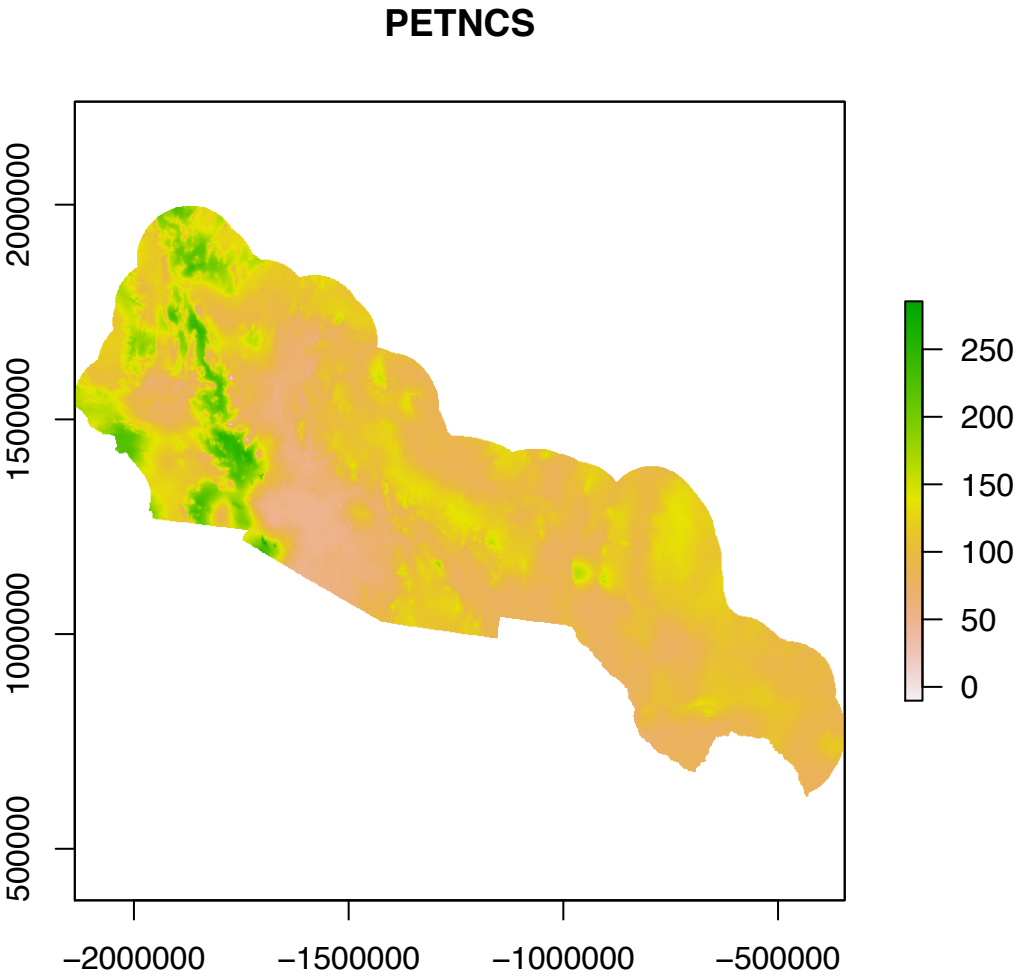
PETNCS
2000000
1500000
1000000
500000
−2000000
−1500000
−1000000
−500000
250
200
150
100
50
0

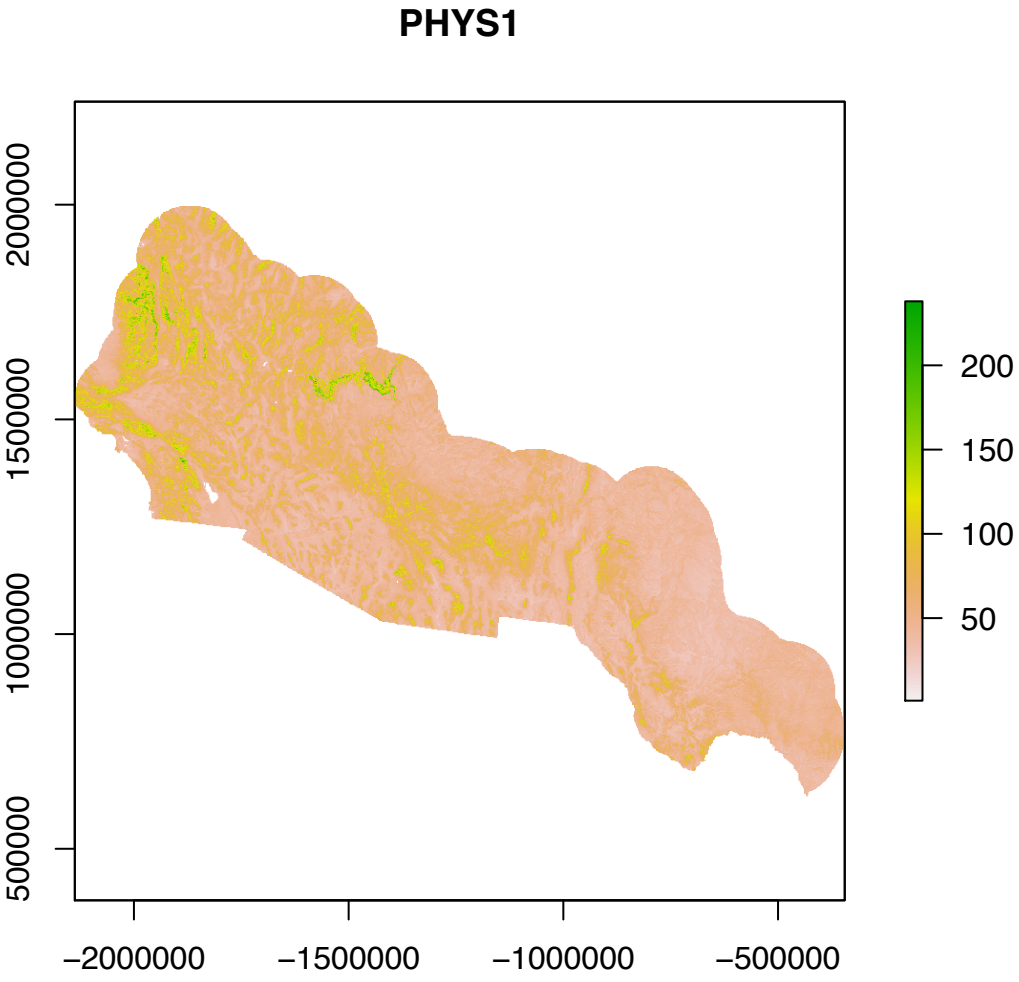
PHYS1
2000000
1500000
1000000
500000
−2000000
−1500000
−1000000
−500000
200
150
100
50

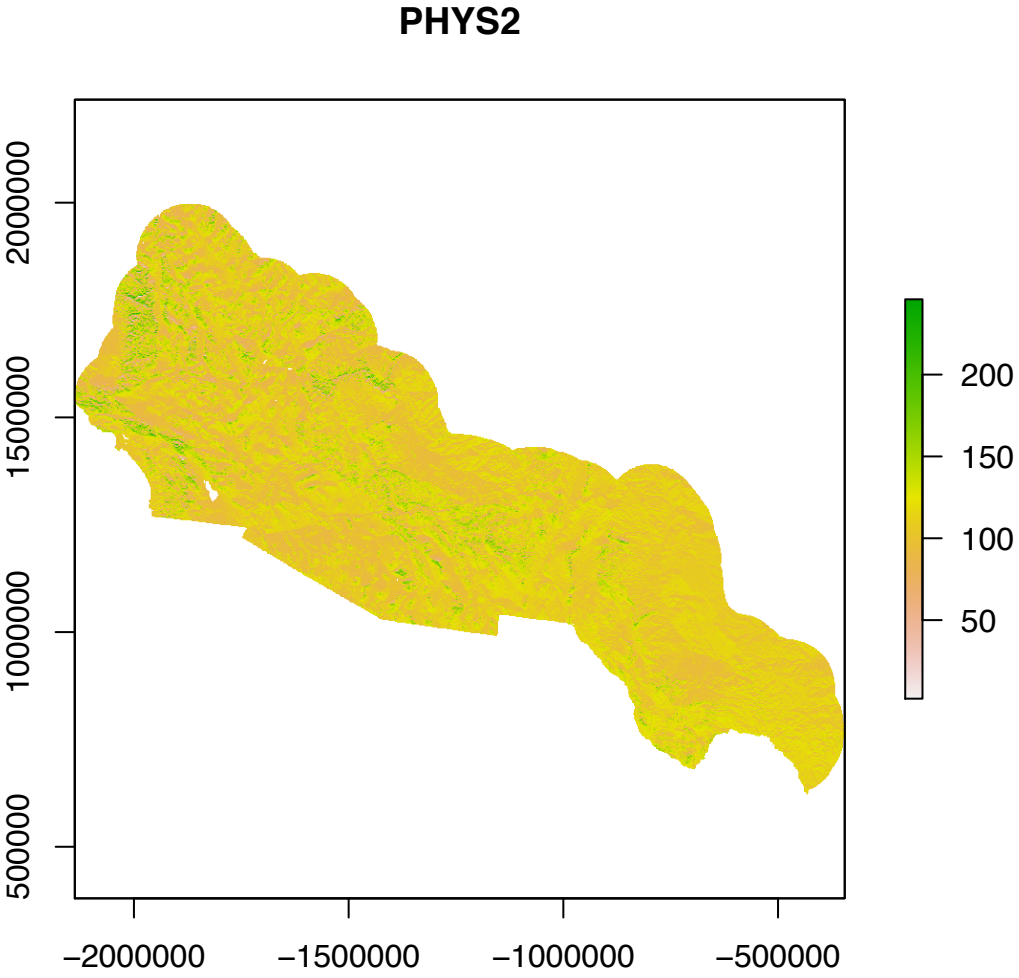
PHYS2
2000000
1500000
1000000
500000
−2000000
−1500000
−1000000
−500000
200
150
100
50

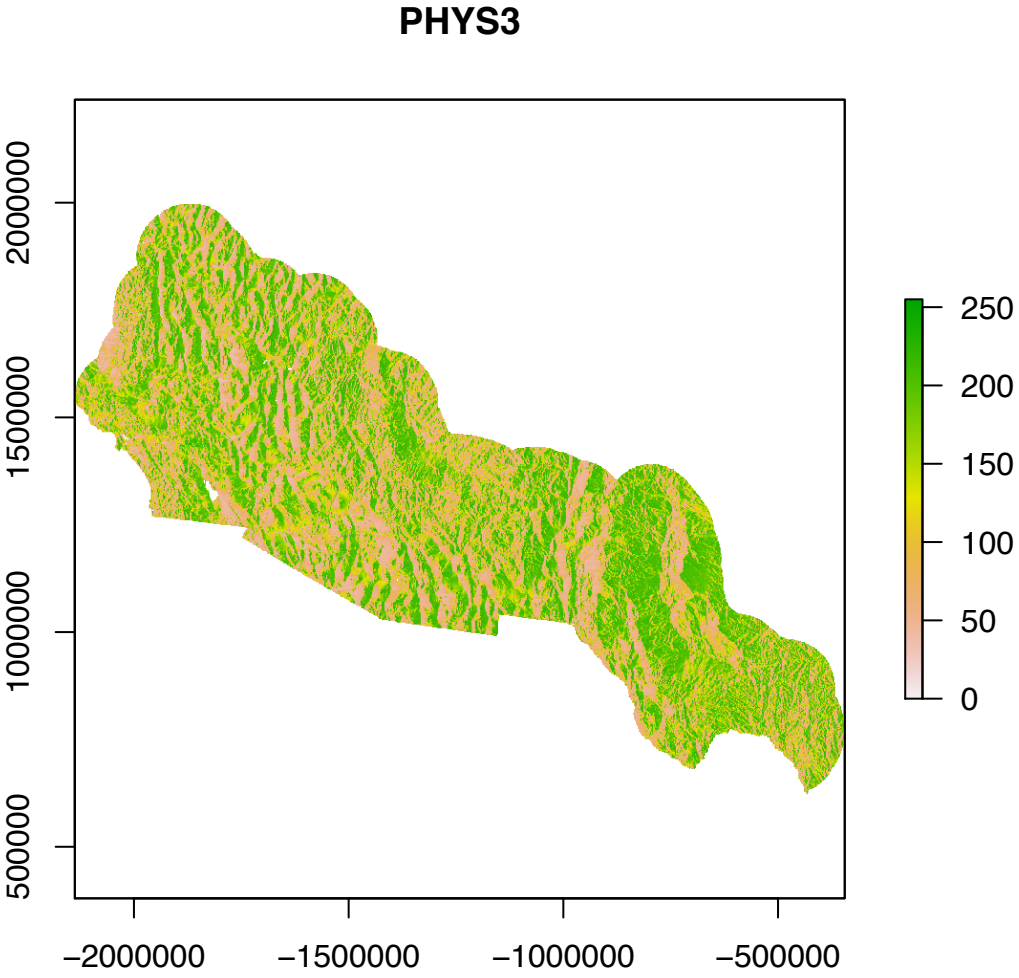
PHYS3
2000000
1500000
1000000
500000
−2000000
−1500000
−1000000
−500000
250
200
150
100
50
0

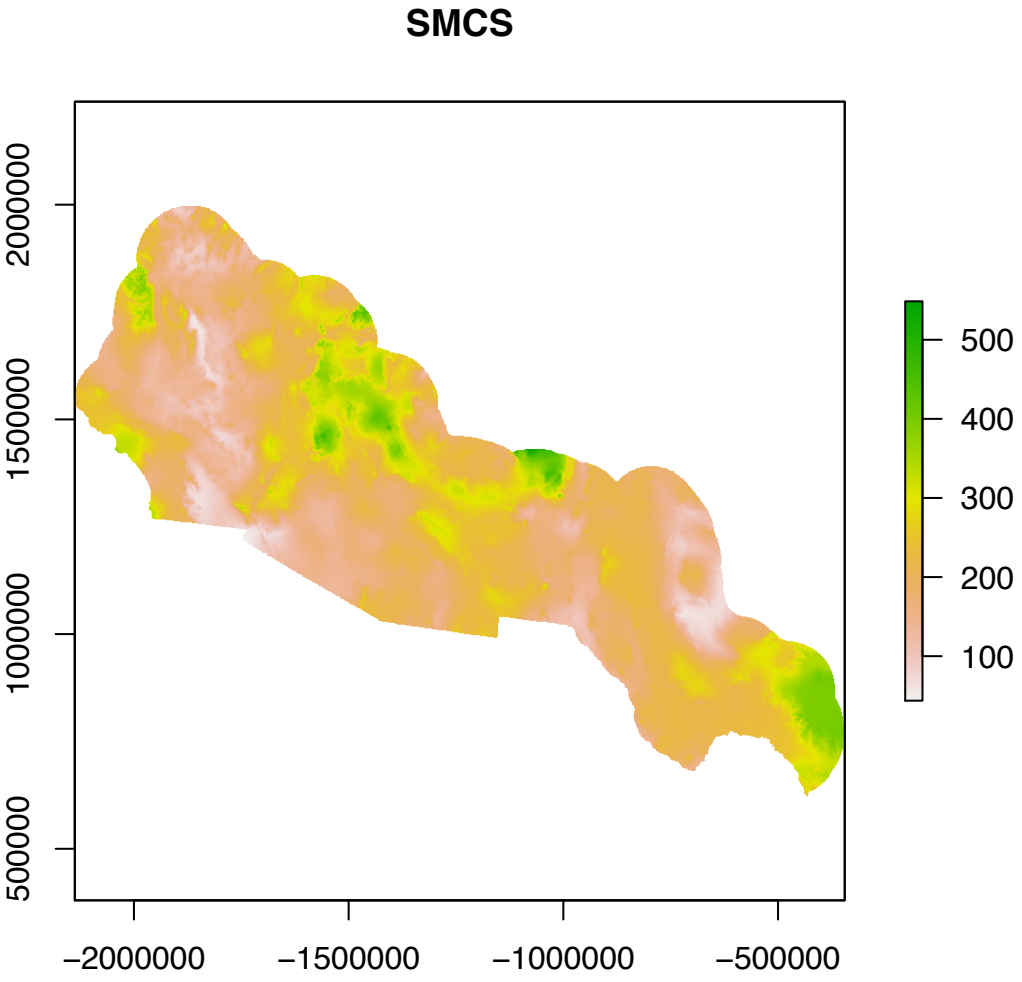
SMCS
2000000
1500000
1000000
500000
−2000000
−1500000
−1000000
−500000
500
400
300
200
100

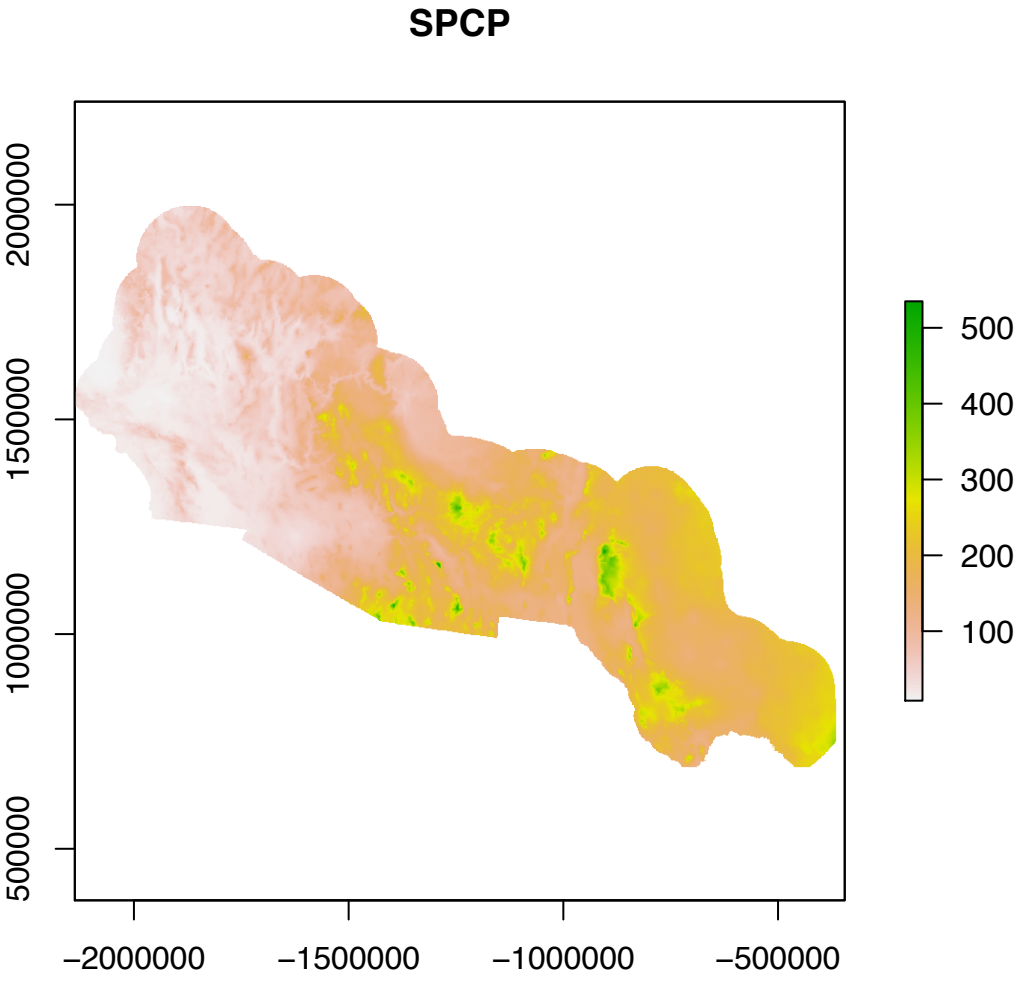
SPCP
2000000
1500000
1000000
500000
−2000000
−1500000
−1000000
−500000
500
400
300
200
100

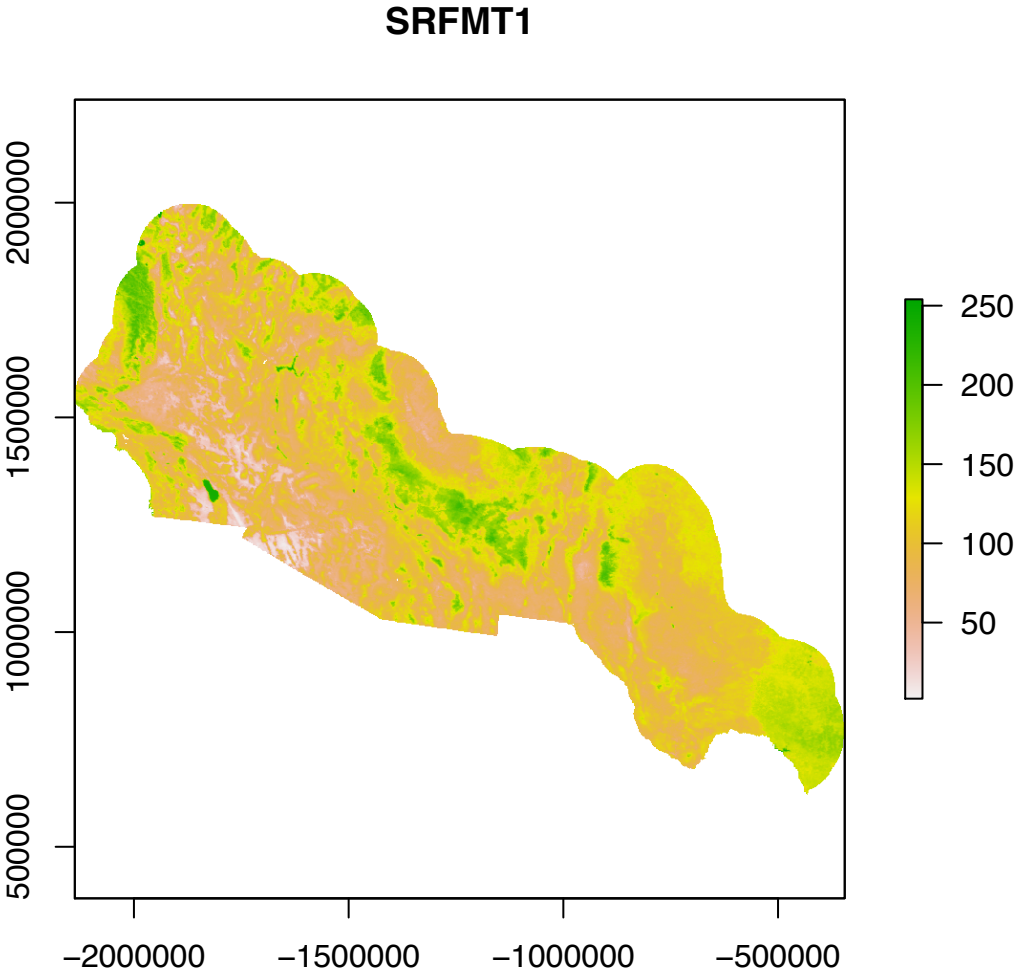
SRFMT1
2000000
1500000
1000000
500000
−2000000
−1500000
−1000000
−500000
250
200
150
100
50

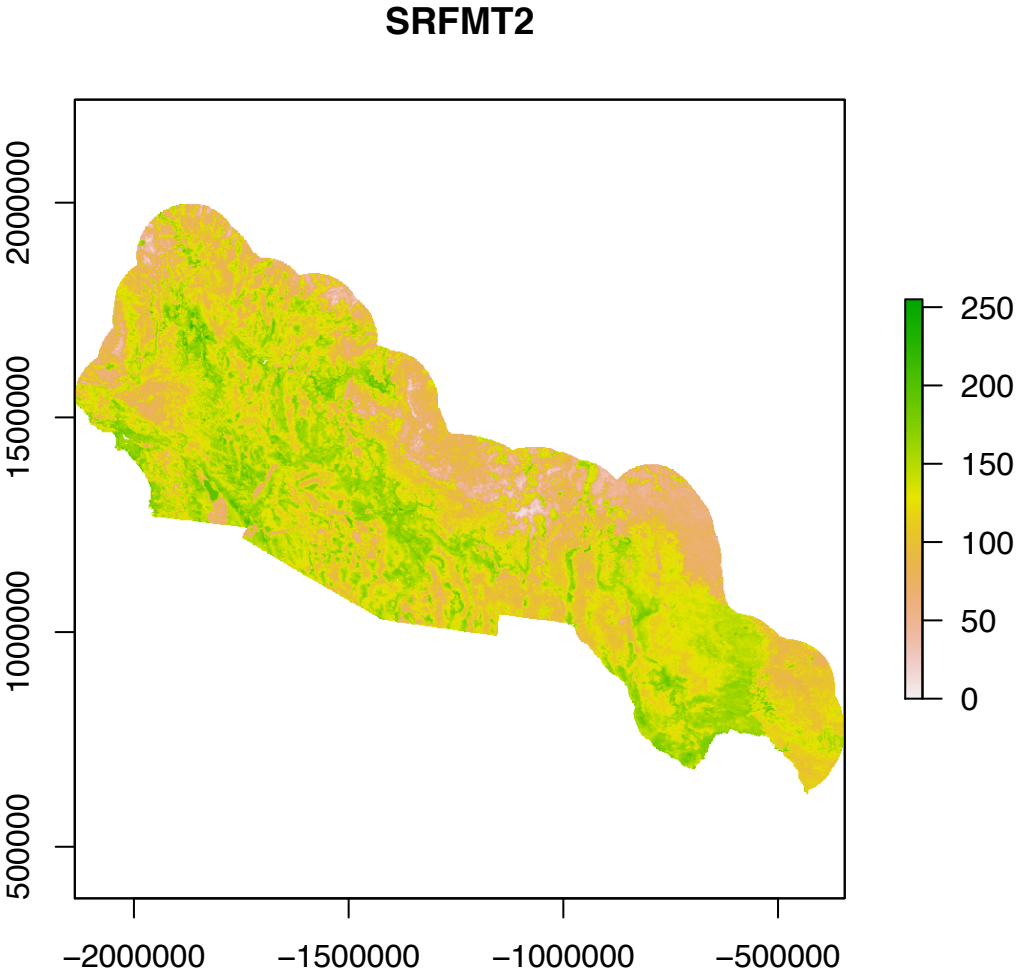
SRFMT2
2000000
1500000
1000000
500000
−2000000
−1500000
−1000000
−500000
250
200
150
100
50
0

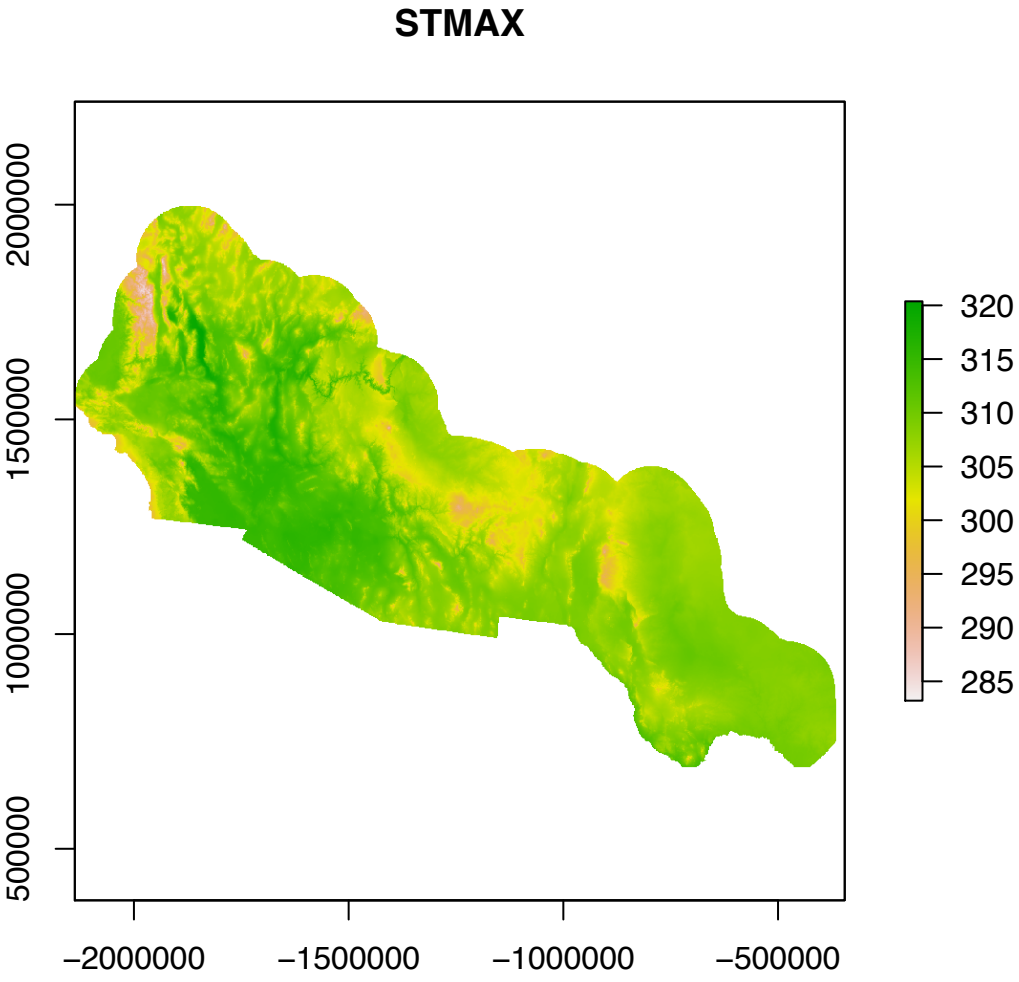
STMAX
2000000
1500000
1000000
500000
−2000000
−1500000
−1000000
−500000
320
315
310
305
300
295
290
285

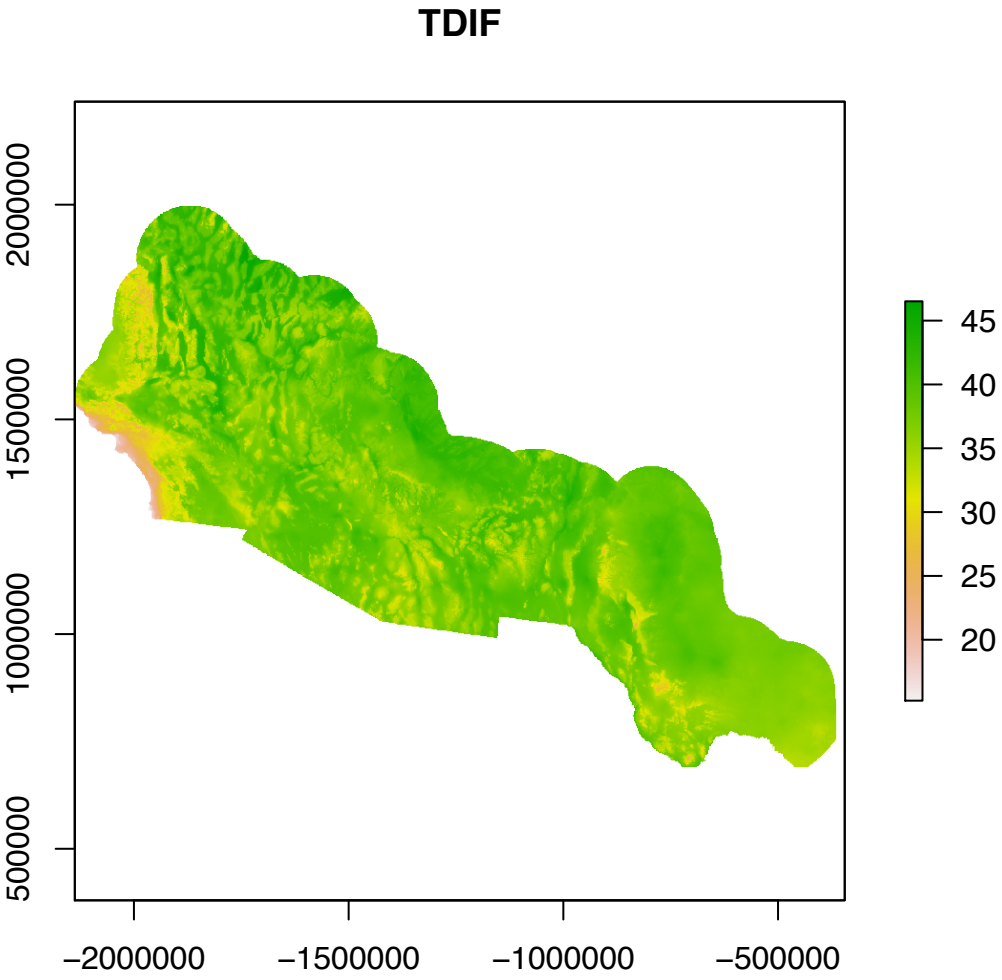
TDIF
2000000
1500000
1000000
500000
−2000000
−1500000
−1000000
−500000
45
40
35
30
25
20

APPENDIX B (2.2)

EXAMPLE RESPONSE CURVE

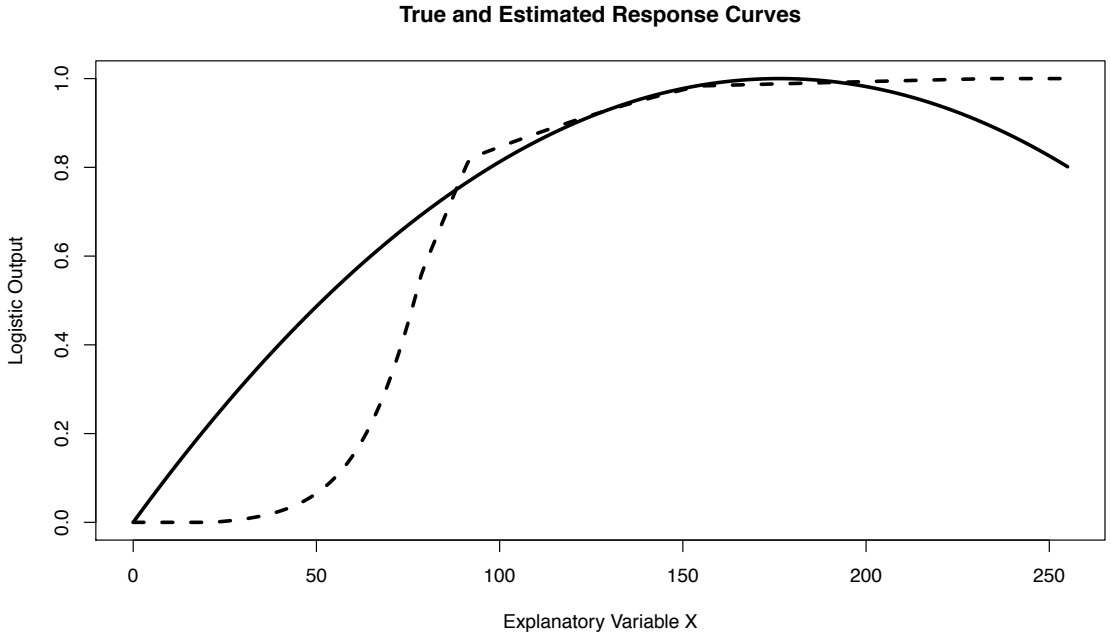

164

True (solid) and estimated (dashed) response curve for an example explanatory variable for a simulated species. Pearson's correlation between the two provided measure of how well the true response curve was estimates.

APPENDIX C (2.3)

GEOGRAPHIC BIODIVERSITY INFORMATION FACILITY OBSERVATIONS

Anaxyrus punctatus: GBIF.org (21st February 2018) GBIF Occurrence

Download https://doi.org/10.15468/dl.bxxybz

Artemisia tridentate: GBIF.org (21st February 2018) GBIF Occurrence

Download https://doi.org/10.15468/dl.2tnmpa

Chaetodipus penicillatus: GBIF.org (21st February 2018) GBIF Occurrence

Download https://doi.org/10.15468/dl.nqlsfu

Chionactis occipitalis: GBIF.org (21st February 2018) GBIF Occurrence

Download https://doi.org/10.15468/dl.8p812c

Larea tridentate: GBIF.org (21st February 2018) GBIF Occurrence

Download https://doi.org/10.15468/dl.zcsgdw

Perognathus longimembris: GBIF.org (21st February 2018) GBIF Occurrence

Download https://doi.org/10.15468/dl.qvxeea

Quercus gambelii: GBIF.org (21st February 2018) GBIF Occurrence

Download https://doi.org/10.15468/dl.jwoiop

Sceloporus magister: GBIF.org (21st February 2018) GBIF Occurrence

Download https://doi.org/10.15468/dl.zqohri

Toxostoma crissale: GBIF.org (21st February 2018) GBIF Occurrence

Download https://doi.org/10.15468/dl.l6n3rz

APPENDIX D (3.1)

ENVIRONMENTAL DATA REPRESENTING PRESENT-DAY AND EARLY/MID HOLOCENE CONDITIONS

Abbreviation	Name	Description	Source
BIO12n	Annual Precipitation	Annual cumulative precipition	Hijmans, R.J., S.E. Cameron, J.L. Parra, P.G. Jones and A. Jarvis, 2005. Very high resolution interpolated climate surfaces for global land areas. International Journal of Climatology 25: 1965-1978.
BIO14n	Precipitation of Driest Month	Precipitation of Driest Month	Hijmans, R.J., S.E. Cameron, J.L. Parra, P.G. Jones and A. Jarvis, 2005. Very high resolution interpolated climate surfaces for global land areas. International Journal of Climatology 25: 1965-1978.
BIO2n	Mean Diurnal Range	(Mean of monthly (max temp - min temp))	Hijmans, R.J., S.E. Cameron, J.L. Parra, P.G. Jones and A. Jarvis, 2005. Very high resolution interpolated climate surfaces for global land areas. International Journal of Climatology 25: 1965-1978.
BIO3n	Isothermality	(BIO2/BIO7) (* 100)	Hijmans, R.J., S.E. Cameron, J.L. Parra, P.G. Jones and A. Jarvis, 2005. Very high resolution interpolated climate surfaces for global land areas. International Journal of Climatology 25: 1965-1978.
BIO6n	Min Temperature of Coldest Month	Min Temperature of Coldest Month	Hijmans, R.J., S.E. Cameron, J.L. Parra, P.G. Jones and A. Jarvis, 2005. Very high resolution interpolated climate surfaces for global land areas. International Journal of Climatology 25: 1965-1978.
fGEOL	Geologic Units	Bedrock geologic map units of the conterminous United States	Schruben, Paul G., Arndt, Raymond E., Bawiec, Walter J., King, Philip B., and Beikman, Helen M., 1994, Geology of the Conterminous United States at 1:2,500,000 Scale -- A Digital Representation of the 1974 P.B. King and H.M. Beikman Map: U.S. Geological Survey Digital Data Series DDS-11, U.S. Geological Survey, Reston, VA. https://pubs.usgs.gov/dds/dds11/
fLITH	Surficial Lithology	A new classification of the lithology of surficial materials to be used in creating maps depicting standardized, terrestrial ecosystem models for the conterminous United States.	Cress, Jill, Soller, David, Sayre, Roger, Comer, Patrick, and Warner, Harumi, 2010, Terrestrial ecosystems—Surficial lithology of the conterminous United States: U.S. Geological Survey Scientific Investigations Map 3126, scale 1:5,000,000, 1 sheet.
PHYS1n	Primary Physiographic Variable	1st Component of Physiographic Variables PCA; 43% Variance	Aspect, Apparent Thermal Inertia, Eastness, Horizon Angle, Albedo, Northness, Slope, Smoothness, Surface Roughness, Terrain Position Index
PHYS2n	Secondary Physiographic Variable	2nd Component of Physiographic Variables PCA; 30% Variance	

PHYS3n	Tertiary Physiographic Variable	3rd Component of Physiographic Variables PCA; 9% Variance	
SLR2n	Secondary Solar Variable	2nd Component of Solar Insolation Variables PCA; 17% Variance	Mean Annual Beam Solar Insoltion, Mean Summer Diffuse Solar Insolation

Raster data were compiled at a spatial scale of 1 km for present-day and the mid-Holocene. Only climatic variables were assumed to have changed between periods.

APPENDIX E (3.2)

GEOGRAPHIC BIODIVERSITY INFORMATION FACILITY OBSERVATIONS OF PRESENT-DAY CONDITIONS

Abies concolor: GBIF.org (9th February 2018) GBIF Occurrence

Download https://doi.org/10.15468/dl.bjkxnk

Artemisia tridentate: GBIF.org (9th February 2018) GBIF Occurrence

Download https://doi.org/10.15468/dl.eql8i1

Coleogyne ramosissima: GBIF.org (9th February 2018) GBIF Occurrence

Download https://doi.org/10.15468/dl.yyx4ij

Juniperus communis: GBIF.org (9th February 2018) GBIF Occurrence

Download https://doi.org/10.15468/dl.1lqipx

Pinus ponderosa: GBIF.org (9th February 2018) GBIF Occurrence

Download https://doi.org/10.15468/dl.dtwshp

Quercus gambelii: GBIF.org (9th February 2018) GBIF Occurrence

Download https://doi.org/10.15468/dl.bahqyp

APPENDIX F (3.3)

ENVIRONMENTAL DATA REPRESENTING PRESERVATION STATISTICAL MODEL

Abbreviation	Name	Description	Source
BIO12n	Annual Precipitation	Annual cumulative precipitation	Hijmans, R.J., S.E. Cameron, J.L. Parra, P.G. Jones and A. Jarvis, 2005. Very high resolution interpolated climate surfaces for global land areas. International Journal of Climatology 25: 1965-1978.
fGEOL	Geologic Units	Bedrock geologic map units of the conterminous United States	Schruben, Paul G., Arndt, Raymond E., Bawiec, Walter J., King, Philip B., and Beikman, Helen M., 1994, Geology of the Conterminous United States at 1:2,500,000 Scale -- A Digital Representation of the 1974 P.B. King and H.M. Beikman Map: U.S. Geological Survey Digital Data Series DDS-11, U.S. Geological Survey, Reston, VA. https://pubs.usgs.gov/dds/dds11/
fLANDF	Land Surface Forms	A biophysical stratification approach to classify surfaces with slope and local relief.	Cress, J.J., Sayre, Roger, Comer, Patrick, and Warner, Harumi, 2009, Terrestrial Ecosystems—Land Surface Forms of the Conterminous United States: U.S. Geological Survey Scientific Investigations Map 3085, scale 1:5,000,000, 1 sheet.
fLITH	Surficial Lithology	A new classification of the lithology of surficial materials to be used in creating maps depicting standardized, terrestrial ecosystem models for the conterminous United States.	Cress, Jill, Soller, David, Sayre, Roger, Comer, Patrick, and Warner, Harumi, 2010, Terrestrial ecosystems—Surficial lithology of the conterminous United States: U.S. Geological Survey Scientific Investigations Map 3126, scale 1:5,000,000, 1 sheet.
PHYS1n	Primary Physiographic Variable	1st Component of Physiographic Variables PCA; 43% Variance	Aspect, Apparent Thermal Inertia, Eastness, Horizon Angle, Albedo, Northness, Slope, Smoothness, Surface Roughness, Terrain Position Index

Raster data were compiled at a spatial scale of 1 km for the mid-Holocene.

APPENDIX G (3.4)

SPATIAL PREDICTIONS OF EACH STATISTICAL MODEL USED TO REPRESENT σ

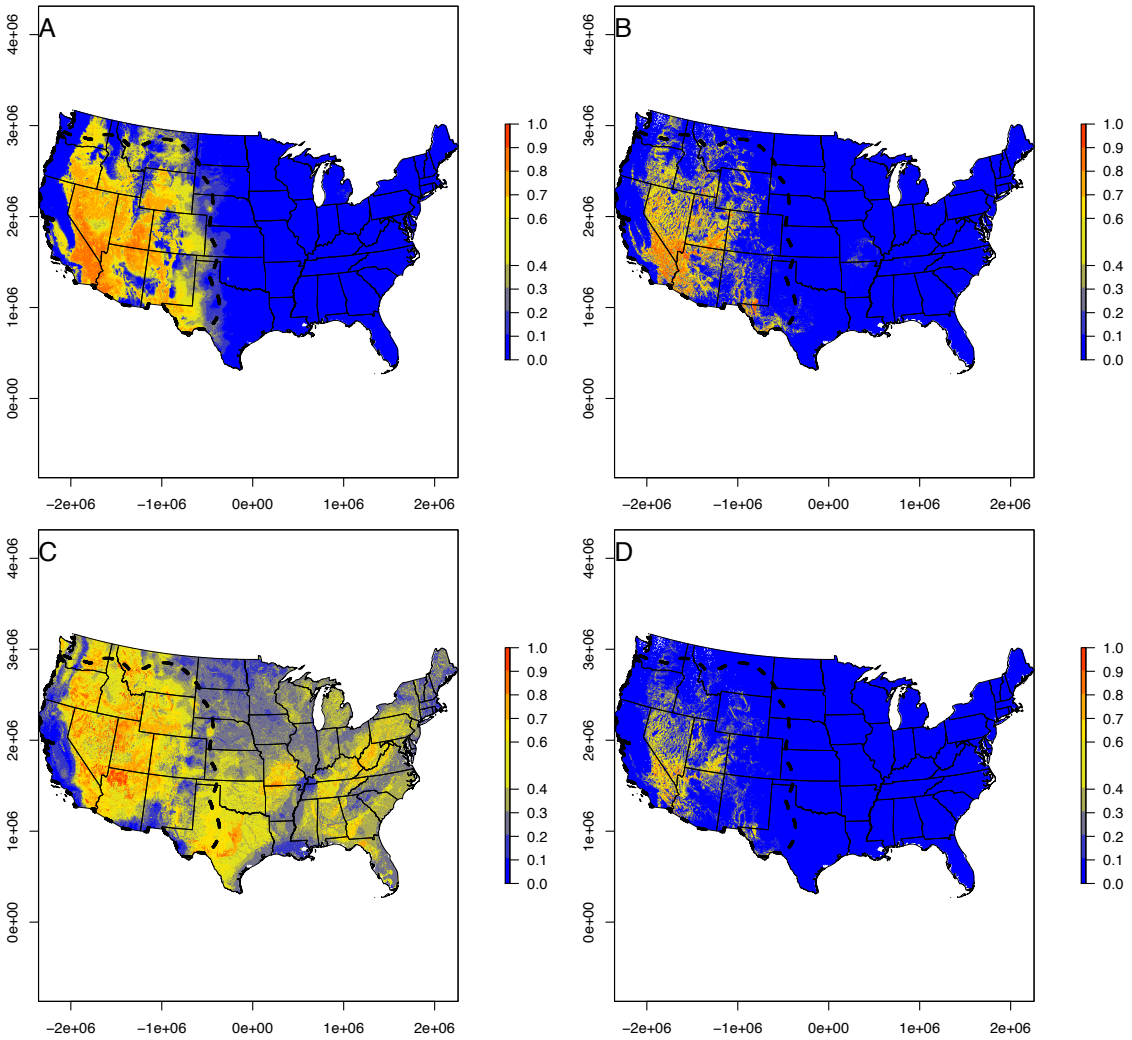

Spatial predictions for the three statistical models (Availability, A; Preservation, B; Discovery, C) used to estimate σ (D). Dashed line represents study area for paleo-SDM.

APPENDIX H (3.5)

POLLEN SAMPLES FROM LAKE SEDIMENT CORES

ACER project members; Sanchez Goñi, Maria Fernanda; Desprat, Stéphanie; Daniau, Anne-Laure; Jiménez-Moreno, Gonzalo; Anderson, R Scott; Fawcett, Peter J (2017): CLAM age model and pollen profile of sediment core Bear_Lake. PANGAEA, https://doi.org/10.1594/PANGAEA.872848

ACER project members; Sanchez Goñi, Maria Fernanda; Desprat, Stéphanie; Daniau, Anne-Laure; Allen, Judy R M; Anderson, R Scott; Behling, Hermann; Bonnefille, Raymonde; Cheddadi, Rachid; Combourieu-Nebout, Nathalie; Dupont, Lydie M; Fletcher, William J; González, Catalina; Grigg, Laurie D; Grimm, Eric C; Hayashi, Ryoma; Helmens, Karin F; Hessler, Ines; Heusser, Linda E; Hooghiemstra, Henry; Huntley, Brian; Igarashi, Yaeko; Irino, Tomohisa; Jacobs, Bonnie Fine; Jiménez-Moreno, Gonzalo; Kawai, Sayuri; Kumon, Fujio; Lawson, Ian T; Lebamba, Judicael; Ledru, Marie-Pierre; Lézine, Anne-Marie; Liew, Ping-Mei; Londeix, Laurent; López-Martinez, Constancia; Magri, Donatella; Maley, Jean; Margari, Vasiliki; Marret, Fabienne; Müller, Ulrich C; Naughton, Filipa; Novenko, Elena Y; Oba, Tadamichi; Roucoux, Katherine H; Takahara, Hikaru; Tzedakis, Polychronis C; Vincens, Annie; Whitlock, Cathy L; Willard, Debra A; Yamamoto, Masanobu (2017): CLAM age model and biomes of sediment core Bear_Lake. PANGAEA, https://doi.org/10.1594/PANGAEA.872779

ACER project members; Sanchez Goñi, Maria Fernanda; Desprat, Stéphanie; Daniau, Anne-Laure; Pisias, Nicklas G; Mix, Alan C; Heusser, Linda E (2017): CLAM age model and pollen profile of sediment core W8709A-13. PANGAEA, https://doi.org/10.1594/PANGAEA.872919

ACER project members; Sanchez Goñi, Maria Fernanda; Desprat, Stéphanie; Daniau, Anne-Laure; Grigg, Laurie D; Whitlock, Cathy L; Dean, Walter E (2017): CLAM age model and pollen profile of sediment core Little_Lake. PANGAEA, https://doi.org/10.1594/PANGAEA.872891

ACER project members; Sanchez Goñi, Maria Fernanda; Desprat, Stéphanie; Daniau, Anne-Laure; Allen, Judy R M; Anderson, R Scott; Behling, Hermann; Bonnefille, Raymonde; Cheddadi, Rachid; Combourieu-Nebout, Nathalie; Dupont, Lydie M; Fletcher, William J; González, Catalina; Grigg, Laurie D; Grimm, Eric C; Hayashi, Ryoma; Helmens, Karin F; Hessler, Ines; Heusser, Linda E; Hooghiemstra, Henry; Huntley, Brian; Igarashi, Yaeko; Irino, Tomohisa; Jacobs, Bonnie Fine; Jiménez-Moreno, Gonzalo; Kawai, Sayuri; Kumon, Fujio; Lawson, Ian T; Lebamba, Judicael; Ledru, Marie-Pierre; Lézine, Anne-Marie; Liew, Ping-Mei; Londeix, Laurent; López-Martinez, Constancia; Magri, Donatella; Maley, Jean; Margari, Vasiliki; Marret, Fabienne; Müller, Ulrich C; Naughton, Filipa; Novenko, Elena Y; Oba, Tadamichi; Roucoux, Katherine H; Takahara, Hikaru; Tzedakis, Polychronis C; Vincens, Annie; Whitlock, Cathy L; Willard, Debra A; Yamamoto, Masanobu (2017): CLAM age model and biomes of sediment core Potato_Lake. PANGAEA, https://doi.org/10.1594/PANGAEA.872817

ACER project members; Sanchez Goñi, Maria Fernanda; Desprat, Stéphanie; Daniau, Anne-Laure; Heusser, Linda E (2017): CLAM age model and pollen profile of sediment core Rice_Lake_81. PANGAEA, https://doi.org/10.1594/PANGAEA.872909

ACER project members; Sanchez Goñi, Maria Fernanda; Desprat, Stéphanie; Daniau, Anne-Laure; Heusser, Linda E (2017): CLAM age model and pollen profile of sediment core 146-893A. PANGAEA, https://doi.org/10.1594/PANGAEA.872839

ACER project members; Sanchez Goñi, Maria Fernanda; Desprat, Stéphanie; Daniau, Anne-Laure; Jacobs, Bonnie Fine (2017): CLAM age model and pollen profile of sediment core Hay_Lake. PANGAEA, https://doi.org/10.1594/PANGAEA.872866

ACER project members; Sanchez Goñi, Maria Fernanda; Desprat, Stéphanie; Daniau, Anne-Laure; Anderson, R Scott (2017): CLAM age model and pollen profile of sediment core Potato_Lake. PANGAEA, https://doi.org/10.1594/PANGAEA.872907

Kennett, Douglas J; Kennett, James P; West, G J; Erlandson, Jon M; Johnson, John R; Hendy, Ingrid L; West, A; Culleton, B J; Jones, T L; Stafford, Thomas W (2008): Age determination, carbon geochemistry and palynology of section AC003. PANGAEA, https://doi.org/10.1594/PANGAEA.817597, Supplement to: Kennett, DJ et al. (2008): Wildfire and abrupt ecosystem disruption on California's Northern Channel Islands at the Ållerød-Younger Dryas boundary (13.0-12.9ka). Quaternary Science Reviews, 27(27-28), 2530-2545, https://doi.org/10.1016/j.quascirev.2008.09.006

Kennett, Douglas J; Kennett, James P; West, G J; Erlandson, Jon M; Johnson, John R; Hendy, Ingrid L; West, A; Culleton, B J; Jones, T L; Stafford, Thomas W (2008): (Table 5) Palynology of section AC-003 samples. PANGAEA, https://doi.org/10.1594/PANGAEA.817596, In supplement to: Kennett, DJ et al. (2008): Wildfire and abrupt ecosystem disruption on California's Northern Channel Islands at the Ållerød-Younger Dryas boundary (13.0-12.9ka). Quaternary Science Reviews, 27(27-28), 2530-2545, https://doi.org/10.1016/j.quascirev.2008.09.006

APPENDIX I (3.6)

OVERLAP AMONG PALEO-DISTRIBUTIONS

Abies concolor	Hindcast	σ-naïve	σ-standard	σ-modeled
Hindcast	1	0.177	0.212	0.456
σ-naïve		1	0.398	0.228
σ-standard		19.5%	1	0.279
σ-modeled		156.9%		1

Artemisia tridentata	Hindcast	σ-naïve	σ-standard	σ-modeled
Hindcast	1	0.247	0.314	0.434
σ-naïve		1	0.448	0.309
σ-standard		26.9%	1	0.362
σ-modeled		75.5%		1

Coleogyne ramosissima	Hindcast	σ-naïve	σ-standard	σ-modeled
Hindcast	1	0.322	0.409	0.406
σ-naïve		1	0.388	0.304
σ-standard		27.0%	1	0.359
σ-modeled		25.9%		1

Juniperus communis	Hindcast	σ-naïve	σ-standard	σ-modeled
Hindcast	1	0.196	0.306	0.483
σ-naïve		1	0.381	0.266
σ-standard		56.0%	1	0.397
σ-modeled		146.0%		1

Pinus ponderosa	Hindcast	σ-naïve	σ-standard	σ-modeled
Hindcast	1	0.272	0.333	0.586
σ-naïve		1	0.437	0.292
σ-standard		22.2%	1	0.363
σ-modeled		115.1%		1

Quercus gambelii	Hindcast	σ-naïve	σ-standard	σ-modeled
Hindcast	1	0.362	0.372	0.461
σ-naïve		1	0.560	0.561
σ-standard		2.8%	1	0.602
σ-modeled		27.5%		1

Overlap (ESP) scores among each of the paleo-distributions shows that the σ-modeled method resulted in the highest agreement to the assumed true paleo-distributions (hindcast). Percent improvement scores shown in lower right section.

APPENDIX J (4.1)

PRINCIPLE COMPONENT SCORES AND LOADINGS FOR PHYSIOGRAPHIC, CLIMATIC, SOILS AND VEGETATION EXPLANATORY VARIABLES.

Climate PCA loadings.

Name	PCA	% Importance	Eigen values	PCPsmRt	PCPsm	TDIFF	TSMX	PCPwnt	TWMN
CLIM1	PC1	50.78	3.05	0.2479	-0.4934	0.361	0.4784	-0.5141	0.2677
CLIM2	PC2	25.30	1.52	-0.6392	0.3412	-0.0696	0.3873	-0.0299	0.5651
CLIM3	PC3	17.32	1.04	-0.3196	0.2186	0.7469	0.1655	0.0478	-0.5125
CLIM4	PC4	5.87	0.35	0.4687	0.1382	0.213	0.3638	0.7177	0.2616
CLIM5	PC5	0.74	0.04	0.4563	0.7572	0.0126	0.0224	-0.4663	0.0204
CLIM6	PC6	0.00	0.00	-0.0017	-0.0006	0.5114	-0.6789	0.0016	0.5269

Physiographic PCA loadings

Name	PCA	% Importance	Eigen values	Eastness	Northness	North Slope	Slope	Rockiness	Horizon Angle	TPX	Solar Insolation
PHYS1	PC1	37.35	2.99	-0.0273	0.1154	0.1067	0.5305	0.5412	0.4147	-0.3738	-0.2975
PHYS2	PC2	25.99	2.08	-0.0469	-0.5481	-0.6234	0.1679	0.1641	0.0837	-0.1514	0.4729
PHYS3	PC3	12.49	1.00	0.9915	0.0102	-0.0192	0.0349	0.0275	-0.064	-0.0921	0.0446
PHYS4	PC4	10.42	0.83	0.1172	-0.1916	-0.0887	-0.052	0.0141	0.6295	0.7095	-0.198
PHYS5	PC5	6.28	0.50	0.0131	-0.7527	0.21	-0.0454	-0.0618	-0.228	-0.1351	-0.5596
PHYS6	PC6	3.96	0.32	0.0133	0.0093	-0.0655	-0.4852	-0.3595	0.5664	-0.5541	-0.0547
PHYS7	PC7	2.95	0.24	0.0018	-0.2878	0.737	0.0387	0.0386	0.2013	-0.002	0.5748
PHYS8	PC8	0.53	0.05	0.0013	0.0029	-0.0099	0.6689	-0.738	0.0861	-0.0165	-0.0115

Vegetation PCA loadings

Name	PCA	% Importance	Eigen values	AMP	DUR	EOSN	EOST	MAXN	MAXT	SOSN	SOST	TIN
VEG1	PC1	46.88	4.22	0.3915	-0.1088	0.4121	0.1989	0.4617	0.2231	0.4049	0.2269	0.3836
VEG2	PC2	29.48	2.65	-0.1774	0.276	-0.1372	0.5361	-0.1784	0.5157	-0.137	0.507	-0.1117
VEG3	PC3	12.02	1.08	-0.4493	0.3485	0.4575	-0.0801	0.0866	0.0317	0.4808	-0.111	-0.4571
VEG4	PC4	9.35	0.84	0.2053	0.8532	-0.0685	0.074	0.0421	-0.1554	-0.0786	-0.2617	0.3453
VEG5	PC5	1.23	0.11	0.1179	0.1262	-0.115	-0.6683	0.0926	0.7015	-0.0771	-0.0578	-0.0185
VEG6	PC6	0.57	0.05	0.2176	0.2146	-0.0282	-0.3508	0.1918	-0.3978	-0.0891	0.7102	-0.2746
VEG7	PC7	0.41	0.04	-0.5574	-0.0009	0.1011	-0.2889	-0.2243	-0.0834	0.0802	0.3113	0.6596
VEG8	PC8	0.04	0.00	-0.3397	-0.022	0.2768	0.066	0.6006	0.0117	-0.6603	-0.076	0.0212
VEG9	PC9	0.02	0.00	0.2896	0.012	0.7046	-0.0603	-0.5379	0.0402	-0.3515	0.0169	-0.0328

APPENDIX K (4.2)

TOP 100 CANDIDATE MODELS FOR GLOBAL POOLED SDM

Model Name & Explanatory Variables	nCoeff	nTerms	nVariables	nTrain	nTest	UBREave	UBREcv	AUCave	AUCcv	RMSEave	RMSEcv	MXEave	MXEcv
sTPXn_SurfMat1n_SurfMat2n_TDIFFn_TWMNn_PCPsmwtRtn_SMCdiffn_SMCsmm_VEG1n_VEG2n	91	10	10	930	398	-0.070	48.125	0.848	2.054	0.390	3.227	0.463	5.768
sTPXn_SurfMat1n_SurfMat2n_SurfMat3n_TDIFFn_TWMNn_PCPsmwtRtn_SMCdiffn_SMCsmrn_VEG1n_VEG2n	100	11	11	930	398	-0.071	48.006	0.848	2.092	0.390	3.210	0.463	5.734
sTPXn_SurfMat1n_SurfMat2n_TDIFFn_TWMNn_PCPsmwtRtn_SMCdiffn_SMCsmm_VEG1n_VEG2n_VEG3n	100	11	11	930	398	-0.069	49.123	0.848	1.989	0.390	3.204	0.463	5.688
sSRFn_TPXn_SurfMat1n_SurfMat2n_SurfMat3n_TDIFFn_TWMNn_PCPsmwtRtn_SMCdiffn_SMCsmrn_VEG1n_VEG2n	109	12	12	930	398	-0.075	45.238	0.850	2.027	0.389	3.274	0.464	5.883
sSRFn_TPXn_SurfMat1n_SurfMat2n_TDIFFn_TWMNn_PCPsmwtRtn_SMCdiffn_SMCsmm_VEG1n_VEG2n	100	11	11	930	398	-0.074	45.214	0.849	1.977	0.389	3.252	0.465	5.781
sSRFn TPXn SurfMat1n SurfMat2n SurfMat3n TDIFFn TWMNn PCPsmwtRtn SMCdiffn SMCsmrn_VEG1n_VEG2n_VEG3n	118	13	13	930	398	-0.074	45.880	0.849	1.915	0.390	3.192	0.466	5.736
sSurfMat1n_SurfMat2n_TDIFFn_TWMNn_PCPsmwtRtn_SMCdiffn_SMCsmrn_VEG1n_VEG2n	82	9	9	930	398	-0.068	49.416	0.846	2.152	0.391	3.266	0.464	5.844
sTPXn_SurfMat1n_SurfMat2n_SurfMat3n_TDIFFn_TWMNn_PCPsmwtRtn_SMCdiffn_SMCsmrn_VEG1n_VEG2n_VEG3n	109	12	12	930	398	-0.070	48.689	0.848	2.029	0.391	3.200	0.464	5.691
sTPXn_SurfMat1n_TDIFFn_TWMNn_PCPsmwtRtn_SMCdiffn_SMCsmrn_VEG1n_VEG2n	82	9	9	930	398	-0.066	51.150	0.848	2.111	0.391	3.273	0.464	5.692
sTPXn_SurfMat1n_SurfMat2n_SurfMat3n_TDIFFn_TWMNn_PCPsmwtRtn_SMCdiffn_SMCsmrn_VEG2n	91	10	10	930	398	-0.066	51.553	0.846	2.170	0.391	3.298	0.464	5.801
sSurfMat1n_SurfMat2n_TDIFFn_TWMNn_PCPsmwtRtn_SMCdiffn_SMCsmm_VEG1n_VEG2n_VEG3n	91	10	10	930	398	-0.066	50.550	0.846	2.154	0.391	3.256	0.465	5.795
sSurfMat1n_SurfMat2n_SurfMat3n_TDIFFn_TWMNn_PCPsmwtRtn_SMCdiffn_SMCsmrn_VEG1n_VEG2n	91	10	10	930	398	-0.069	49.630	0.846	2.135	0.391	3.221	0.465	5.739
sTPXn_SurfMat1n_SurfMat2n_TDIFFn_TWMNn_PCPsmwtRtn_SMCdiffn_SMCsmm_VEG1n	82	9	9	930	398	-0.069	49.366	0.845	2.131	0.391	3.253	0.465	5.820
sTPXn_SurfMat1n_SurfMat3n_TDIFFn_TWMNn_PCPsmwtRtn_SMCdiffn_SMCsmm_VEG1n_VEG2n	91	10	10	930	398	-0.067	50.602	0.847	2.132	0.391	3.253	0.465	5.770
sTPXn_SurfMat1n_SurfMat2n_SurfMat3n_TDIFFn_TWMNn_PCPsmwtRtn_SMCdiffn_VEG1n_VEG2n	91	10	10	930	398	-0.066	53.225	0.846	2.141	0.391	3.221	0.465	5.688
sTPXn_SurfMat1n_SurfMat2n_TDIFFn_TWMNn_PCPsmwtRtn_SMCdiffn_SMCsmm_VEG2n	82	9	9	930	398	-0.066	51.952	0.846	2.103	0.391	3.251	0.465	5.810
sTPXn_SurfMat1n_SurfMat2n_TDIFFn_TWMNn_PCPsmwtRtn_SMCdiffn_VEG1n_VEG2n	82	9	9	930	398	-0.066	52.999	0.846	2.094	0.391	3.208	0.465	5.589
sTPXn_SurfMat1n_SurfMat2n_SurfMat3n_TDIFFn_TWMNn_PCPsmwtRtn_SMCdiffn_SMCsmrn_VEG1n	91	10	10	930	398	-0.069	49.292	0.845	2.108	0.391	3.204	0.465	5.653
sSTn_TPXn_SurfMat2n_SurfMat3n_TDIFFn_TWMNn_PCPsmwtRtn_SMCdiffn_SMCsmrn_VEG1n_VEG2n	100	11	11	930	398	-0.062	52.918	0.846	2.157	0.392	3.307	0.465	5.715
sTPXn_SurfMat1n_SurfMat2n_SurfMat3n_TDIFFn_TWMNn_PCPsmwtRtn_SMCdiffn_VEG1n_VEG2n_VEG3n	100	11	11	930	398	-0.066	54.141	0.846	2.136	0.392	3.199	0.465	5.568
sTPXn_SurfMat1n_SurfMat2n_TDIFFn_TWMNn_PCPsmwtRtn_SMCdiffn_VEG1n_VEG2n_VEG3n	91	10	10	930	398	-0.065	54.387	0.846	2.125	0.392	3.261	0.465	5.681
sSurfMat1n_SurfMat2n_SurfMat3n_TDIFFn_TWMNn_PCPsmwtRtn_SMCdiffn_SMCsmrn_VEG1n_VEG2n_VEG3n	100	11	11	930	398	-0.067	50.595	0.846	2.129	0.391	3.218	0.465	5.788
sTPXn_SurfMat1n_TDIFFn_TWMNn_PCPsmwtRtn_SMCdiffn_SMCsmrn_VEG1n_VEG2n_VEG3n	91	10	10	930	398	-0.065	51.832	0.847	2.114	0.391	3.307	0.465	5.744
sSRFn_TPXn_SurfMat1n_SurfMat2n_TDIFFn_TWMNn_PCPsmwtRtn_SMCdiffn_SMCsmm_VEG1n_VEG2n_VEG3n	109	12	12	930	398	-0.072	46.270	0.849	1.961	0.390	3.273	0.465	5.840
sTPXn_SurfMat1n_SurfMat2n_SurfMat3n_TDIFFn_TWMNn_PCPsmwtRtn_SMCdiffn_SMCsmrn_VEG2n_VEG3n	100	11	11	930	398	-0.064	53.010	0.846	2.168	0.392	3.288	0.465	5.768
sTPXn_SurfMat1n_SurfMat2n_TDIFFn_TWMNn_PCPsmwtRtn_SMCdiffn_SMCsmm_VEG1n_VEG3n	91	10	10	930	398	-0.067	50.407	0.845	2.112	0.392	3.250	0.465	5.773
sTPXn_SurfMat1n_SurfMat3n_TDIFFn_TWMNn_PCPsmwtRtn_SMCdiffn_SMCsmm_VEG1n_VEG2n_VEG3n	100	11	11	930	398	-0.066	51.597	0.847	2.146	0.392	3.279	0.465	5.770
sTPXn_SurfMat1n_SurfMat2n_SurfMat3n_TDIFFn_TWMNn_PCPsmwtRtn_SMCdiffn_SMCsmrn_VEG1n_VEG3n	100	11	11	930	398	-0.068	50.149	0.845	2.117	0.392	3.225	0.466	5.749
sSurfMat1n_SurfMat2n_SurfMat3n_TDIFFn_TWMNn_PCPsmwtRtn_SMCdiffn_VEG1n_VEG2n	82	9	9	930	398	-0.065	54.208	0.845	2.252	0.392	3.302	0.466	5.920
sSurfMat1n_SurfMat2n_TDIFFn_TWMNn_PCPsmwtRtn_SMCdiffn_SMCsmm_VEG1n	73	8	8	930	398	-0.067	50.389	0.843	2.240	0.392	3.321	0.466	5.909
sSTn_TPXn_SurfMat2n_SurfMat3n_TDIFFn_TSMXn_PCPsmwtRtn_SMCdiffn_SMCsmm_VEG1n_VEG2n	100	11	11	930	398	-0.069	45.848	0.847	2.052	0.391	3.186	0.466	5.480
sSurfMat1n_SurfMat2n_TDIFFn_TWMNn_PCPsmwtRtn_SMCdiffn_VEG1n_VEG2n	73	8	8	930	398	-0.064	53.917	0.844	2.218	0.392	3.271	0.466	5.779
sTPXn_SurfMat1n_SurfMat2n_SurfMat3n_TDIFFn_TWMNn_PCPsmwtRtn_SMCdiffn_SMCsmrn	82	9	9	930	398	-0.065	52.526	0.844	2.221	0.392	3.219	0.466	5.530
sSurfMat1n_SurfMat2n_SurfMat3n_TDIFFn_TWMNn_PCPsmwtRtn_SMCdiffn_SMCsmrn_VEG1n	82	9	9	930	398	-0.067	50.805	0.843	2.214	0.392	3.243	0.466	5.785
sTPXn_SurfMat1n_SurfMat3n_TDIFFn_TWMNn_PCPsmwtRtn_SMCdiffn_VEG1n_VEG2n	82	9	9	930	398	-0.063	55.225	0.846	2.125	0.392	3.157	0.466	5.542
sSRFn_TPXn_SurfMat1n_SurfMat2n_SurfMat3n_TDIFFn_TWMNn_PCPsmwtRtn_SMCdiffn_SMCsmrn_VEG1n	100	11	11	930	398	-0.074	45.816	0.848	2.056	0.390	3.242	0.466	5.860
sTPXn_SurfMat1n_SurfMat2n_TDIFFn_TWMNn_PCPsmwtRtn_SMCdiffn_SMCsmm_VEG2n_VEG3n	91	10	10	930	398	-0.064	53.705	0.845	2.115	0.392	3.261	0.466	5.665
sSurfMat1n_SurfMat2n_SurfMat3n_TDIFFn_TWMNn_PCPsmwtRtn_SMCdiffn_VEG1n_VEG2n_VEG3n	91	10	10	930	398	-0.063	55.334	0.844	2.293	0.392	3.342	0.466	5.856
sSTn_TPXn_SurfMat2n_TDIFFn_TWMNn_PCPsmwtRtn_SMCdiffn_SMCsmrn_VEG1n_VEG2n	91	10	10	930	398	-0.061	53.985	0.845	2.107	0.392	3.294	0.466	5.670
sTPXn_SurfMat1n_SurfMat2n_TDIFFn_TWMNn_PCPsmwtRtn_SMCdiffn_SMCsmm	73	8	8	930	398	-0.064	53.253	0.844	2.206	0.392	3.264	0.466	5.711

Model Name & Explanatory Variables	nCoeff	nTerms	nVariables	nTrain	nTest	UBREave	UBREcv	AUCave	AUCcv	RMSEave	RMSEcv	MXEave	MXEcv
sSTn_TPXn_SurfMat2n_SurfMat3n_TDIFFn_TWMNn_PCPsmwtRtn_SMCdiffn_SMCsmrn_VEG1n_VEG2n_VEG3n	109	12	12	930	398	-0.061	54.344	0.845	2.179	0.392	3.402	0.466	5.866
sTPXn_SurfMat1n_SurfMat3n_TDIFFn_TWMNn_PCPsmwtRtn_SMCdiffn_SMCsmrn_VEG2n	82	9	9	930	398	-0.062	53.938	0.845	2.240	0.392	3.301	0.466	5.669
sTPXn_SurfMat1n_SurfMat2n_TDIFFn_TWMNn_PCPsmwtRtn_SMCdiffn_VEG1n	73	8	8	930	398	-0.065	53.499	0.843	2.153	0.392	3.228	0.466	5.643
sTPXn_SurfMat1n_TDIFFn_TWMNn_PCPsmwtRtn_SMCdiffn_VEG1n_VEG2n	73	8	8	930	398	-0.062	56.628	0.846	2.087	0.392	3.169	0.466	5.516
sTPXn_SurfMat1n_SurfMat2n_SurfMat3n_TDIFFn_TWMNn_PCPsmwtRtn_SMCdiffn_VEG2n	82	9	9	930	398	-0.062	57.473	0.844	2.247	0.392	3.233	0.466	5.646
sTPXn_SurfMat3n_TDIFFn_TWMNn_PCPsmwtRtn_SMCdiffn_SMCsmrn_VEG1n_VEG2n	82	9	9	930	398	-0.061	54.733	0.845	2.219	0.392	3.324	0.466	5.675
sSRFn_TPXn_SurfMat1n_SurfMat2n_TDIFFn_TWMNn_PCPsmwtRtn_SMCdiffn_SMCsmm_VEG1n	91	10	10	930	398	-0.073	45.779	0.847	2.051	0.390	3.277	0.466	5.879
sTPXn_SurfMat1n_SurfMat2n_TDIFFn_TWMNn_PCPsmwtRtn_SMCdiffn_VEG2n	73	8	8	930	398	-0.061	57.921	0.844	2.231	0.392	3.279	0.467	5.725
sSurfMat1n_SurfMat2n_TDIFFn_TWMNn_PCPsmwtRtn_SMCdiffn_VEG1n_VEG2n_VEG3n	82	9	9	930	398	-0.063	55.150	0.844	2.203	0.392	3.248	0.467	5.652
sTPXn_SurfMat1n_SurfMat3n_TDIFFn_TWMNn_PCPsmwtRtn_SMCdiffn_SMCsmm_VEG1n	82	9	9	930	398	-0.064	52.728	0.845	2.147	0.392	3.210	0.467	5.583
sTPXn_SurfMat1n_SurfMat3n_TDIFFn_TWMNn_PCPsmwtRtn_SMCdiffn_VEG1n_VEG2n_VEG3n	91	10	10	930	398	-0.062	56.749	0.846	2.145	0.392	3.191	0.467	5.552
sSTn_TPXn_SurfMat3n_TDIFFn_TWMNn_PCPsmwtRtn_SMCdiffn_SMCsmrn_VEG1n_VEG2n	91	10	10	930	398	-0.061	55.110	0.845	2.221	0.393	3.338	0.467	5.762
sTPXn_SurfMat2n_SurfMat3n_TDIFFn_TWMNn_PCPsmwtRtn_SMCdiffn_SMCsmm_VEG1n_VEG2n	91	10	10	930	398	-0.061	55.518	0.845	2.196	0.392	3.325	0.467	5.699
sTPXn_SurfMat1n_SurfMat2n_SurfMat3n_TDIFFn_TWMNn_PCPsmwtRtn_SMCdiffn_VEG1n	82	9	9	930	398	-0.066	53.126	0.844	2.178	0.392	3.198	0.467	5.581
sTPXn_SurfMat1n_SurfMat2n_TDIFFn_TWMNn_PCPsmwtRtn_SMCdiffn_VEG1n_VEG3n	82	9	9	930	398	-0.064	54.833	0.843	2.190	0.393	3.276	0.467	5.677
sSTn_TPXn_SurfMat2n_SurfMat3n_TDIFFn_TSMXn_PCPsmwtRtn_SMCsmrn_VEG1n_VEG2n	91	10	10	930	398	-0.063	50.085	0.846	2.050	0.392	3.128	0.467	5.541
sTPXn_SurfMat1n_SurfMat2n_SurfMat3n_TDIFFn_TWMNn_PCPsmwtRtn_SMCdiffn_VEG1n_VEG3n	91	10	10	930	398	-0.065	54.792	0.843	2.233	0.393	3.281	0.467	5.707
sSTn_TPXn_SurfMat2n_TDIFFn_TSMXn_PCPsmwtRtn_SMCdiffn_SMCsmrn_VEG1n_VEG2n	91	10	10	930	398	-0.068	46.449	0.847	2.151	0.391	3.195	0.467	5.506
sSurfMat1n_SurfMat2n_TDIFFn_TWMNn_PCPsmwtRtn_SMCdiffn_SMCsmm_VEG1n_VEG3n	82	9	9	930	398	-0.065	51.511	0.843	2.171	0.392	3.258	0.467	5.780
sTPXn_SurfMat1n_TDIFFn_TWMNn_PCPsmwtRtn_SMCdiffn_SMCsmrn_VEG2n	73	8	8	930	398	-0.061	54.908	0.845	2.179	0.392	3.307	0.467	5.708
sTPXn_SurfMat1n_TDIFFn_TWMNn_PCPsmwtRtn_SMCdiffn_VEG1n_VEG2n_VEG3n	82	9	9	930	398	-0.061	57.573	0.845	2.097	0.393	3.203	0.467	5.536
sTPXn_SurfMat1n_TDIFFn_TWMNn_PCPsmwtRtn_SMCdiffn_SMCsmrn_VEG1n	73	8	8	930	398	-0.064	53.569	0.845	2.168	0.392	3.280	0.467	5.674
sSurfMat1n_SurfMat2n_TDIFFn_TWMNn_PCPsmwtRtn_SMCdiffn_VEG1n	64	7	7	930	398	-0.064	54.683	0.841	2.305	0.393	3.308	0.467	5.816
sTPXn_SurfMat1n_SurfMat2n_SurfMat3n_TWMNn_PCPsmwtRtn_SMCdiffn_SMCsmm_VEG1n_VEG2n	91	10	10	930	398	-0.065	51.670	0.846	2.066	0.392	3.056	0.467	5.653
sSTn_TPXn_SurfMat2n_TDIFFn_TSMXn_PCPsmwtRtn_SMCsmrn_VEG1n_VEG2n	82	9	9	930	398	-0.062	50.909	0.846	2.145	0.392	3.123	0.467	5.467
sTPXn_SurfMat3n_TDIFFn_TWMNn_PCPsmwtRtn_SMCdiffn_SMCsmrn_VEG1n_VEG2n_VEG3n	91	10	10	930	398	-0.060	56.611	0.845	2.221	0.392	3.351	0.467	5.698
sSRFn_TPXn_SurfMat1n_SurfMat2n_TDIFFn_TWMNn_PCPsmwtRtn_SMCdiffn_SMCsmm_VEG1n_VEG3n	100	11	11	930	398	-0.071	46.679	0.847	2.022	0.391	3.299	0.467	5.924
sTPXn_SurfMat2n_TDIFFn_TWMNn_PCPsmwtRtn_SMCdiffn_SMCsmrn_VEG1n_VEG2n	82	9	9	930	398	-0.059	56.404	0.845	2.169	0.392	3.329	0.467	5.695
sSurfMat1n_SurfMat2n_SurfMat3n_TDIFFn_TWMNn_PCPsmwtRtn_SMCdiffn_SMCsmrn_VEG1n_VEG3n	91	10	10	930	398	-0.066	51.768	0.843	2.211	0.393	3.267	0.467	5.786
sTPXn_TDIFFn_TWMNn_PCPsmwtRtn_SMCdiffn_SMCsmrn_VEG1n_VEG2n	73	8	8	930	398	-0.060	55.767	0.845	2.208	0.392	3.351	0.467	5.719
sSTn_TPXn_SurfMat2n_SurfMat3n_TDIFFn_TSMXn_PCPsmwtRtn_SMCdiffn_SMCsmm_VEG1n_VEG2n_VEG3n	109	12	12	930	398	-0.068	47.444	0.846	2.079	0.391	3.195	0.467	5.507
sSurfMat1n_SurfMat2n_TDIFFn_TWMNn_PCPsmwtRtn_SMCdiffn_SMCsmm_VEG2n	73	8	8	930	398	-0.061	55.485	0.843	2.195	0.393	3.250	0.467	5.714
sSTn_TPXn_SurfMat2n_TDIFFn_TWMNn_PCPsmwtRtn_SMCdiffn_SMCsmrn_VEG1n_VEG2n_VEG3n	100	11	11	930	398	-0.060	55.212	0.845	2.122	0.393	3.335	0.467	5.773
sTPXn_SurfMat2n_SurfMat3n_TDIFFn_TSMXn_PCPsmwtRtn_SMCdiffn_SMCsmm_VEG1n_VEG2n	91	10	10	930	398	-0.068	47.938	0.846	2.079	0.391	3.171	0.467	5.407
sTPXn_SurfMat1n_SurfMat2n_SurfMat3n_TDIFFn_TWMNn_PCPsmwtRtn_SMCdiffn_VEG2n_VEG3n	91	10	10	930	398	-0.060	59.385	0.844	2.311	0.393	3.276	0.467	5.695
sSTn_TPXn_SurfMat3n_TDIFFn_TWMNn_PCPsmwtRtn_SMCdiffn_SMCsmrn_VEG1n_VEG2n_VEG3n	100	11	11	930	398	-0.059	56.666	0.845	2.249	0.393	3.419	0.467	5.832
sTPXn_SurfMat1n_SurfMat2n_TDIFFn_TWMNn_PCPsmwtRtn_SMCdiffn_VEG2n_VEG3n	82	9	9	930	398	-0.059	59.649	0.843	2.214	0.393	3.229	0.467	5.615
sTPXn_SurfMat3n_TDIFFn_TSMXn_PCPsmwtRtn_SMCdiffn_SMCsmrn_VEG1n_VEG2n	82	9	9	930	398	-0.068	47.594	0.846	2.129	0.391	3.240	0.467	5.555
sTPXn_SurfMat1n_SurfMat3n_TDIFFn_TWMNn_PCPsmwtRtn_SMCdiffn_SMCsmm_VEG1n_VEG3n	91	10	10	930	398	-0.063	53.631	0.844	2.243	0.393	3.342	0.467	5.817
sTPXn_TDIFFn_TSMXn_PCPsmwtRtn_SMCdiffn_SMCsmrn_VEG1n_VEG2n	73	8	8	930	398	-0.066	48.245	0.846	2.150	0.391	3.263	0.467	5.561
sTPXn_SurfMat1n_TDIFFn_TWMNn_PCPsmwtRtn_SMCdiffn_SMCsmrn_VEG1n_VEG3n	82	9	9	930	398	-0.062	54.610	0.844	2.209	0.393	3.358	0.467	5.782
sSTn_TPXn_SurfMat3n_TDIFFn_TSMXn_PCPsmwtRtn_SMCdiffn_SMCsmrn_VEG1n_VEG2n	91	10	10	930	398	-0.067	48.519	0.846	2.104	0.391	3.268	0.467	5.562
sTPXn_SurfMat1n_SurfMat2n_SurfMat3n_TDIFFn_TWMNn_PCPsmwtRtn_SMCdiffn	73	8	8	930	398	-0.061	57.659	0.842	2.321	0.393	3.214	0.467	5.554
sTPXn_SurfMat1n_SurfMat2n_SurfMat3n_TWMNn_PCPsmwtRtn_SMCdiffn_SMCsmm_VEG1n_VEG2n_VEG3n	100	11	11	930	398	-0.064	52.774	0.846	2.043	0.392	3.074	0.467	5.679
sSurfMat1n_SurfMat2n_SurfMat3n_TDIFFn_TWMNn_PCPsmwtRtn_SMCdiffn_VEG1n	73	8	8	930	398	-0.064	54.754	0.841	2.367	0.393	3.377	0.467	6.031
sSTn_TPXn_SurfMat2n_SurfMat3n_TDIFFn_TSMXn_PCPsmwtRtn_SMCdiffn_SMCsmm_VEG2n	91	10	10	930	398	-0.063	50.445	0.845	2.084	0.392	3.249	0.468	5.503
sTPXn_SurfMat1n_SurfMat2n_TDIFFn_TWMNn_PCPsmwtRtn_SMCdiffn	64	7	7	930	398	-0.061	58.434	0.842	2.233	0.393	3.173	0.468	5.406
sSTn_TPXn_TDIFFn_TSMXn_PCPsmwtRtn_SMCdiffn_SMCsmrn_VEG1n_VEG2n	82	9	9	930	398	-0.066	48.663	0.846	2.190	0.391	3.331	0.468	5.678
sTPXn_SurfMat1n_SurfMat3n_TDIFFn_TWMNn_PCPsmwtRtn_SMCdiffn_SMCsmrn_VEG2n_VEG3n	91	10	10	930	398	-0.060	55.661	0.844	2.271	0.393	3.344	0.468	5.752

Model Name & Explanatory Variables	nCoeff	nTerms	nVariables	nTrain	nTest	UBREave	UBREcv	AUCave	AUCcv	RMSEave	RMSEcv	MXEave	MXEcv
sSRFn_TPXn_SurfMat1n_SurfMat2n_TDIFFn_TWMNn_PCPsmwtRtn_SMCdiffn_SMCsmrn_VEG2n	91	10	10	930	398	-0.070	47.983	0.848	2.037	0.390	3.332	0.468	6.207
sSTn_TPXn_SurfMat2n_SurfMat3n_TDIFFn_TWMNn_PCPsmwtRtn_SMCdiffn_SMCsmrn_VEG1n	91	10	10	930	398	-0.060	54.867	0.843	2.211	0.393	3.305	0.468	5.700
sTPXn_SurfMat2n_SurfMat3n_TDIFFn_TWMNn_PCPsmwtRtn_SMCdiffn_SMCsmrn_VEG1n_VEG2n_VEG3n	100	11	11	930	398	-0.059	57.265	0.844	2.171	0.393	3.328	0.468	5.685
sTPXn_SurfMat1n_TDIFFn_TWMNn_PCPsmwtRtn_SMCdiffn_SMCsmrn_VEG2n_VEG3n	82	9	9	930	398	-0.059	57.073	0.844	2.208	0.393	3.274	0.468	5.646
sSTn_TPXn_SurfMat2n_SurfMat3n_TDIFFn_TSMXn_PCPsmwtRtn_SMCdiffn_SMCsmrn_VEG1n	91	10	10	930	398	-0.069	46.281	0.845	2.112	0.392	3.250	0.468	5.541
sSTn_TPXn_TDIFFn_TWMNn_PCPsmwtRtn_SMCdiffn_SMCsmrn_VEG1n_VEG2n	82	9	9	930	398	-0.059	56.249	0.845	2.253	0.393	3.373	0.468	5.788
sSurfMat1n_SurfMat2n_SurfMat3n_TDIFFn_TWMNn_PCPsmwtRtn_SMCdiffn_SMCsmrn_VEG2n_VEG3n	91	10	10	930	398	-0.059	57.318	0.842	2.271	0.393	3.294	0.468	5.785
sTPXn_SurfMat2n_SurfMat3n_TDIFFn_TSMXn_PCPsmwtRtn_SMCdiffn_SMCsmm_VEG1n	82	9	9	930	398	-0.068	47.848	0.844	2.090	0.391	3.205	0.468	5.497
sTPXn_SurfMat1n_SurfMat2n_SurfMat3n_TDIFFn_TWMNn_PCPsmwtRtn_SMCdiffn_SMCsmrn_VEG3n	91	10	10	930	398	-0.063	54.141	0.843	2.269	0.393	3.326	0.468	5.758
sSTn_TPXn_SurfMat2n_SurfMat3n_TDIFFn_TSMXn_PCPsmwtRtn_SMCsmrn_VEG1n_VEG2n_VEG3n	100	11	11	930	398	-0.061	52.380	0.845	2.040	0.392	3.108	0.468	5.535

APPENDIX L (4.3)

TOP 100 OLS MODELS EXPLAINING RESIDUALS FROM POOLED SDM

Model Name: Explanatory Variables	nCoeff	Deviance	nullDeviance	AIC	BIC	R2	maxVIF
ns(PHYS1n, 2) + ns(PHYS2n, 3) + ns(CLIM1n, 2) + ns(CLIM3n, 3) + ns(SOIL2n, 3) + ns(SOIL3n, 2) + LU2n + VEG1n + VEG3n	19	154.922	221.762	481.528	595.048	0.301	5.038502
ns(PHYS1n, 2) + ns(CLIM1n, 2) + ns(CLIM3n, 3) + ns(SOIL2n, 3) + ns(SOIL3n, 2) + LU2n + VEG1n + VEG3n	16	156.668	221.762	499.687	596.180	0.294	4.452492
ns(PHYS1n, 2) + ns(PHYS2n, 3) + ns(CLIM1n, 2) + ns(SOIL2n, 3) + ns(SOIL3n, 2) + LU2n + VEG1n + VEG3n	16	156.751	221.762	500.835	597.327	0.293	4.802353
ns(PHYS1n, 2) + ns(PHYS2n, 3) + ns(CLIM1n, 2) + ns(CLIM3n, 3) + ns(SOIL2n, 3) + ns(SOIL3n, 2) + VEG1n + VEG3n	18	155.753	221.762	491.062	598.906	0.298	5.028685
ns(PHYS1n, 2) + ns(CLIM1n, 2) + ns(CLIM3n, 3) + ns(SOIL2n, 3) + ns(SOIL3n, 2) + VEG1n + VEG3n	15	157.478	221.762	508.808	599.625	0.290	4.440763
ns(PHYS1n, 2) + ns(PHYS2n, 3) + ns(SurfMat3n, 2) + ns(CLIM1n, 2) + ns(CLIM3n, 3) + ns(SOIL2n, 3) + ns(SOIL3n, 2) + LU2n + VEG1n + VEG3n	21	154.173	221.762	475.079	599.951	0.305	5.302458
ns(PHYS1n, 2) + ns(PHYS2n, 3) + ns(SurfMat3n, 2) + ns(CLIM1n, 2) + ns(CLIM3n, 3) + ns(SOIL2n, 3) + ns(SOIL3n, 2) + VEG1n + VEG3n	20	154.852	221.762	482.547	601.743	0.302	5.283595
ns(PHYS1n, 2) + ns(PHYS2n, 3) + ns(CLIM1n, 2) + CLIM2n + ns(CLIM3n, 3) + ns(SOIL2n, 3) + ns(SOIL3n, 2) + LU2n + VEG1n + VEG3n	20	154.866	221.762	482.742	601.938	0.302	6.410887
ns(PHYS1n, 2) + ns(PHYS2n, 3) + ns(SurfMat3n, 2) + ns(CLIM1n, 2) + CLIM2n + ns(CLIM3n, 3) + ns(SOIL2n, 3) + ns(SOIL3n, 2) + VEG1n + VEG3n	21	154.673	221.762	482.063	606.935	0.303	6.946181
ns(PHYS1n, 2) + ns(SurfMat3n, 2) + ns(CLIM1n, 2) + ns(CLIM3n, 3) + ns(SOIL2n, 3) + ns(SOIL3n, 2) + LU2n + VEG1n + VEG3n	18	155.806	221.762	491.786	599.630	0.297	4.684349
ns(PHYS1n, 2) + ns(PHYS2n, 3) + ns(CLIM1n, 2) + CLIM2n + ns(SOIL2n, 3) + ns(SOIL3n, 2) + LU2n + VEG1n + VEG3n	17	156.364	221.762	497.506	599.674	0.295	5.03245
ns(PHYS1n, 2) + ns(PHYS2n, 3) + ns(CLIM1n, 2) + ns(SOIL2n, 3) + ns(SOIL3n, 2) + VEG1n + VEG3n	15	157.547	221.762	509.751	600.567	0.290	4.793397
ns(PHYS1n, 2) + ns(SurfMat3n, 2) + ns(CLIM1n, 2) + ns(CLIM3n, 3) + ns(SOIL2n, 3) + ns(SOIL3n, 2) + VEG1n + VEG3n	17	156.463	221.762	498.861	601.029	0.294	4.663756
ns(PHYS1n, 2) + ns(PHYS2n, 3) + ns(CLIM1n, 2) + CLIM2n + ns(SOIL2n, 3) + ns(SOIL3n, 2) + VEG1n + VEG3n	16	157.035	221.762	504.728	601.220	0.292	5.025987
SurfMat2n + ns(CLIM1n, 2) + ns(CLIM3n, 3) + ns(SOIL2n, 3) + ns(SOIL3n, 2) + VEG1n + VEG3n	14	158.177	221.762	516.353	601.493	0.287	3.845897
ns(PHYS1n, 2) + ns(CLIM1n, 2) + ns(SOIL2n, 3) + ns(SOIL3n, 2) + LU2n + VEG1n + VEG3n	13	158.796	221.762	522.776	602.240	0.284	4.277122
ns(PHYS1n, 2) + ns(CLIM1n, 2) + CLIM2n + ns(SOIL2n, 3) + ns(SOIL3n, 2) + LU2n + VEG1n + VEG3n	14	158.259	221.762	517.475	602.615	0.286	4.455256
ns(PHYS1n, 2) + ns(PHYS2n, 3) + PHYS3n + ns(CLIM1n, 2) + ns(CLIM3n, 3) + ns(SOIL2n, 3) + ns(SOIL3n, 2) + LU2n + VEG1n + VEG3n	20	154.917	221.762	483.454	602.651	0.301	5.173315
ns(PHYS1n, 2) + ns(PHYS2n, 3) + ns(CLIM1n, 2) + ns(CLIM3n, 3) + ns(SOIL2n, 3) + ns(SOIL3n, 2) + LU1n + LU2n + VEG1n + VEG3n	20	154.922	221.762	483.519	602.715	0.301	5.17715
ns(PHYS1n, 2) + ns(CLIM1n, 2) + CLIM2n + ns(CLIM3n, 3) + ns(SOIL2n, 3) + ns(SOIL3n, 2) + LU2n + VEG1n + VEG3n	17	156.604	221.762	500.807	602.975	0.294	6.181493
ns(PHYS1n, 2) + PHYS3n + ns(CLIM1n, 2) + ns(CLIM3n, 3) + ns(SOIL2n, 3) + ns(SOIL3n, 2) + LU2n + VEG1n + VEG3n	17	156.656	221.762	501.520	603.688	0.294	4.555803
ns(PHYS1n, 2) + ns(CLIM1n, 2) + CLIM2n + ns(SOIL2n, 3) + ns(SOIL3n, 2) + VEG1n + VEG3n	13	158.907	221.762	524.287	603.752	0.283	4.448015
ns(PHYS1n, 2) + ns(CLIM1n, 2) + ns(CLIM3n, 3) + ns(SOIL2n, 3) + ns(SOIL3n, 2) + LU1n + LU2n + VEG1n + VEG3n	17	156.664	221.762	501.635	603.803	0.294	4.581585
SurfMat2n + ns(CLIM1n, 2) + ns(SOIL2n, 3) + ns(SOIL3n, 2) + VEG1n + VEG3n	11	160.092	221.762	536.305	604.417	0.278	3.68583
ns(PHYS1n, 2) + ns(PHYS2n, 3) + ns(SurfMat3n, 2) + ns(CLIM1n, 2) + ns(SOIL2n, 3) + ns(SOIL3n, 2) + LU2n + VEG1n + VEG3n	18	156.163	221.762	496.726	604.570	0.296	5.043904
ns(PHYS1n, 2) + ns(PHYS2n, 3) + ns(SurfMat3n, 2) + ns(CLIM1n, 2) + CLIM2n + ns(SOIL2n, 3) + ns(SOIL3n, 2) + VEG1n + VEG3n	18	156.167	221.762	496.781	604.625	0.296	5.229518
ns(PHYS1n, 2) + ns(PHYS2n, 3) + PHYS3n + ns(CLIM1n, 2) + ns(SOIL2n, 3) + ns(SOIL3n, 2) + LU2n + VEG1n + VEG3n	17	156.746	221.762	502.754	604.922	0.293	4.93181
ns(PHYS1n, 2) + ns(PHYS2n, 3) + ns(CLIM1n, 2) + ns(SOIL2n, 3) + ns(SOIL3n, 2) + LU1n + LU2n + VEG1n + VEG3n	17	156.751	221.762	502.832	605.000	0.293	4.938606
ns(PHYS1n, 2) + ns(PHYS2n, 3) + ns(CLIM1n, 2) + CLIM2n + ns(CLIM3n, 3) + ns(SOIL2n, 3) + ns(SOIL3n, 2) + VEG1n + VEG3n	19	155.647	221.762	491.591	605.112	0.298	6.321409
ns(PHYS1n, 2) + ns(PHYS2n, 3) + ns(SurfMat3n, 2) + ns(CLIM1n, 2) + CLIM2n + ns(SOIL2n, 3) + ns(SOIL3n, 2) + LU2n + VEG1n + VEG3n	19	155.648	221.762	491.608	605.128	0.298	5.240826
ns(PHYS1n, 2) + ns(CLIM1n, 2) + ns(SOIL2n, 3) + ns(SOIL3n, 2) + VEG1n + VEG3n	12	159.589	221.762	531.521	605.309	0.280	4.268156
ns(PHYS1n, 2) + ns(SurfMat3n, 2) + ns(CLIM1n, 2) + CLIM2n + ns(CLIM3n, 3) + ns(SOIL2n, 3) + ns(SOIL3n, 2) + LU2n + VEG1n + VEG3n	19	155.678	221.762	492.022	605.542	0.298	6.755709
ns(PHYS1n, 2) + ns(CLIM1n, 2) + CLIM2n + ns(CLIM3n, 3) + ns(SOIL2n, 3) + ns(SOIL3n, 2) + VEG1n + VEG3n	16	157.362	221.762	509.216	605.708	0.290	6.095116
ns(PHYS1n, 2) + ns(SurfMat3n, 2) + ns(CLIM1n, 2) + CLIM2n + ns(SOIL2n, 3) + ns(SOIL3n, 2) + VEG1n + VEG3n	15	157.926	221.762	514.934	605.751	0.288	4.620415
ns(PHYS1n, 2) + ns(PHYS2n, 3) + ns(SurfMat3n, 2) + ns(CLIM1n, 2) + ns(SOIL2n, 3) + ns(SOIL3n, 2) + VEG1n + VEG3n	17	156.823	221.762	503.822	605.990	0.293	5.026148
ns(PHYS1n, 2) + ns(SurfMat3n, 2) + ns(CLIM1n, 2) + CLIM2n + ns(CLIM3n, 3) + ns(SOIL2n, 3) + ns(SOIL3n, 2) + VEG1n + VEG3n	18	156.267	221.762	498.157	606.001	0.295	6.643892
ns(PHYS1n, 2) + ns(PHYS2n, 3) + ns(CLIM1n, 2) + ns(CLIM3n, 3) + ns(SOIL2n, 3) + ns(SOIL3n, 2) + LU1n + VEG1n + VEG3n	19	155.741	221.762	492.890	606.410	0.298	5.159331
ns(PHYS1n, 2) + ns(PHYS2n, 3) + PHYS3n + ns(CLIM1n, 2) + ns(CLIM3n, 3) + ns(SOIL2n, 3) + ns(SOIL3n, 2) + VEG1n + VEG3n	19	155.751	221.762	493.026	606.546	0.298	5.161699
ns(PHYS1n, 2) + ns(SurfMat3n, 2) + ns(CLIM1n, 2) + CLIM2n + ns(SOIL2n, 3) + ns(SOIL3n, 2) + LU2n + VEG1n + VEG3n	16	157.430	221.762	510.150	606.642	0.290	4.681774
ns(PHYS1n, 2) + ns(CLIM1n, 2) + ns(CLIM3n, 3) + ns(SOIL2n, 3) + ns(SOIL3n, 2) + LU1n + VEG1n + VEG3n	16	157.457	221.762	510.518	607.010	0.290	4.561585
ns(PHYS1n, 2) + PHYS3n + ns(SurfMat3n, 2) + ns(CLIM1n, 2) + ns(CLIM3n, 3) + ns(SOIL2n, 3) + ns(SOIL3n, 2) + LU2n + VEG1n + VEG3n	19	155.793	221.762	493.606	607.126	0.297	4.790131
ns(PHYS1n, 2) + ns(SurfMat3n, 2) + ns(CLIM1n, 2) + ns(CLIM3n, 3) + ns(SOIL2n, 3) + ns(SOIL3n, 2) + LU1n + LU2n + VEG1n + VEG3n	19	155.794	221.762	493.625	607.145	0.297	4.787478
ns(PHYS1n, 2) + PHYS3n + ns(CLIM1n, 2) + ns(CLIM3n, 3) + ns(SOIL2n, 3) + ns(SOIL3n, 2) + VEG1n + VEG3n	16	157.471	221.762	510.707	607.199	0.290	4.542199
ns(PHYS1n, 2) + ns(PHYS2n, 3) + ns(CLIM1n, 2) + CLIM2n + ns(SOIL2n, 3) + ns(SOIL3n, 2) + LU1n + LU2n + VEG1n + VEG3n	18	156.363	221.762	499.486	607.330	0.295	5.16955
ns(PHYS1n, 2) + ns(PHYS2n, 3) + PHYS3n + ns(CLIM1n, 2) + CLIM2n + ns(SOIL2n, 3) + ns(SOIL3n, 2) + LU2n + VEG1n + VEG3n	18	156.364	221.762	499.496	607.340	0.295	5.148982
ns(PHYS1n, 2) + ns(PHYS2n, 3) + ns(CLIM1n, 2) + ns(SOIL2n, 3) + ns(SOIL3n, 2) + LU1n + VEG1n + VEG3n	16	157.538	221.762	511.621	608.113	0.290	4.92228
ns(PHYS1n, 2) + ns(PHYS2n, 3) + PHYS3n + ns(CLIM1n, 2) + ns(SOIL2n, 3) + ns(SOIL3n, 2) + VEG1n + VEG3n	16	157.543	221.762	511.701	608.193	0.290	4.921556
ns(PHYS1n, 2) + ns(SurfMat3n, 2) + ns(CLIM1n, 2) + ns(SOIL2n, 3) + ns(SOIL3n, 2) + LU2n + VEG1n + VEG3n	15	158.126	221.762	517.663	608.479	0.287	4.483039
ns(PHYS1n, 2) + PHYS3n + ns(SurfMat3n, 2) + ns(CLIM1n, 2) + ns(CLIM3n, 3) + ns(SOIL2n, 3) + ns(SOIL3n, 2) + VEG1n + VEG3n	18	156.454	221.762	500.744	608.588	0.294	4.766959
ns(PHYS1n, 2) + ns(SurfMat3n, 2) + ns(CLIM1n, 2) + ns(CLIM3n, 3) + ns(SOIL2n, 3) + ns(SOIL3n, 2) + LU1n + VEG1n + VEG3n	18	156.461	221.762	500.835	608.680	0.294	4.759726
ns(PHYS1n, 2) + ns(PHYS2n, 3) + ns(CLIM1n, 2) + CLIM2n + ns(SOIL2n, 3) + ns(SOIL3n, 2) + LU1n + VEG1n + VEG3n	17	157.021	221.762	506.543	608.711	0.292	5.156612
SurfMat2n + ns(CLIM1n, 2) + CLIM2n + ns(CLIM3n, 3) + ns(SOIL2n, 3) + ns(SOIL3n, 2) + VEG1n + VEG3n	15	158.144	221.762	517.900	608.716	0.287	6.548641
SurfMat2n + ns(CLIM1n, 2) + ns(CLIM3n, 3) + ns(SOIL2n, 3) + ns(SOIL3n, 2) + LU1n + VEG1n + VEG3n	15	158.145	221.762	517.913	608.729	0.287	3.943095
SurfMat2n + ns(SurfMat3n, 2) + ns(CLIM1n, 2) + ns(CLIM3n, 3) + ns(SOIL2n, 3) + ns(SOIL3n, 2) + VEG1n + VEG3n	16	157.587	221.762	512.293	608.785	0.289	4.033159
ns(PHYS1n, 2) + ns(PHYS2n, 3) + PHYS3n + ns(CLIM1n, 2) + CLIM2n + ns(SOIL2n, 3) + ns(SOIL3n, 2) + VEG1n + VEG3n	17	157.035	221.762	506.727	608.896	0.292	5.141185
SurfMat2n + ns(CLIM1n, 2) + ns(CLIM3n, 3) + ns(SOIL2n, 3) + ns(SOIL3n, 2) + LU2n + VEG1n + VEG3n	15	158.158	221.762	518.097	608.913	0.287	3.957263
PHYS3n + SurfMat2n + ns(CLIM1n, 2) + ns(CLIM3n, 3) + ns(SOIL2n, 3) + ns(SOIL3n, 2) + VEG1n + VEG3n	15	158.177	221.762	518.347	609.163	0.287	3.934755
ns(PHYS1n, 2) + ns(PHYS2n, 3) + ns(SurfMat3n, 2) + ns(CLIM1n, 2) + ns(CLIM3n, 3) + ns(SOIL2n, 3) + ns(SOIL3n, 2) + LU1n + VEG1n + VEG3n	21	154.848	221.762	484.498	609.371	0.302	5.388698
ns(PHYS1n, 2) + ns(PHYS2n, 3) + PHYS3n + ns(SurfMat3n, 2) + ns(CLIM1n, 2) + ns(CLIM3n, 3) + ns(SOIL2n, 3) + ns(SOIL3n, 2) + VEG1n + VEG3n	21	154.849	221.762	484.508	609.380	0.302	5.419798
ns(PHYS1n, 2) + PHYS3n + ns(CLIM1n, 2) + ns(SOIL2n, 3) + ns(SOIL3n, 2) + LU2n + VEG1n + VEG3n	14	158.772	221.762	524.443	609.584	0.284	4.366355
ns(PHYS1n, 2) + ns(SurfMat3n, 2) + ns(CLIM1n, 2) + ns(SOIL2n, 3) + ns(SOIL3n, 2) + VEG1n + VEG3n	14	158.784	221.762	524.617	609.757	0.284	4.466215
ns(PHYS1n, 2) + ns(CLIM1n, 2) + ns(SOIL2n, 3) + ns(SOIL3n, 2) + LU1n + LU2n + VEG1n + VEG3n	14	158.795	221.762	524.761	609.901	0.284	4.398633
ns(PHYS1n, 2) + PHYS3n + ns(CLIM1n, 2) + CLIM2n + ns(SOIL2n, 3) + ns(SOIL3n, 2) + LU2n + VEG1n + VEG3n	15	158.250	221.762	519.352	610.168	0.286	4.534891
ns(PHYS1n, 2) + ns(CLIM1n, 2) + CLIM2n + ns(SOIL2n, 3) + ns(SOIL3n, 2) + LU1n + LU2n + VEG1n + VEG3n	15	158.256	221.762	519.426	610.242	0.286	4.577949
ns(PHYS1n, 2) + PHYS3n + ns(CLIM1n, 2) + CLIM2n + ns(CLIM3n, 3) + ns(SOIL2n, 3) + ns(SOIL3n, 2) + LU2n + VEG1n + VEG3n	18	156.594	221.762	502.667	610.511	0.294	6.36656
ns(PHYS1n, 2) + ns(CLIM1n, 2) + CLIM2n + ns(CLIM3n, 3) + ns(SOIL2n, 3) + ns(SOIL3n, 2) + LU1n + LU2n + VEG1n + VEG3n	18	156.600	221.762	502.748	610.592	0.294	6.23605
ns(PHYS1n, 2) + ns(CLIM1n, 2) + CLIM2n + ns(SOIL2n, 3) + ns(SOIL3n, 2) + LU1n + VEG1n + VEG3n	14	158.889	221.762	526.036	611.176	0.284	4.564317
ns(PHYS1n, 2) + PHYS3n + ns(CLIM1n, 2) + ns(CLIM3n, 3) + ns(SOIL2n, 3) + ns(SOIL3n, 2) + LU1n + LU2n + VEG1n + VEG3n	18	156.653	221.762	503.481	611.325	0.294	4.703188
ns(PHYS1n, 2) + PHYS3n + ns(CLIM1n, 2) + CLIM2n + ns(SOIL2n, 3) + ns(SOIL3n, 2) + VEG1n + VEG3n	14	158.902	221.762	526.219	611.359	0.283	4.526373
SurfMat2n + ns(CLIM1n, 2) + ns(SOIL2n, 3) + ns(SOIL3n, 2) + LU1n + VEG1n + VEG3n	12	160.049	221.762	537.715	611.503	0.278	3.773404
SurfMat2n + ns(CLIM1n, 2) + CLIM2n + ns(SOIL2n, 3) + ns(SOIL3n, 2) + VEG1n + VEG3n	12	160.086	221.762	538.220	612.008	0.278	4.493187
ns(PHYS1n, 2) + ns(PHYS2n, 3) + ns(SurfMat3n, 2) + ns(CLIM1n, 2) + ns(SOIL2n, 3) + ns(SOIL3n, 2) + LU1n + LU2n + VEG1n + VEG3n	19	156.149	221.762	498.532	612.052	0.296	5.152384
SurfMat2n + ns(CLIM1n, 2) + ns(SOIL2n, 3) + ns(SOIL3n, 2) + LU2n + VEG1n + VEG3n	12	160.091	221.762	538.280	612.068	0.278	3.789049

Model Name: Explanatory Variables	nCoeff	Deviance	nullDeviance	AIC	BIC	R2	maxVIF
PHYS3n + SurfMat2n + ns(CLIM1n, 2) + ns(SOIL2n, 3) + ns(SOIL3n, 2) + VEG1n + VEG3n	12	160.092	221.762	538.301	612.089	0.278	3.766611
ns(PHYS1n, 2) + ns(PHYS2n, 3) + PHYS3n + ns(SurfMat3n, 2) + ns(CLIM1n, 2) + ns(SOIL2n, 3) + ns(SOIL3n, 2) + LU2n + VEG1n + VEG3n	19	156.157	221.762	498.640	612.160	0.296	5.176132
ns(PHYS1n, 2) + ns(PHYS2n, 3) + ns(SurfMat3n, 2) + ns(CLIM1n, 2) + CLIM2n + ns(SOIL2n, 3) + ns(SOIL3n, 2) + LU1n + VEG1n + VEG3n	19	156.164	221.762	498.745	612.265	0.296	5.334984
ns(PHYS1n, 2) + ns(PHYS2n, 3) + PHYS3n + ns(SurfMat3n, 2) + ns(CLIM1n, 2) + CLIM2n + ns(SOIL2n, 3) + ns(SOIL3n, 2) + VEG1n + VEG3n	19	156.167	221.762	498.781	612.301	0.296	5.34844
ns(PHYS1n, 2) + ns(PHYS2n, 3) + PHYS3n + ns(CLIM1n, 2) + ns(SOIL2n, 3) + ns(SOIL3n, 2) + LU1n + LU2n + VEG1n + VEG3n	18	156.745	221.762	504.752	612.596	0.293	5.088318
ns(PHYS1n, 2) + ns(PHYS2n, 3) + ns(CLIM1n, 2) + CLIM2n + ns(CLIM3n, 3) + ns(SOIL2n, 3) + ns(SOIL3n, 2) + LU1n + VEG1n + VEG3n	20	155.634	221.762	493.408	612.604	0.298	6.369728
ns(PHYS1n, 2) + PHYS3n + ns(CLIM1n, 2) + ns(SOIL2n, 3) + ns(SOIL3n, 2) + VEG1n + VEG3n	13	159.570	221.762	533.263	612.727	0.280	4.356206
ns(PHYS1n, 2) + ns(CLIM1n, 2) + ns(CLIM3n, 3) + ns(SOIL2n, 3) + ns(SOIL3n, 2) + LU2n + VEG1n	15	158.439	221.762	521.920	612.736	0.286	3.998355
ns(PHYS1n, 2) + ns(PHYS2n, 3) + PHYS3n + ns(CLIM1n, 2) + CLIM2n + ns(CLIM3n, 3) + ns(SOIL2n, 3) + ns(SOIL3n, 2) + VEG1n + VEG3n	20	155.646	221.762	493.574	612.770	0.298	6.515055
ns(PHYS1n, 2) + ns(CLIM1n, 2) + ns(SOIL2n, 3) + ns(SOIL3n, 2) + LU1n + VEG1n + VEG3n	13	159.577	221.762	533.345	612.810	0.280	4.382783
ns(PHYS1n, 2) + ns(PHYS2n, 3) + ns(CLIM1n, 2) + ns(CLIM3n, 3) + ns(SOIL2n, 3) + ns(SOIL3n, 2) + LU2n + VEG1n	18	156.763	221.762	504.989	612.833	0.293	4.559868
ns(PHYS1n, 2) + ns(CLIM1n, 2) + CLIM2n + ns(CLIM3n, 3) + ns(SOIL2n, 3) + ns(SOIL3n, 2) + LU1n + VEG1n + VEG3n	17	157.340	221.762	510.916	613.084	0.291	6.142886
ns(PHYS1n, 2) + PHYS3n + ns(CLIM1n, 2) + CLIM2n + ns(CLIM3n, 3) + ns(SOIL2n, 3) + ns(SOIL3n, 2) + VEG1n + VEG3n	17	157.356	221.762	511.140	613.309	0.290	6.273415
ns(PHYS1n, 2) + PHYS3n + ns(SurfMat3n, 2) + ns(CLIM1n, 2) + CLIM2n + ns(SOIL2n, 3) + ns(SOIL3n, 2) + VEG1n + VEG3n	16	157.921	221.762	516.865	613.357	0.288	4.736269
ns(PHYS1n, 2) + ns(SurfMat3n, 2) + ns(CLIM1n, 2) + CLIM2n + ns(SOIL2n, 3) + ns(SOIL3n, 2) + LU1n + VEG1n + VEG3n	16	157.924	221.762	516.901	613.394	0.288	4.713046
ns(PHYS1n, 2) + PHYS3n + ns(SurfMat3n, 2) + ns(CLIM1n, 2) + CLIM2n + ns(CLIM3n, 3) + ns(SOIL2n, 3) + ns(SOIL3n, 2) + VEG1n + VEG3n	19	156.261	221.762	500.075	613.595	0.295	6.839842
ns(PHYS1n, 2) + ns(PHYS2n, 3) + PHYS3n + ns(SurfMat3n, 2) + ns(CLIM1n, 2) + ns(SOIL2n, 3) + ns(SOIL3n, 2) + VEG1n + VEG3n	18	156.819	221.762	505.766	613.611	0.293	5.156537
ns(PHYS1n, 2) + ns(PHYS2n, 3) + ns(SurfMat3n, 2) + ns(CLIM1n, 2) + ns(SOIL2n, 3) + ns(SOIL3n, 2) + LU1n + VEG1n + VEG3n	18	156.820	221.762	505.779	613.624	0.293	5.128116
ns(PHYS1n, 2) + ns(SurfMat3n, 2) + ns(CLIM1n, 2) + CLIM2n + ns(CLIM3n, 3) + ns(SOIL2n, 3) + ns(SOIL3n, 2) + LU1n + VEG1n + VEG3n	19	156.264	221.762	500.124	613.644	0.295	6.739965
ns(PHYS1n, 2) + ns(PHYS2n, 3) + PHYS3n + ns(CLIM1n, 2) + ns(CLIM3n, 3) + ns(SOIL2n, 3) + ns(SOIL3n, 2) + LU1n + VEG1n + VEG3n	20	155.739	221.762	494.865	614.061	0.298	5.312534
ns(PHYS1n, 2) + ns(SurfMat3n, 2) + ns(CLIM1n, 2) + CLIM2n + ns(SOIL2n, 3) + ns(SOIL3n, 2) + LU1n + LU2n + VEG1n + VEG3n	17	157.419	221.762	512.002	614.170	0.290	4.751665
ns(PHYS1n, 2) + PHYS3n + ns(SurfMat3n, 2) + ns(CLIM1n, 2) + CLIM2n + ns(SOIL2n, 3) + ns(SOIL3n, 2) + LU2n + VEG1n + VEG3n	17	157.422	221.762	512.032	614.200	0.290	4.844527
SurfMat2n + ns(SurfMat3n, 2) + ns(CLIM1n, 2) + ns(SOIL2n, 3) + ns(SOIL3n, 2) + VEG1n + VEG3n	13	159.697	221.762	534.975	614.439	0.280	3.841956
ns(PHYS1n, 2) + PHYS3n + ns(CLIM1n, 2) + ns(CLIM3n, 3) + ns(SOIL2n, 3) + ns(SOIL3n, 2) + LU1n + VEG1n + VEG3n	17	157.451	221.762	512.439	614.607	0.290	4.679819
ns(PHYS2n, 3) + SurfMat2n + ns(CLIM1n, 2) + ns(CLIM3n, 3) + ns(SOIL2n, 3) + ns(SOIL3n, 2) + VEG1n + VEG3n	17	157.469	221.762	512.681	614.849	0.290	4.2444
SurfMat2n + ns(SurfMat3n, 2) + ns(CLIM1n, 2) + ns(CLIM3n, 3) + ns(SOIL2n, 3) + ns(SOIL3n, 2) + LU1n + VEG1n + VEG3n	17	157.488	221.762	512.945	615.113	0.290	4.107915

APPENDIX M (4.4)

MAPPED LOCAL PARAMETER SURFACES FOR 9 STANDARDIZED EXPLANATORY VARIABLES

Local parameter surfaces for the 9 standardized explanatory variables specified in the MGWR model of SDM residuals. Local parameter estimates ranged from -3.56 to 3.02 and are shown with standardized color breaks for CLIM1 (A), CLIM3 (B), PHYS1 (C), PHYS2 (D), SOIL2 (E), SOIL3 (F), VEG1 (G), VEG3 (H), and LU2 (I). Explanations of each explanatory variable are given in Tables 4.1 and Appendix 4.1. The Colorado River (blue) separates California and Arizona and creates the division between the two species the two species of desert tortoise, *Gopherus agassizii* (Agassiz's tortoise) and *Gopherus morafkai* (Morafkai's tortoise).

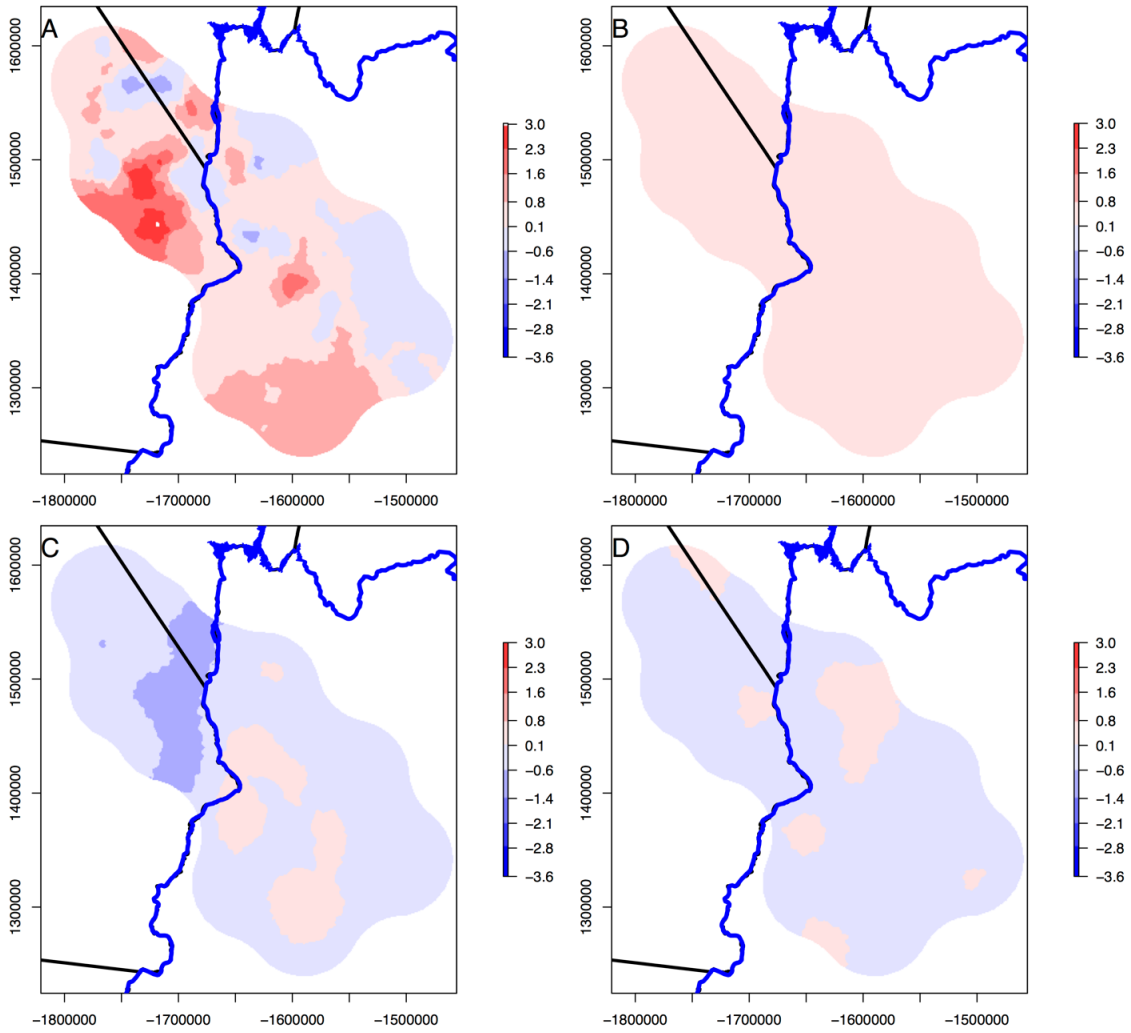

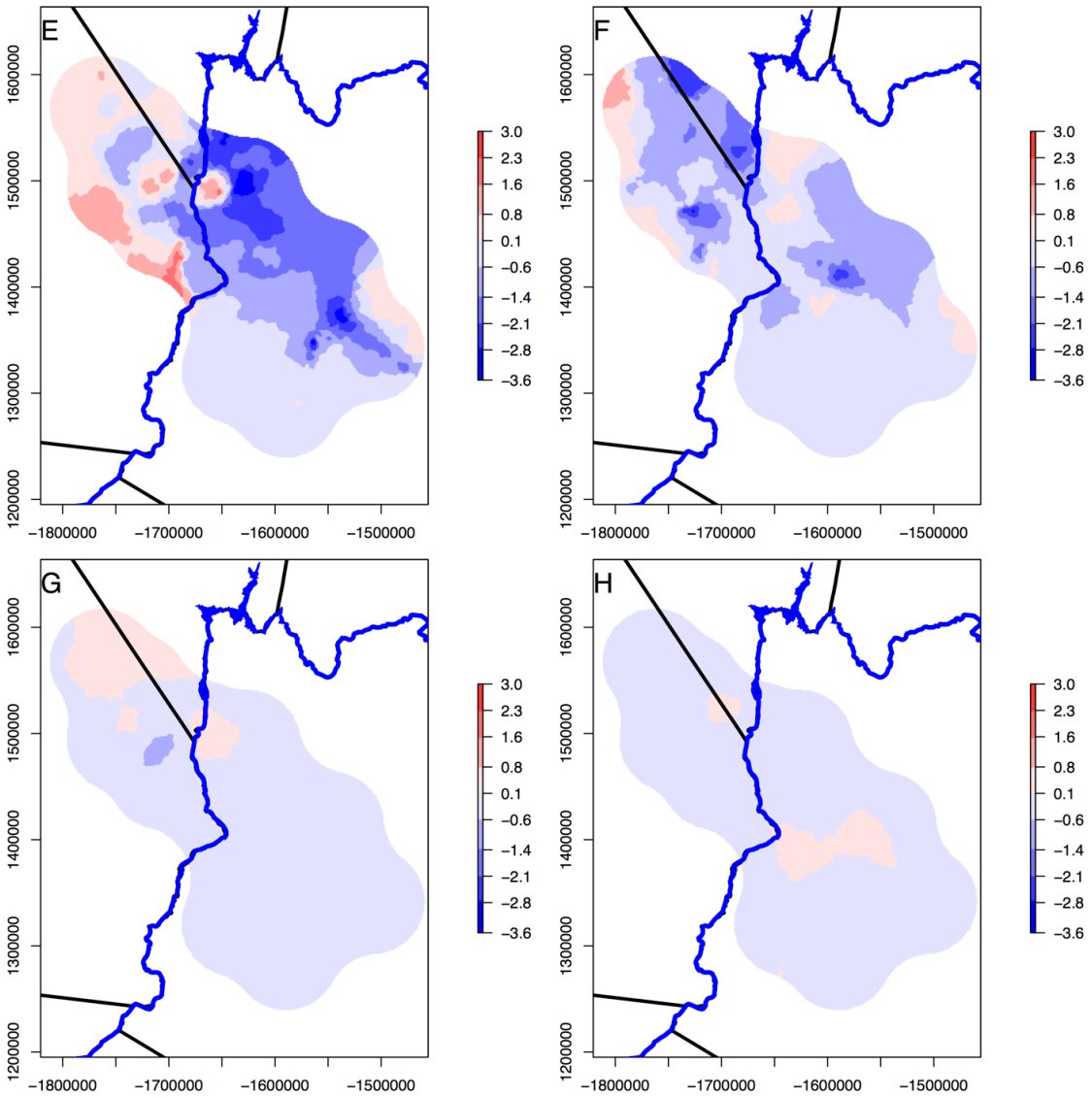
E
F
G
H
1600000
1500000
1400000
1300000
1200000
−1800000
−1700000
−1600000
−1500000
3.0
2.3
1.6
0.8
0.1
−0.6
−1.4
−2.1
−2.8
−3.6